Technology Collaboration Programme
by iea

International Energy Agency
Photovoltaic Power Systems Programme

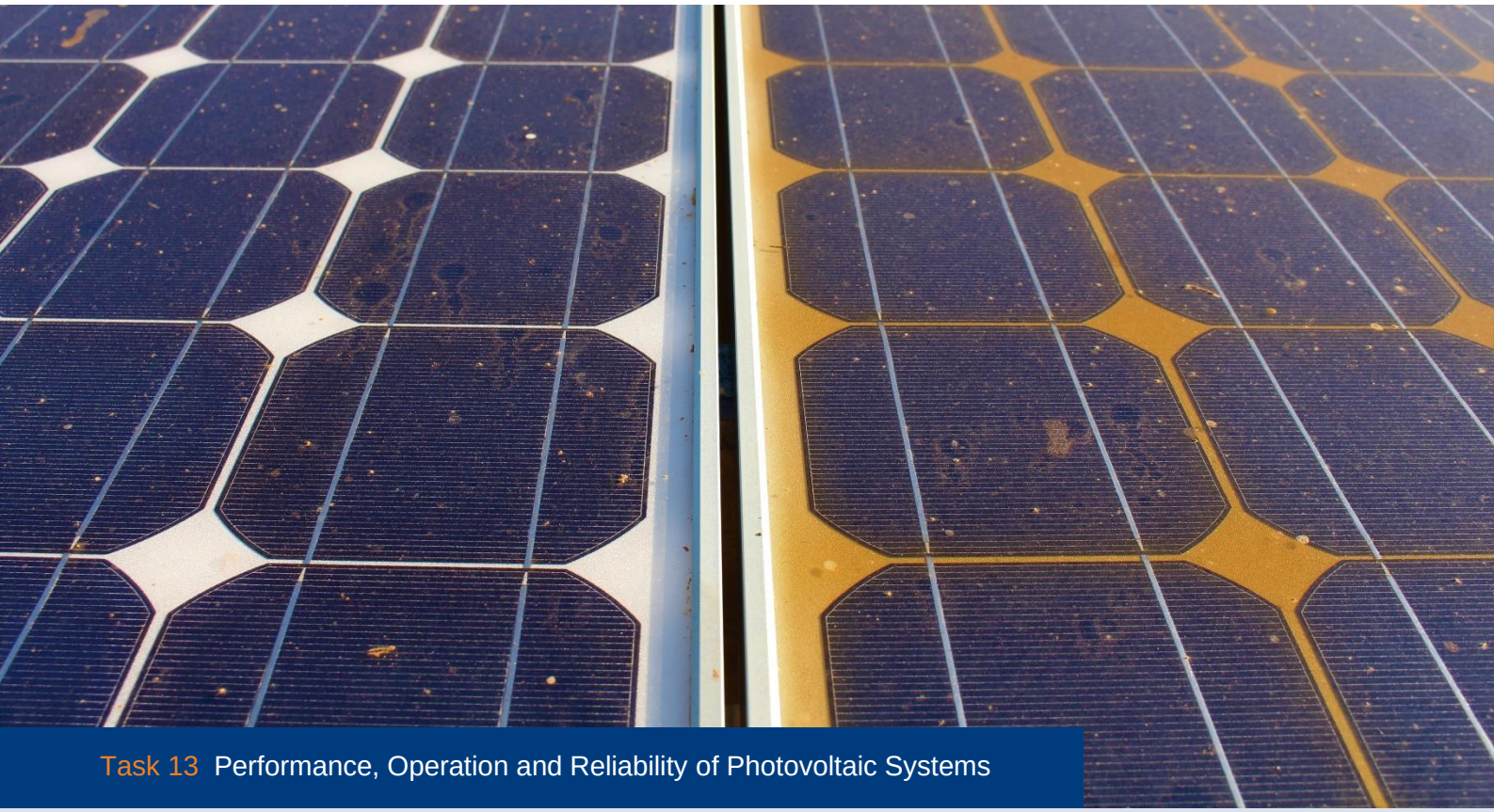

Task 13 Performance, Operation and Reliability of Photovoltaic Systems

PVPS

Designing New Materials for Photovoltaics: Opportunities for Lowering Cost and Increasing Performance through Advanced Material Innovations

2021

Report IEA-PVPS T13-13:2021

What is IEA PVPS TCP?

The International Energy Agency (IEA), founded in 1974, is an autonomous body within the framework of the Organization for Economic Cooperation and Development (OECD). The Technology Collaboration Programme (TCP) was created with a belief that the future of energy security and sustainability starts with global collaboration. The programme is made up of 6.000 experts across government, academia, and industry dedicated to advancing common research and the application of specific energy technologies.

The IEA Photovoltaic Power Systems Programme (IEA PVPS) is one of the TCP's within the IEA and was established in 1993. The mission of the programme is to "enhance the international collaborative efforts which facilitate the role of photovoltaic solar energy as a cornerstone in the transition to sustainable energy systems." In order to achieve this, the Programme's participants have undertaken a variety of joint research projects in PV power systems applications. The overall programme is headed by an Executive Committee, comprised of one delegate from each country or organisation member, which designates distinct 'Tasks,' that may be research projects or activity areas.

The IEA PVPS participating countries are Australia, Austria, Belgium, Canada, Chile, China, Denmark, Finland, France, Germany, Israel, Italy, Japan, Korea, Malaysia, Mexico, Morocco, the Netherlands, Norway, Portugal, South Africa, Spain, Sweden, Switzerland, Thailand, Turkey, and the United States of America. The European Commission, Solar Power Europe, the Smart Electric Power Alliance (SEPA), the Solar Energy Industries Association and the Cop- per Alliance are also members.

Visit us at: www.iea-pvps.org

What is IEA PVPS Task 13?

Within the framework of IEA PVPS, Task 13 aims to provide support to market actors working to improve the operation, the reliability and the quality of PV components and systems. Operational data from PV systems in different climate zones compiled within the project will help provide the basis for estimates of the current situation regarding PV reliability and performance.

The general setting of Task 13 provides a common platform to summarize and report on technical aspects affecting the quality, performance, reliability and lifetime of PV systems in a wide variety of environments and applications. By working together across national boundaries we can all take advantage of research and experience from each member country and combine and integrate this knowledge into valuable summaries of best practices and methods for ensuring PV systems perform at their optimum and continue to provide competitive return on investment.

Task 13 has so far managed to create the right framework for the calculations of various parameters that can give an indication of the quality of PV components and systems. The framework is now there and can be used by the industry who has expressed appreciation towards the results included in the high-quality reports.

The IEA PVPS countries participating in Task 13 are Australia, Austria, Belgium, Canada, Chile, China, Denmark, Finland, France, Germany, Israel, Italy, Japan, the Netherlands, Norway, Spain, Sweden, Switzerland, Thailand, and the United States of America.

COVER PICTURE

Backsheet yellowing. Photo by Gernot Oreski (PCCL, AUT)

ISBN 978-3-907281-02-4: Designing new materials for photovoltaics: Opportunities for lowering cost and increasing performance through advanced material innovations

INTERNATIONAL ENERGY AGENCY

PHOTOVOLTAIC POWER SYSTEMS PROGRAMME

IEA PVPS Task 13

Performance, Operation and Reliability of Photovoltaic Systems

Designing New Materials for Photovoltaics: Opportunities for Lowering Cost and Increasing Performance through Advanced Material Innovations

Report IEA-PVPS T13-13:2021

April 2021

ISBN 978-3-907281-02-4

AUTHORS

Main Authors

Gernot Oreski, Polymer Competence Center Leoben (PCCL), Austria
Joshua Stein, Sandia National Labs, USA
Gabriele Eder, Austrian Research Institute for Chemistry and Technology (OFI), Austria
Karl Berger, Austrian Institute of Technology (AIT), Austria
Laura S. Bruckman, Case Western Reserve University (CRWU), USA
Jan Vedde, European Energy, Denmark
Karl-Anders Weiss, Fraunhofer ISE, Germany
Tadanori Tanahashi, National Institute of Advanced Industrial Science and Technology （AIST), Japan
Roger H. French, Case Western Reserve University (CRWU), USA
Samuli Ranta, Turku University of Applied Sciences, Finland

Contributing Authors

Chiara Barretta, Polymer Competence Center Leoben, Austria
Luis Castillon, Polymer Competence Center Leoben, Austria
Menghong Wang, Case Western Reserve University, USA
Raymond J. Wieser, Case Western Reserve University, USA
Sameera Nalin Venkat, Case Western Reserve University, USA
William Gambogi, DuPont, USA
Kaushik Roy Choudhury, DuPont, USA
Mauro Caccivio, SUPSI, Switzerland
Markus Klenk, ZHAW, Switzerland
Hartmut Nussbaumer, ZHAW, Switzerland
Gianluca Cattaneo, CSEM, Switzerland
Sang Han, Osazda Energy, USA
Hoi Ng, Sunpower, USA
David C. Miller, NREL, USA

Editors

Gernot Oreski, Polymer Competence Center Leoben, Austria
Joshua Stein, Sandia National Labs, USA
Boris Farnung, VDE Renewables, Germany

TABLE OF CONTENTS

Acknowledgements 6
List of abbreviations 7
Executive summary 11
1 Introduction 15
2 State of the Art in PV Module Materials and Technology 16
2.1 Frontsheets and coatings 16
2.2 Encapsulants 17
2.3 Cells and cell interconnects 19
2.4 Backsheets 20
2.5 Junction boxes and connectors 21
2.6 Module frame 21
3 Motivation, benefits, and opportunities for new material & module developments 22
3.1 Decrease of LCOE: Cost reduction and performance improvement 22
3.2 Sustainability and legal regulations 23
3.3 New technological requirements 24
3.4 Impact and consequences of new materials and module designs 28
4 Reliability of advanced materials, components and modules 37
4.1 Frontsheets and coatings 37
4.2 Backsheets 43
4.3 Encapsulants 50
4.4 Cell interconnection and metallization 55
4.5 Reliability of new module concepts - Lightweight module approaches 67
5 Conclusion 70
6 References 71

ACKNOWLEDGEMENTS

This paper received valuable contributions from several IEA-PVPS Task 13 members and other international experts. Many thanks to:

Marc Köntges (ISFH, Germany) for reviewing of the document.

This report is supported by the Austrian Federal Government, represented by the Austrian Research Promotion Agency (FFG) under contract no. 876736.

This report is supported by the Danish Energy Agency under the Energy Technology Development and Demonstration Program (EUDP) contract no 64018-0081

This report is supported by the German Federal Ministry for Economic Affairs and Energy (BMWi) under contract no. 0324304B and 0324304C.

This report is supported by the by the New Energy and Industrial Technology Development Organization (NEDO), Japan, under contract #15100576-0.

This report is supported by the Swiss Federal Office of Energy (SFOE) under contract no.: SI/501788-01. Contributions described in section 3.4.2 are part of the PV-Enerate research project - Advanced PV Energy Rating (co-financed by EMPIR programme and from the European Union's Horizon 2020 research and innovation programme under the project number 16ENG02) and the BIPVBOOST project (European Union's Horizon 2020 research and innovation programme under grant agreement No 817991). Part of the presented concepts have been developed with the support of the BIPVBOOST partners TECNALIA and CSTB.

Sandia National Laboratories is a multimission laboratory managed and operated by National Technology and Engineering Solutions of Sandia, LLC, a wholly owned subsidiary of Honeywell International Inc., for the U.S. Department of Energy's National Nuclear Security Administration under contract DE-NA0003525.

Laura Bruckman and Raymond Weiser were supported by the U.S. Department of Energy's Office of Energy Efficiency and Renewable Energy (EERE) under Solar Energy Technologies Office (SETO) Agreement Number DE-EE-0008748. Roger French, Sameera Venkat, and Menghong Wang were supported by the U.S. Department of Energy's Office of Energy Efficiency and Renewable Energy (EERE) under Solar Energy Technologies Office (SETO) Agreement Number DE-EE-0008550.

This work was authored in part by the NREL, operated by Alliance for Sustainable Energy, LLC for the US DOE under contract no. DE-AC36-08GO28308. Funding was provided under Agreement DE-EE00034357 by the U.S. Department of Energy (DOE), Office of Energy Efficiency.

The contribution of Osazda Energy is based upon work supported by the U.S. Department of Energy's Office of Energy Efficiency and Renewable Energy under the DuraMAT Program Award Numbers RGJ-7-70325 and NGJ-9-92069-01 and under the Solar Energy Technologies Office Award Number DE-EE0009013. We also want to thank DuPont for providing commercial silver paste products to be used in metal matrix composite formulations.

LIST OF ABBREVIATIONS

2D	Two-dimensional
AAA	PA/PA/PA backsheet
AATR	Acetic acid transmission rate
ACA	Anisotropic Conductive adhesive
Ag	Silver
Al-BSF	Aluminum back surface field
APA	PA/aluminum/PET/PA backsheet
AR	Anti-reflective
ARC	Anti-reflective coating
AS	Antisoiling
a-Si:H	Amorphous hydrogenated silicon
ASTM	American Society for Testing and Materials
aTc	Accelerated thermal cycling
BAPV	Building applied photovoltaics
BB	Busbar
BIPV	Building integrated photovoltaic module
BNPI	Bifacial nameplate irradiance
BOM	Bill of Materials
BOS	Balance of System
BPR	Bypass diode thermal runaway
BPT	Bypass diode temperature
BSI	Bifacial stress irradiance
CAPEX	Capital expenditure
C-AST	Combined and Accelerated Stress Testing
CdTe	Cadmium-telluride
CIGS	Copper indium gallium selenide
CPC	Coating/PET/coating backsheet
CPO	Co-extruded polypropylene backsheet
CPR	Construction products regulation
c-Si	Crystalline silicon
DH	Damp heat
DIC	Digital image correlation

DMA	Dynamical mechanical analysis
DML	Dynamic Mechanical Load test
DSC	Differential scanning calorimetry
ECA	Electrically conductive adhesive
EL	Electroluminescence
EN	European standard
ETFE	Ethylene tetrafluoroethylene
EU	European union
EVA	Ethylene-vinyl acetate
FDIS	Final draft international standard
FEVE	Fluoroethylene vinyl ether
FF	Fill factor
FWC	Foil wire assembly
GB	Glass backsheet
GG	Glass-glass
HF	Humidity-freeze test
IBC	Interdigitated back contact
ICA	Isotropic conductive adhesive
IEA	International energy agency
IEC	International energy commission
IEC CO	IEC central office
IEC SMB	IEC standardization management board
IEC TC	IEC technical committee
IEC TR	IEC technical report
IR	Infrared
ITO	Indium tin oxide
JPL	Jet Propulsion Laboratory
KPE	PVDF/PET/polyolefin backsheet
KPK	PVDF/PET/PVDF backsheet
LC	Longitudinal crack
LED	Light emitting diode
LCOE	Levelized cost of electricity
LDPE	Low-density polyethylene

LeTID	Light and elevated temperature induced degradation
LID	Light induced degradation
MBB	Multi busbar
mDH	Modified damp heat
MENA	Middle East and North Africa
ML	Mechanical lad test
MMC	Metal matrix composite
µ-PCD	Microwave detected photo conductance decay
MQT	Module quality test
MST	Module safety test
MWCNT	Multi-walled carbon nanotube
NIR	Near infrared
nZEB	Nearly zero energy building
PA	Polyamide
PC	Polycarbonate
PDMS	Polydimethylsiloxane
PE	Polyethylene
PEF	Product environmental footprint
PERC	Passivated emitter and rear solar cell
PERT	Passivated emitter rear totally diffused solar cell
PET	Polyethylene terephthalate
PID	Potential induced degradation
PO	Polyolefin
POE	Polyolefin elastomer
PP	Polypropylene
PPE	PET/PET/Polyolefin backsheet
PV	Photovoltaic
PVB	Polyvinyl butyral
PVDF	Polyvinyl difluoride
PVF	Polyvinyl fluoride
PVQAT	International PV Quality Assurance Task Force
QSSPC	Quasi-steady-state photoconductance
RACK	Resistance across cleaves and cracks

R&D	Research and development
RH	Relative humidity
SAM	Scanning acoustic microscopy
SC	Squared crack
SGS	Solar grade silicon
SHJ	Silicon heterojunction cells
SLP	Service life prediction
S-N	Cycling stress (S) against the cycles to failure (N)
SQTW	Solar quantum efficiency weighted transmission
SWCT™	Smartwire Connection Technology
TC	Thermal cycling
TCO	Transparent conductive oxide
TPE	PVF/PET/polyolefin backsheet
TPO	Thermoplastic polyolefin
TPT	PVF/PET/PVF backsheet
TPX	PVF/PET backsheet
UV	Ultraviolet
VAc	Vinyl acetate content
WVTR	Water vapor transmission rate
XML	Extensible markup language
YI	Yellowness index

EXECUTIVE SUMMARY

In the last decade and longer, photovoltaic module manufacturers have experienced a rapidly growing market along with a dramatic decrease in module prices. Such cost pressures have resulted in a drive to develop and implement new module designs, which either increase performance and/or lifetime of the modules or decrease the cost to produce them. Many of these innovations include the use of new and novel materials in place of more conventional materials or designs. As a result, modules are being produced and sold without a long-term understanding about the performance and reliability of these new materials. This presents a technology risk for the industry.

This report provides a global survey from IEA PVPS member countries of efforts being made to design new materials for photovoltaic cell and module applications. The report is organized by module component and includes reviews of material innovations being made in: (1) frontsheets, (2) encapsulants, (3) backsheets, (4) cell metallization, and (5) cell interconnects. Section 1 is an introduction. Section 2 presents the state of the art in PV module materials including the functional requirements of each component and the common materials typically used to meet these requirements. Section 3 discusses the motivations for applying new material solutions to PV modules. Section 4 presents the global survey of novel material solutions being developed and tested for the next generation of PV modules.

There are several motivations for investigating new materials for PV modules. Reducing or replacing expensive materials is important for the overall economics of module production. For example, reducing the use of or replacing silver with copper or aluminum leads to a significant cost reduction for manufacturers. Another example is using thinner glass for top sheets or converting from more expensive PVF to less expensive PVDF materials for backsheets. Accelerating the manufacturing process is another way to decrease production costs. Lamination is typically the slowest step in a module production line and manufacturers are very interested in materials that can speed up this process step. For example, fast or ultra-fast cure EVA encapsulants have reduced the time needed for crosslinking from 25 min to 10 min today. Converting to thermoplastic encapsulants, which do not crosslink, may help reduce these times even further. Increasing performance is an obvious motivation for material innovations. This can be achieved with increasing the number of busbars, increasing the active area by using shingling, or increasing light absorption using anti-reflective coatings, or increasing internal reflections with highly reflective backsheets or white templates between cells. The trend to increasing wafer size also leads to performance gains. Making modules more sustainable is another strong motivating factor. Life Cycle Assessment (LCA) is a methodology to quantify the environmental impact of a product. Some manufacturers seek recognition of ecologically responsible material choices by using various labeling standards to identify good sustainability practices.

A survey of the PV manufacturing industry today shows that there are clear trends in material improvements. Crystalline silicon wafer sizes are projected to continue to increase over time as silicon production improves and results in larger mono-crystals that can reach 300 mm in diameter. Cell sizes are expected to increase up to 210 x 210 mm² (M12) in the next several years. New cell interconnection methods are moving to production lines. Manufacturers are instead trying lead-free solder based on bismuth, ECAs, or smart-wire technology. Back contact cells (IBC, MWT, etc.) allow the use of conductive backsheets to interconnect cells. This approach has the advantage of minimizing cell warpage and stress on interconnects due to

fact that busbars do not need to cross from the back to the front of the cells, which results in a much flatter package design.

Less developed ideas for module improvement include modules designed for specific climates (e.g., desert, tropical, arctic, high wind or snow loads) or environments (i.e., floating, agriculture). Modules for building integrated applications typically value aesthetic properties as much as or more than energy production. For roof-mounted PV modules, weight can be a limiting factor for deployments. Concepts for making lightweight modules using ultrathin glass and glass-fibre reinforced composite structures or support lattices are being investigated. Vehicle integrated PV requires curved modules, which likely will require materials innovations.

The process of material innovation for PV is further complicated by the complex interactions within a PV module. The advantage of one material may be outweighed by its interaction with another component. For example, EVA is inexpensive and highly effective for encapsulation, however it degrades to form acetic acid which can cause corrosion of the metallization if it is not allowed to escape the module package due to use of an impermeable backsheet. New materials must work within the whole module package and in concert with the other materials present. Consumers and manufacturers rely on international standards, such as those from Technical Committee “Solar Photovoltaic Energy Systems” TC 82 to ensure that new materials do not result in unexpected performance or reliability problems. Another issue is that module manufacturers do not typically advertise their bill of materials (BOM) and the BOM for a particular module model can vary depending on when and where it was made. There exist several nondestructive methods to characterize and identify module materials including FTIR, NIR and Raman spectroscopy.

Frontsheets: PV module frontsheets provide transparency for incoming light, structural protection of the solar cells, electrical insulation and a barrier for moisture and oxygen ingress. While low iron float glass is the most common material used in PV modules, it is heavy, requires tempering for safety, and sometimes presents adhesion problems that can lead to delamination. Frontsheets also typically include anti-reflective and anti-soiling coatings.

Innovations discussed in the area of frontsheets include the use of thinner glass, flexible polymeric materials, and abrasion resistant coatings. Innovations in ultra-thin glass include (1) very low iron contents (100 ppm) that reduces optical absorption, (2) advances in surface texturing, (3) thicknesses between 1.6 mm and 3.2 mm, (4) use of clean room coating step and (5) advances in tempering to reduce built in stresses. The aim is to increase transmission and bending strength while using less material. Fifteen varieties of polymeric frontsheet materials are compared for cost and UV durability. ETFE and PVDF materials have the highest cost while PET based materials have medium to low costs in comparison. Loss in transmission following UV exposure shows a large variability depending on the material. Anti-reflective and anti-soiling coatings can increase performance but there is concern about the durability of these coatings over time. Results of abrasion testing done on various coatings is presented.

Encapsulants: Polymers are used to encapsulate the interconnected strings of PV cells and metal busbars between the frontsheet material and the backsheet. The functional requirements of this component include protection of the cells and metallization from moisture and other environmental contaminates, provide and maintain electrical insulation, and provide adhesion and support between the layered components of the modules. The encapsulant material in front of the cell typically differs slightly in composition from that used on the back side of the cells. The front layer typically is transparent to UV in order to increase light absorption by the cells and UV absorbing in the back layer to protect the backsheet from aging. Ethylene vinyl acetate (EVA) is the most widely used material in PV modules but there is a concern about

using this material in glass-glass modules, where diffusion rates are low, since EVA can generate acetic acid as the result of a photolytic degradation reaction. Recently various polyolefin (PO) elastomers and thermoplastic elastomers (POE and TPO, respectively) are being used for PV modules, especially glass-glass designs. Other materials such as ionomers, polyvinyl butyral (PVB) and silicones are also being considered and used sometimes.

Innovations discussed in the area of encapsulants include the increasing use of POE and TPO materials instead of EVA. The results of accelerated aging tests comparing TPO, POE and EVA samples show mixed results with some studies reporting TPO and POE samples performing better than EVA and others not. It may be that performance differences may depend as much on the additives added to the bulk material (e.g. UV absorbers) than the specific material used. Recent innovations have resulted in the production of silicone encapsulants in the form of sheets designed to be laminated using conventional equipment. Silicone has been used as a PV encapsulant for especially high reliability applications, but the material has typically had to be applied as a liquid resulting in high costs. Silicone encapsulated modules can survive DH6000 without any signs of corrosion unlike EVA modules cannot.

Cells and cell interconnects: Commercial PV cells come in a variety of different types including Si-wafer based technologies (c-Si), thin films (e.g., CdTe, amorphous silicon, and copper indium gallium selenide (CIGS). Currently most PV modules are made from c-Si cells (e.g., Al-BSF, PERC, IBC, HIT, PERT, etc.). C-Si cells are interconnected in series to raise voltage and lower resistive losses. Conventional interconnection involves connecting metal ribbons or wires to the cells using solder bonds or electrically conductive adhesives (ECA).

Innovations discussed in the area of cell-interconnects include multiwire and low temperature solders, electrically conductive adhesives and advances in cell metallization. The current trend in c-Si PV cell interconnection is to increase the number of busbars while reducing their width in order to reduce the amount of silver for the cell metallization and increase the module efficiency. This has led to cells with front metallization schemes without busbars, referred as busbar-less cells interconnected by means of multi wires. Electrical connection is made during lamination, which avoids the high temperatures required for soldering. This technology has reduced silver usage in modules by as much as 40% compared with a standard 4BB soldered ribbon design. Multiwire interconnection results in less cell cracking, less shading, greater internal reflections and more interconnection points resulting in better performance of modules with cracked cells. Electrically conductive adhesives are composite materials based on a conductive filler and an insulating polymeric adhesive. They are being considered for use in place of solder (e.g., ribbon-based interconnection) for new designs (e.g., shingled) and for attaching conductive backsheets to PV cells. Research is being made on the thermomechanical properties and performance of ECAs in modules. Early results suggest that the use of ECAs can reduce the stress on PV cells compared with soldering. However, there is a wide variety in formulations of available ECAs and differences in performance may partially reflect these differences. Researchers in the US are working to develop a new metal paste formulation designed to be less susceptible to power loss from cell cracks. They have shown that by adding carbon nanotubes to the silver paste used for cell metallization, they can create cells that continue to function normally even when cracked. They have shown that the carbon nanotubes can bridge crack widths up to 70 µm. In addition, even when the cracks resulted in loss of electrical continuity, they were shown to “heal” as thermal and mechanical stresses lessened.

Backsheets: Backsheet materials serve to protect the cells and metallization from moisture and environmental contaminants such as dirt, salt, acids, etc. They also must provide electrical insulation and sometimes even mechanical stability. Multilayered polymeric films are a popular choice as PV backsheet materials. But recently with the market growth in bifacial PV, glass is

also becoming a popular backsheet material. Polymer backsheets come in a variety of different materials including polyvinyl fluoride (PVF), polyethylene terephthalate (PET), low density polyethylene (LDPE), polyvinylidene fluoride (PVDF), polyamide (PA) and polypropylene (PP). Backsheet manufacturers also layer different materials and supply commercial names such as TPT (Tedlar-PET from DuPont).

Innovations discussed in the area of backsheets include development of co-extruded backsheets and transparent backsheets. Co-extrusion has better thickness control, reduced processing steps, and allows expensive fluoropolymers (PVF, PVDF) to be replaced by less costly polymers (PET, PA, PP, PE derivatives). Early examples of co-extruded backsheets were made of layers of PA and experienced cracking failures in the field. More recently, co-extruded backsheets made of PE, PO, and PP have been developed. It is too early for extensive field results, but early accelerated tests are promising. Transparent backsheets made of PVF have been available from DuPont for over 20 years and used in BIPV applications. More recently a new formulation has been developed that is designed to be resistant to UV damage and last for over 20 years. One of the main applications of this would be for bifacial modules in order to reduce the weight and other process complexities of glass-glass modules. In addition, development of transparent backsheets should further advance the development of polymeric frontsheets since both require UV durability.

Lightweight modules: A typical PV module weighs about 12 kg/m^2. Making modules lighter makes sense as it would decrease shipping and installation costs and open up new application spaces such as large buildings with limits on the load bearing capacity of their roofs. There are several examples of certified lightweight and flexible thin film solar modules with weights as low as 2 kg/m^2 that need to be bonded directly to a flat roof. Research is also being done to design standalone lightweight modules using a glass-backsheet designs along with a lightweight lattice and beam structure. Early prototypes have achieved 8 kg/m^2.

1 INTRODUCTION

Over the past decade there has been an enormous growth in the production capacity of PV modules worldwide: in 2019 an estimated 120 to 140 GW of PV was produced [1]. With significantly increasing production capacity, PV module prices have fallen dramatically. The current PV market shows an extremely high cost pressure, which is also the driving factor for the development and implementation of new module designs and the use of new materials and components. New technologies, which promise either higher efficiency for the same cost or cost reduction at same efficiency, are very often quickly introduced to the market [2]. With current production capacities, many Gigawatts of modules with new technologies and materials can be produced and installed without having sufficient experience about long term reliability. In the worst case this has led to unexpected degradation mechanisms several years after field deployment, which were not predicted in laboratory accelerated testing, such as Potential Induced Degradation (PID) [3], Light and elevated Temperature Induced Degradation (LeTID) [4, 5] or backsheet cracking [6, 7].

The main objectives of this report are to provide a global survey of technical efforts aimed at lowering cost and increasing performance and reliability of PV modules by employing new designs, materials and concepts. The report aims to (1) increase the exchange of information about promising materials, design concepts, (2) provide the means for increasing the value of PV modules, (3) provide recommendations on characterization methods for new technologies and (4) give input regarding new requirements for standardization.

In recent years a special focus was given to materials with specific functional properties like selective optical transmission or absorption or permeation properties. The properties and benefits of such materials and their expected lifetimes as well as interactions with other module components and different climates is of great interest. This report will summarize the state of the art in PV materials and introduce readers to the efforts being made internationally to improve PV modules so that eventually they will perform better and last longer in the field.

The report focuses on recent developments in the following PV module components:

- Frontsheet
- Encapsulant
- Backsheet
- Cell metallization
- Cell interconnection

The report does not claim to give a complete overview on all ongoing developments regarding new PV module materials and components. Instead it provides selected summaries of results on materials development activities and durability testing from IEA-PVPS member countries.

2 STATE OF THE ART IN PV MODULE MATERIALS AND TECHNOLOGY

The general architecture of modern crystalline silicon wafer based PV modules was developed in the late 1970s and early 1980s within the Flat-Plate Solar Array Project and has not significantly changed since then [8]. A 2020 standard PV module consists of a number of interconnected solar cells encapsulated by a polymer (encapsulant) and covered on the frontside by glass and at the rear by a polymeric backsheet into a long-lasting multi-material composite. In most cases this panel is surrounded by a frame providing the necessary structural support and means for module mounting. The actual module architecture has a layered encapsulation structure designed to protect the solar cells and their interconnecting wires from the harsh environment in which they are typically used.

Despite most PV modules being constructed according to this rather standardized composition in layers, PV modules can come in a variety of different form factors and designs using a range of different materials. To enable such variability, the fundamental functional requirements for the materials have to be well understood.

The primary objective of a PV module is to convert as much irradiation into electricity as possible. To achieve this goal, on the one hand high transmission of sunlight to the solar cells is required while on the other hand the optical and electrical components need to be protected from damage from chemical stressors such as water, corrosive gases, oxygen and from thermal and mechanical stresses for at least 25 years. In order to be successful in the market, these ambitious objectives must be accomplished using low cost materials and high volume manufacturing processes. In the following, we provide an overview of (i) the current state of the art in module materials, (ii) their role within the module and principal requirements, (iii) guidelines for material selection, and (iv) suggest opportunities for improvements.

2.1 Frontsheets and coatings

Frontsheets usually serve at least four functions: (1) transparency for incoming light, (2) structural protection and support of the solar cells, (3) electrical insulation and (4) barrier for moisture and oxygen ingress.

The most common material used for PV module frontsheets is low iron (<120 ppm Fe) float glass. Functional coatings are added to the surfaces of the glass to increase light adsorption (anti-reflective coatings) and/or to reduce the accumulation of dirt and debris on the module in the field (anti-soiling coatings).

Anti-reflective coatings (ARC) operate on the principle of trying to match the refractive indices at the interface of the adjoining materials. For a glass front sheet, the ideal single-layer ARC would have a refractive index of ~1.2 to 1.3 (geometric mean of the refractive indices of glass (~1.5) and air (~1)) and a thickness of about 100 nm (~1/4 of the wavelength of light, which promotes destructive interference of reflected light). While there are other more complex ARCs such as multilayer or graded index coatings, these are generally too expensive for PV module applications.

2.2 Encapsulants

Encapsulants must perform several key roles including: (1) protect cells and metallization from water and other environmental chemicals, (2) maintain electrical insulation, (3) provide adhesion between layers of the laminate, and (4) provide high transparency of irradiation for PV-relevant wavelengths (e.g. for c-Si cells 300 to 1200 nm) over many years [9]. In addition, it is desired that the encapsulant is available in sheet or roll form prior to lamination in order to be easily integrated into the module manufacturing process.

Key technical specifications of encapsulants include:

- Melting temperature,
- Volume resistivity,
- Moisture transmission rate,
- Light absorption,
- Young's modulus,
- Glass transition temperature,
- Breathability/ diffusion rates.

There are a few common polymer materials that are generally used as encapsulants in PV modules. Their chemical structure and main characteristics can be seen in Figure 1 and Figure 2, respectively.

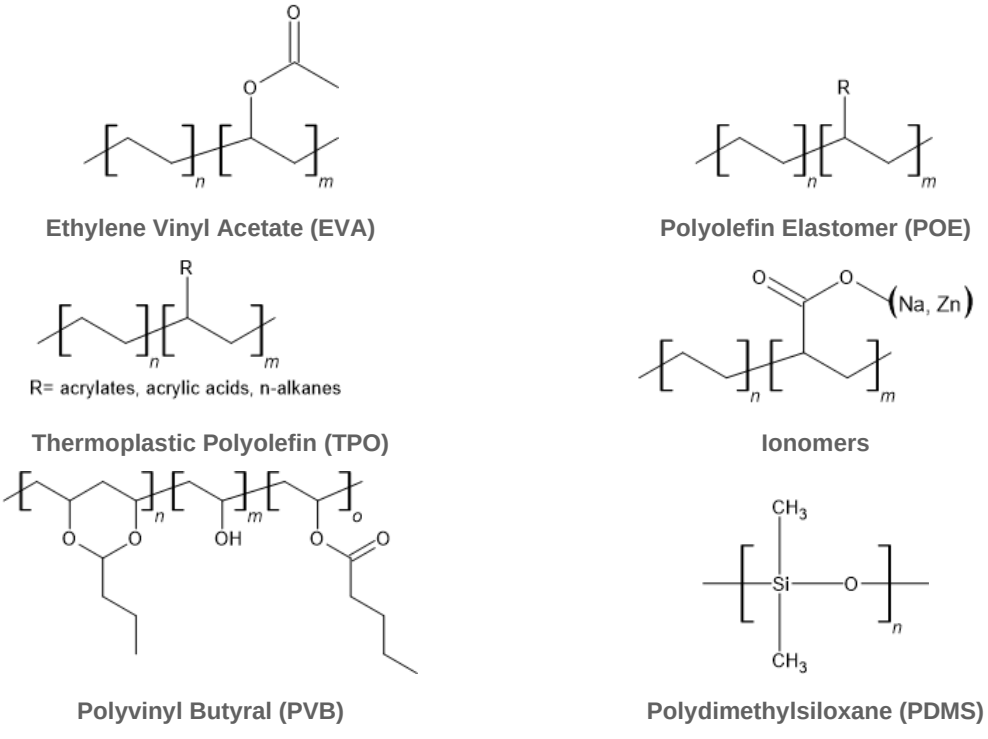

Figure 1: Chemical structure of encapsulant materials used in PV.

- Poly(ethylene-co-vinyl acetate) (EVA) is the most widely used material. It is a copolymer of ethylene and vinyl acetate units, generally with a vinyl acetate weight percentage between 27 % and 33 % [10]. Nowadays, EVA is the state of the art encapsulant used in PV and its reliability has been extensively studied over the years. The main drawback of using

EVA is the production of acetic acid due to the effect of high temperature and photo-oxidation processes.

- Polyolefin (PO) elastomers and thermoplastic elastomers (POE and TPO, respectively) are recently developed encapsulation materials which show higher transmittance and higher chemical inertness than EVA (no hydrolysis and no acetic acid formation). Additionally, POE encapsulants are less prone to develop PID [11, 12]. POE and TPO are currently not considered as state of the art encapsulants because their use is rather limited. Nevertheless, they are very promising materials that might replace EVA. More details regarding reliability of these encapsulants will be given in Chapter 4.
- Ionomers exhibit very low water vapor transmission rate (WVTR) and are thus often used for the protection of humidity sensitive thin film materials [13]. Ionomers show lower susceptibility to PID and higher resistance to discoloration than EVA, but also lower adhesion to the glass and to the cell surface [14].
- Poly vinyl butyral (PVB) is a thermoplastic resin mostly used for applications requiring strong binding, toughness and flexibility and is thus preferentially used in glass/glass modules for BIPV applications [15, 16]. The downside of using PVB is that the material is very susceptible to hydrolysis because of very high water uptake [17].
- Silicones (curing and non-curing systems) are chemically inert and therefore show very good reliability; have been used in the past but are not popular currently due to high price and difficult lamination [18, 19].

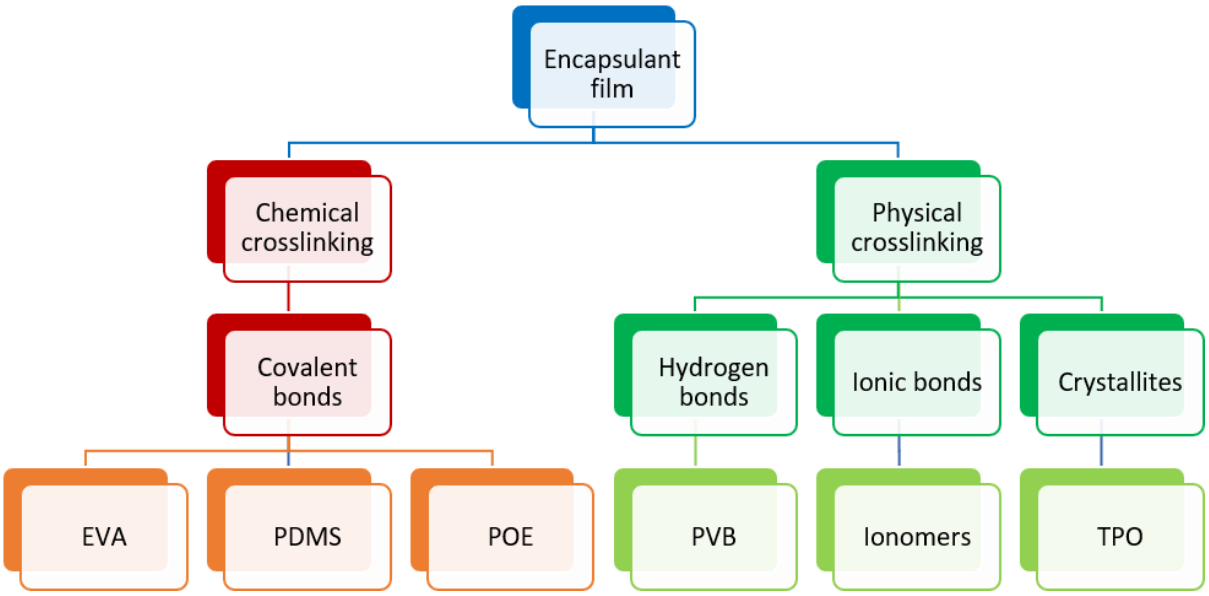

Figure 2: Typical encapsulants and their main characteristics.

In practice, these encapsulants are augmented with additives such as UV-stabilizers, UV absorbers, anti-oxidants (free radical scavengers), crosslinking agents, and adhesion promoters [10]. Recently, PV modules with different additive composition of the front and back encapsulant are fabricated: the back encapsulant includes additives to protect the backsheet from irradiation, while the front encapsulant has UV-absorbers with lower cut-off in order to maximize the throughput of irradiation in the high energy region (UV) to the solar cells.

Typical properties of encapsulants used in PV are listed in Table 1.

Table 1: Properties of PV encapsulants [11, 12, 15, 20–24].

Encapsulant	Polymer type	Glass Transition Temperature	Processing Temperature	Volume Resistivity	WVTR	Young's modulus	Refractive index (n)
		°C	°C	Ω*cm	$g*m^{-2}*day^{-1}$	MPa	-
EVA	Elastomer	-40 to 34	140to 160	10^{14}	34	≤ 68	1.49
POE	Elastomer	-50 to -40	140 to160	10^{15} to 10^{16}	3.30	≤ 30	1.49
PDMS	Elastomer	≤ -100	80 (vacuum process)	10^{14} to 10^{15}	130 to 200	≤ 10	1.38 to 1.58
PVB	Thermo-plastic	-12 to +20	140 to 160	10^{10} to 10^{12}	40.05	≤ 11	1.48
Iono-mer	Thermo-plastic	-40 to -50	140 to 160	10^{16}	0.19	≤ 300	1.49
TPO	Thermo-plastic elastomer	-60 to -40	140 to 160	10^{14}-10^{18}	2.85	≤ 32	1.48

2.3 Cells and cell interconnects

Si-wafer based technology is currently the market share leader. It produces about 95% of the total photovoltaic energy in 2019, whereas thin films produce the remaining 5 % [25].

The three major thin films technologies include: cadmium telluride (CdTe), amorphous silicon, and copper indium gallium selenide (CIGS), among which CdTe technologies share about 4% of the total market [25]. Thin films are especially used in BIPV and amorphous silicon solar cells are mostly used in consumer electronics, such as calculators, watches and so on [26]. The advantage of using thin films is mainly economic because of the very low amount of active material used, higher shading tolerance and the possibility to build flexible modules. But thin films have lower efficiencies compared to c-Si based technologies. Additionally, the materials used are often toxic or not easily available [26, 27].

The focus of this report is on Si-wafer based technologies, as they represent the most widespread technology. PERC solar cells have quickly gained prominence in the PV market due to improved efficiency in comparison to Al-BSF cells. Some of the major advantages of using PERC include reduced rear-surface recombination and enhanced rear-surface reflectivity. According to the International Technology Roadmap for PV, in 2017, the market share of PERC was about 20% but is expected to be greater than 50% after 2020 [28].

Crystalline Si cells are connected via electrically conductive metallic ribbons or wires mainly made of copper (Cu) or silver (Ag). These metallic connectors are adhered to the cells either via solder bonds (typically with tin-lead solders or lead free systems) or electrically conductive adhesive (ECA) with a polymeric base material and µm-scale Ag-particles to achieve the re-

quired conductivity [29]. The recently very popular Smart Wire [30, 31], multi-wire [32, 33] technologies use thin metal wires (200 to 300 µm in diameter) while shingling interconnection [34, 35] uses ECA directly applied to glue the top edge of one cell to the bottom edge of the adjacent cell. These new interconnection technologies allow for new module designs. More in-depth details regarding cell interconnections and metallization will be given in Chapter 4.

2.4 Backsheets

Standard PV modules use multilayer polymeric or glass backsheets to protect the rear side. Backsheets have to provide protection from environmental stressors like (1) UV radiation, (2) humidity and vapor penetration, and (3) dryness, wind, dust, sand, and chemicals (e.g., salt, pollution). Furthermore, the backsheet has to ensure total electrical insulation of the PV panel and provide mechanical support. In addition, the color (reflectivity) of the backsheet can influence and contribute to increased internal reflections that result in higher efficiency and affect module operating temperatures.

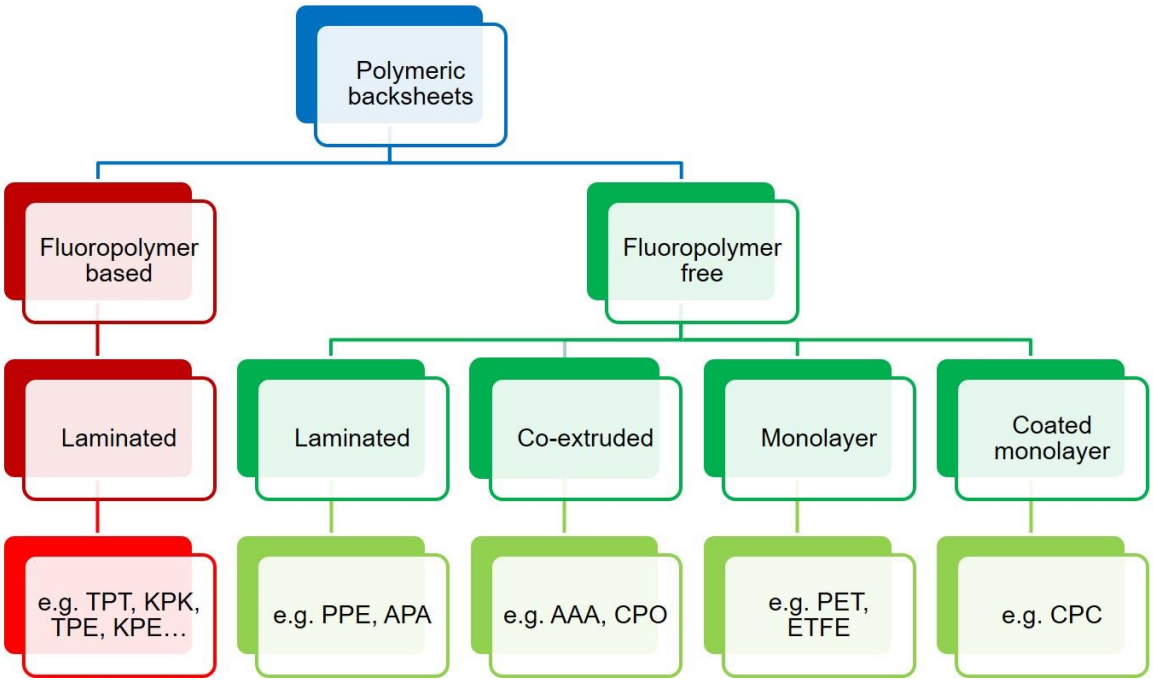

Figure 3: Typical backsheet types and their layer structure.

Some common polymer materials used for multi-layer backsheets include:

- Polyvinyl fluoride (PVF): very reliable and stable against environmental impacts (inert); Used extensively and has a proven track record. The commercial name from DuPont for this material is Tedlar. DuPont uses this material in a layered laminated film of Tedlar-PET - Tedlar or TPT [36].
- Polyethylene terephthalate (PET): high mechanical strength and electrical resistivity; is used as the inner core of most backsheet stacks; hydrolysis-stabilized PET can also be used as outer layer and laminated to a PET core; low cost monolayer PET-backsheets also exist in the market [37].
- Low density Polyethylene (LDPE) or EVA: provides good adhesion to the encapsulant; used as an inner layer material (Tie-layer).
- Polyvinylidene fluoride (PVDF): good stability against environmental impact; used as an outer layer; known ageing problems such as yellowing, cracking, and delamination.

- Polyamide (PA): developed as fluoropolymer free alternative for the outer and inner layer (laminated to a PET core); a coextruded 3-layer all PA-backsheet entered the market ~2010 but disappeared 5 years later, as it suffered from shrinkage and associated cracking after several years in the field [7, 38, 39].
- Polypropylene (PP): new material in the backsheet production; co-extruded all polyolefin 3-layer backsheets are available; fluoropolymer free, sustainable material, good chemical stability [40]. More information regarding reliability of co-extruded PP backsheets will be given in Chapter 4.

2.5 Junction boxes and connectors

PV modules consisting of polymer and glass plates surrounding the electricity conducting parts (cell, connectors and wiring) need to be equipped with components that allow for safe transport of the produced electricity from the panel to the inverter. The wires are backed out of the module and fixed in a polymeric junction box which is mounted at the backsheet via an adhesive (mostly polysiloxane-type) [41]. The junction box contains the electrical connection to the cabling and the bypass diodes [42]. The boxes are filled either with a protective polymer (potting material, mostly transparent silicone resin) or under air. Junction boxes for current PV modules are divided into three part, each part is equipped with a bypass diode and the both outer boxes include the plus and minus wire of the module. PV modules use as quasi-standard MC4 connectors which design is copied by many manufactures.

2.6 Module frame

Some PV modules are mounted without frames, but most of them are protected with an aluminum frame, which is connected to the panel via an adhesive (mostly polysiloxane) or an adhesive tape. With respect to the ingress of moisture into the encapsulant, the adhesive layer and the framing provide an additional diffusion barrier [42]. The frame allows for easier mounting and racking on the supporting structure in the field and protects the glass edges from breakage. The frame is also used as grounding connection depending on local regulations.

3 MOTIVATION, BENEFITS, AND OPPORTUNITIES FOR NEW MATERIAL & MODULE DEVELOPMENTS

3.1 Decrease of LCOE: Cost reduction and performance improvement

Over the past few decades, PV module prices have fallen dramatically, following a price-experience curve (learning curve) with an average learning rate of about 80%, i.e. the average selling price of PV modules fell by 20 % for each doubling of production volume. This development was driven not only by technological improvements but also by changed market conditions [1]. Economy of scale was one of the major driving forces of the falling prices, i.e. the huge expansion of production capacities, not only for PV modules but also for all components and materials in the value chain. Furthermore, advances in manufacturing technology and material science had a significant impact on price reduction. In the following sections, several strategies applied in order to achieve these historical cost reductions are listed:

3.1.1 Reduction and replacement of expensive materials

One approach to lower PV module prices is reduction and/or replacement of expensive materials. The silicon solar cell was and still is the most expensive component of a c-Si PV module, with the silicon wafer accounting for half of the cells price [2]. The thickness of solar cells was reduced from over 300 µm in the early 2000s down to 180 µm in 2020. Further reduction to thicknesses to between 140 and 160 µm is foreseen in the next decade, depending on the wafer technology [2].

Also, the amount of silver used in c-Si based PV modules was reduced from 400 mg to 130 mg between 2007 and 2016 by reducing the metal finger width and the busbar area on the cells. The minimum amount of silver needed to ensure current transport within the conductive system is predicted to be almost halved in the next years to approximately 65 mg by 2028. However, a replacement by non-silver-based solar cell metallization solutions is not expected to gain significant market share in the next decade [43].

Tthe last few years has seen a reduction in the front glass thickness from 3.2 mm and higher down to values between 2 mm and 3 mm [2].

PV backsheet technology changed significantly in the last 20 years. In the early 2000s more than 85% of the backsheets used were so-called “Tedlar” (TPT) backsheets, with a Polyester core layer and inner/outer layers made from PVF [44]. Since then manufacturers are moving to replace the comparably expensive PVF films with more economical fluoropolymers like PVDF or other, fluorine-free, technical polymers like PET, PA or PE derivates [45]. In 2010 co-extruded backsheet-types were introduced into the market, based on commodity polymers like PP, PE and PA [40, 45].

3.1.2 Acceleration of manufacturing processes

The acceleration of the time-consuming PV module lamination process has been a major focus in technology development over the years. The main approach was a reduction of the cross-linking time via adaption of the encapsulant material formulation. Initially, standard cure EVA types needed up to 25 min for the crosslinking reaction [9]. With fast cure and ultra-fast cure

types the crosslinking time was reduced down to 10 min [9, 46–48]. Alternatively, also thermoplastic encapsulants have been developed, where no crosslinking is needed and the total lamination time was reduced to 10 min [49].

3.1.3 Performance increase

Many new materials and components have been developed to achieve a performance increase. When looking at cell interconnection technologies, a transition from three busbars to layouts with up to 12 busbars can be seen. Also busbar-less technologies like the “Smart Wire Interconnection” are on the rise [2, 30, 50]. The increased number of busbars aims to reduce resistive losses by reducing the amount of current that flows in both, the fingers and the busbars. Additionally, also cell shading is reduced and it coincides with additional reduction of the silver content [2]. Also new approaches like shingling of partial cells aim at increasing the active area and therefore the power output per area while reducing the resistive losses [34].

Many developments aim at improving or better matching the optical properties of the components allowing an increased number of photons to reach the solar cells. Encapsulant films with new additive formulations allow for transparency in the UV region of the incoming light, resulting in an increased power output of up to 0.5 % [49, 51, 52]. Similar effects can be achieved using highly reflective backsheets that act as a diffuse mirror and lead to backscattering of light to the cells [40]. Antireflective coatings for improving the transmission of the front glass have become state of the art in recent years, even though that the average service life of these coatings needs to be increased [53].

3.1.4 Production related cost decrease

One important driver for cost reduction since about 2018 is the increase of wafer size. The wafer size increased from about 2008 with so called M0 size with 156^2 mm² to up to M12 with 210^2 mm² wafer technology starting in 2020. The increase in wafer size allows increasing the Wp output of PV manufacturing per year at nearly the same machine and fabrication area costs. Furthermore, the increase in Wp per PV modules reduces the LCOE costs as one needs fewer modules and cables for the same Wp PV system size.

3.2 Sustainability and legal regulations

Awareness regarding sustainability of products is increasing in general. Large deployment of PV installations over the past decade has raised concerns about the environmental impacts of its production and final disposal. Since PV is related to the delivery of renewable “green” energy, the expectation of customers on the sustainability of PV electricity is very high.

The impact of materials incorporated in PV modules on the ecological footprint of produced PV electricity is significant and twofold: First, there is the direct impact related to the material itself, including effects of production of the material, manufacturing related effects and recycling related effects. Second, there is an effect of the chosen materials on the lifetime and yield of modules and systems. Since the effect of lifetime and lifetime-yield on the ecological footprint of PV electricity is enormous, this also translates to the effects of materials and material quality. To analyse the effects of specific materials or material combinations, a Life Cycle Assessment (LCA) covering all the stages in the lifetime of a PV system has to be performed to identify hotspots of environmental burdens and specific effects and influences [54]. Such assessments also should include local (climatic) influences since they have strong effects on the

kWh output per Wp. LCA studies can also help to identify the suitability of materials and material combinations for specific applications, locations or module designs. The results illustrate the potential to further reduce the ecological footprint of PV power generation and to identify possible environmental problems during the PV systems life cycle.

Additionally, sustainability related PV legal regulations and rating systems are expected or have been introduced in several countries in recent years. Such instruments include national regulations such as the Product Environmental Footprint (PEF) as defined by the European Union or French tenders containing the Carbon Footprint of products. Further multi-national policies are under discussion in the European Union [55] at the moment including legally binding regulations, like “Eco Design” in the EU [56], which sets out minimum mandatory requirements to remove non-sustainable products. Another regulatory option is “Energy Labelling” which requires a clear statement regarding the energy related performance of a product [57]. Other possibilities being considered are systems to grant the most sustainable products in the market with a label like the EU “Eco Label” which aims at marking the best 20 % of the products in the market to support manufacturers producing sustainable products [58].

The sustainability and ecologic performance of PV materials is becoming more important and may soon be included in market regulations and standards. Information about calculation methods for sustainability assessments of PV systems as well as impact categories and effects of components and materials can be found in reports and publications of IEA PVPS Task 12.

3.3 New technological requirements

3.3.1 Crystalline silicon wafer – the cell substrate

Although this report mainly addresses packaging materials that are used in making the PV module, it is also relevant to reflect on the important developments in materials and performance related to the crystalline silicon wafer which constitutes the substrate of most solar cells today. The manufacturing sequence for crystalline silicon wafers can be divided into three steps, each of which has undergone significant changes during the last decade and thereby contributed to the observed overall cost reductions.

Silicon Feedstock

In 2000, the only source of feedstock for solar silicon wafers was scrap material from the semiconductor industry. Refinement processes for the hyper-pure silicon material were developed to enable the semiconductor industry. There the objective has been the manufacturing of integrated circuits with nanometre sized transistor elements, where the challenge is to avoid electrical defects (e.g. shunts) originating from impurities in the material. At that time the solar industry did not have such stringent purity requirements. Less expensive alternative processing routes for Solar Grade Silicon, (SGS; e.g. Upgraded Metallurgical Silicon) were developed and production capacities of up to 10.000 MT of SGS were established and in operation for several years. However, with process developments in heat recovery, CAPEX reductions, cost efficiency and productivity enhancement, new production capacities for high purity silicon feedstock have now been brought online in volumes of 30.000 – 40.000 MT per plant. This development has taken place mainly in China and located in areas where electricity is cheap. As a result of these process developments and cost-reductions, the world-wide production capacity for pure silicon feedstock has increased by a factor of 12 since year 2000, without compromising the product performance (purity) and still reducing the manufacturing cost by a factor of at least four (from around 30 USD/kg to less than 7 USD/kg in 2020) [59].

Crystallisation

Although the silicon feedstock comes with purity more than sufficient for solar cells, the brittleness of this material made of many micrometre sized crystals, precludes its direct use as a substrate for solar cell manufacturing. First, the material has to be melted and re-crystallised under controlled conditions to generate larger crystal grains, which also ensure that no (or few) grain boundaries and crystalline defects such as point-, line-, 2D- or bulk features are present, which may act as recombination centres and limit the solar cell performance.

The technology from the semiconductor industry is able to grow mono-crystals up to 300 mm in diameter and more than 200 kg in weight has been transferred to the PV industry and demonstrated capability to obtain solar cell efficiency close to the theoretical upper limit. A simpler and more cost-efficient casting method capable of making multi-crystalline ingots with cm-sized monocrystalline grains, has also been developed and for many years coexisted in the same commercial space [60]. Until recently, the most common solar cell has been based on the Aluminium back surface field (Al-BSF) architecture.

With today's cell architectures being dominated by cells as PERC, PERT and Topcon variants, it has become evident that multi-crystalline wafers cannot ensure the same level of cell performance as a monocrystalline counterpart. A very fast transition of wafer base towards monocrystalline products is therefore predicted. The most important functional performance parameters of crystalline ingots produced for the PV industry are purity (low level of contamination with impurities into the molten silicon during the crystallisation process), lack of crystalline defects (e.g. B-O complexes which will lead to Light Induced Degradation) and stress-control through temperature gradient control while cooling the crystal from the melting temperature. The most important quality assurance characterisation parameter of the silicon ingots is the minority carrier lifetime, as determined by the quasi steady state photoconductivity (QSSPC) or microwave detected photoconductive decay (µ-PCD) methods.

Wafering

In the early days of the PV industry, the silicon ingots were sliced into 0.3 mm thick round silicon wafers by use of an inner diameter saw, one at a time. Today wafers are sliced to a thickness of 0.18 mm by use of wire saws, where the steel wires are diamond coated by use of electroplated nickel and water is used as a cooling media. This process is about to fully replace the alternative wire cutting method that was developed for the solar industry in the late 90s which made use of brass wires and an abrasive grit made from silicon carbide particles and Polyethylene Glycol as cooling media.

The wafer thickness is mostly determined by the solar cell manufacturing specifications, as the wire saw can easily cut even thinner wafers. Thinner wafers however, will become ductile and cannot as easily be transported between cell process steps and inserted into cassettes. After the cutting process wafers are cleaned in a wet chemical process, which also removes saw damage and subsurface micro cracks in order to enhance the optical performance of the finished cell [61, 62].

For many years, the standard size of both, mono- and multi-crystalline wafers were the same (wafer side length of 156 mm being the most common), which also facilitated full flexibility among wafers in use between cell processing equipment. Within the last few years, this consensus on wafer size has been challenged by major Chinese wafer, cell and module manufacturers. More efficient cells mean that higher currents are generated per solar cell. Therefore, a simple method to limit the current and related electrical loss is to cut the cell into half and double the amount of half-cells per electrical string within the module. Once this new concept of divided cells became viable, the opportunity for dividing cells into 1/3 or even 1/4 is possible, which also allows for wafers much larger than today's common size of 156 mm^2 x 156 mm^2.

Currently many new sizes are being promoted: with examples ranging from 156.75 mm^2 x 156.75 mm^2 @ Ø 205 mm; 166 mm^2 x 166 mm^2 @ Ø 223 mm or 182 mm^2 x 182 mm^2 promoted by LONGi or the even bigger by Kwafoo 210 mm^2 x 210 mm^2 @ Ø 295 mm wafer promoted by Zhonghuan Semiconductor [63]. In Table 2 are summarised the evolution of the wafer size as well as effective wafer size area from M0 to M12 [64].

Table 2: Wafer size development from M0 to M12 [64].

Cell Name	Wafer size	Effective wafer size area
	mm	mm^2
M0	156	24092
M1	156.75	24383
M2	156.75	24426
M3	158.75	24991
G1	158.75	25199
M4	161.70	25805
M5	165	26726
M6	166	27410
M8	185	34212
M9	192	36862
M10	200	39997
M12	210	44096

The most important functional performance parameters of wafers to be used in the PV industry are surface morphology and subsurface damage to the crystal, geometrical parameters such as total thickness variation, bow & taper and internal stress and fracture strength.

3.3.2 New cell and interconnection technologies

New cell architectures often require new cell interconnection approaches. As a consequence, interactions between encapsulation and connecting wires/ribbons also must be considered (e.g., thermo-mechanical stresses imposed by the encapsulant as well as chemical interactions or incompatibilities, causing corrosion or discoloration [65, 66]). In general, it is of primary interest to investigate the effect of packaging materials on the type of cell technologies, e.g. aluminium back surface field (Al-BSF) or passivated emitter rear contact (PERC), and study their interaction at the interfaces (potential degradation modes) in greater detail.

Silicon heterojunction cells (SHJ) are one of the promising concepts for high efficiency cells [67, 68]. However, SHJ cells cannot withstand temperatures above 250 °C, so standard soldering process using SnPb coated ribbons are not feasible [67, 69]. Therefore, different interconnection approaches, such as lead-free low-temperature solders based on bismuth [67], electrically conductive adhesives [70] or smart-wire technology (e.g., SWCT) [71] have to be used (see Figure 4). Although currently Cu-ribbons coated with lead based solders are the mainstream, lead free solder ribbons, conductive adhesives and multi-wires are expected to gain importance in the near future [2], in parallel with the rise of SHJ cells.

For back contacted solar cells (e.g., IBC, MWT) it is difficult to apply ribbon-based interconnection technologies with standard production equipment [72]. Furthermore, cell warpage during ribbon attachment is an issue that needs to be overcome [73]. Therefore it is common for structured conductive foils to be used. Here the inner layer of this backsheet is either copper or aluminium. The connection to the cells is then achieved either via laser welding or electrically conductive adhesives. Also here, compatibility between the conductive backsheet, the ECA and the encapsulant has to be ensured [74, 75].

Figure 4: **SWCT-CSEM Façade -Semi-transparent facade of the renovated CSEM building in Neuchâtel, Switzerland, which comprises bifacial SHJ cells interconnected by SWCT™.**

3.3.3 New module designs

New technological requirements for module materials and components also can originate from application driven module concepts with very specific challenges, where conventional module designs with standard components do not meet the specifications.

The development of modules for special environmental conditions has become a trend in R&D, as PV modules perform and degrade differently in different climate zones [66, 76–79]. For desert environments soiling and abrasion, high UV radiation and high temperature cycling are the main challenges [80]. One mentionable initiative is the development of PV modules for the Atacama desert in Chile [81], which has one of the harshest operating conditions worldwide [82]. Here different approaches for glazing, cell and interconnection technology and encapsulant are being tested in order to find the right combination with the required durability [80, 81, 83]. Modules for tropical climates have to withstand higher humidity levels [77, 78] and also higher temperature cycling loads due to partial shading caused by often cloudy skies [84]. PV modules for arctic or alpine regions are often produced with thicker glazing and silicone based encapsulants in order to reduce stress impact and breaking of the solar cells under heavy snow and wind loads.

Next to climatic stress impacts, also micro-climatic loads can be relevant, e.g. for PV modules in agricultural environment or for floating PV systems. Resistance of PV modules against ammonia from agriculture has been widely researched [85–87]. For floating PV humidity ingress, corrosion, and soiling are known issues [88] that need to be addressed. However, such dedicated modules currently only represent a small share of the overall market [2].

As building integrated PV modules (BIPV) are not only energy producing electrical elements but also building products, special requirements need to be met with respect to fire resistance, strength (especially in facades of multi-storey houses thicker glass panes are required), safety in case of glass breakage (security glass, mostly combined with PVB encapsulants) but also long-term reliability. As roofs or facades typically have a lifetime of 50 years, BIPV is also required to have a comparable lifetime to the rest of the building. As BIPV often is used in the urban environment, the aesthetic appearance of the modules is also an important point. Thus, BIPV modules often come in differing shapes, colours and appearance (surface modification of the glass panes e.g. sandblasting) than standard modules. Changes of the colour have a negative impact on the performance with printed or coated front glass or coloured encapsulants causing a performance loss of 10 to 15 % (5 to 50 % are possible see [89]).The reliability of the coloured coatings and prints as well as of pigmented polymers still is subject of long term studies. Interactions of PV components with attached building materials, adhesives and mounting compounds also need to be tested for comparability and reliability.

For some PV applications, the weight of PV modules is an obstacle. This is obvious for some special applications such as solar panels for satellites. The requirements for such special applications are typically quite specific and the products are often based on costly materials and custom designs. However, there are also broader fields of application for lightweight PV modules. Numerous commercial buildings are designed with little to no spare structural capacity due to cost constraints. Therefore, lightweight modules may address this market segment by achieving weights, which still allow an installation on such roofs. Also for some innovative PV system solutions, e.g. PV elements for parking roofs or building Integrated PV (BIPV) [90], but also vehicle integrated PV, lightweight modules can be beneficial.

The main challenge for light-weight PV modules is replacing the glass frontsheet while maintaining the mechanical stability and hail resistance [91–93]. For crystalline silicon cells various approaches from glass-fibre reinforced composite structures [94–96] to support lattices [91] have been implemented. For thin film technologies like CIGS flexible substrates and polymer frontsheets have been applied [97, 98]. Whereas flat lightweight modules are mostly used for PV installations attached to building roofs with static weight limits, curved or free-formed panels are used in building integration and vehicles.

The common challenge for all module designs is to ensure adhesion of all layers over the whole lifetime as well as compatibility of the materials used. In the worst case, large scale delamination or new material degradation effects caused by unwanted interactions can happen after some years of installation.

3.4 Impact and consequences of new materials and module designs

3.4.1 Characterization of novel materials: interactions and new degradation modes

Each material group is known to have its weaknesses and strengths. For example: The most used encapsulant, EVA, is a cheap commodity product fulfilling most requirements for a perfect encapsulation but also has drawbacks like its propensity to produce acetic acid during operation triggering corrosion and delamination [9, 78]. Replacement of EVA by polyolefins as encapsulants can solve the problem of acetic acid formation but challenges with the adhesion of the non-polar polyolefin to glass, cells and backsheets opens up a new field of potential problems/challenges [52].

Furthermore, replacing one component/material in a long-established multi-material composite (as a PV module) can cause unwanted material incompatibilities leading to migration of additives or to harmful chemical reactions at the interfaces resulting in discolouration [66, 99] or delamination [100]. Thus, it is essential that new materials are tested in the material composite of the final product against all potential stressors and combinations of stressors (e.g. accelerated ageing tests) before they are introduced into the market [52, 101].

A more detailed description of observed material interactions and their relation to PV module degradation modes can be found in a previous IEA Task 13 report [66].

For the non-destructive material characterisation of polymers in PV modules several spectroscopic techniques are applicable onsite and/during plant operation: mobile devices of IR, NIR, Raman spectroscopy [102] as well as handheld UV-Fluorescence lamps [103]. In addition, portable Electroluminescence (EL) tools and IR-thermography cameras [66, 104] are available to identify defects in the electrical functionality of PV modules in the field.

Failure analysis and identification of failure modes of aged modules can often not be done directly in the field but requires a detailed (destructive) analysis in a electrical and/or chemical-physical laboratory [6, 7]. One example of a material damage with serious consequences in the PV community is the severe cracking of PVDF-containing or Polyamide based backsheets [105, 106]. The defects can be visually identified in the field; a detailed analysis involves, however, the chemical, physical and thermo-mechanical characterisation of the backsheets and their degradation modes as well as of the adjacent encapsulants.

3.4.2 Impact on module testing procedures and standardization

The trend toward larger wafers results in larger sized modules, many of which do not fit into usual test equipment at PV test labs, such as pulsed and continuous sun simulators, climate chambers, or equipment for mechanical testing. Therefore, in both the performance and safety standard, and also in the standards for PV building integration, IEC 63092 [107] the option is foreseen to test “representative samples”, including all the components of the module, except some repeated parts, instead of extra-large modules. However, at present a clear definition is missing, how test results derived from a class of (smaller) test objects can be extrapolated for another class of modules then manufactured and applied. In present retesting guideline [108] modules have to be retested if their size (or area) is more than 20 % larger than the previous tested ones, but both designs may have an identical “representative”. See also the Report of IEA PVPS Task 15 on the standardization challenges related to the special features of PV modules for building integration, [109].

Characterization and testing of new BIPV module concepts

The growing demand for the use of PV systems integrated in buildings to provide design and multifunctional features beyond the bare energy production, is triggering a profound change in the sector of Building Integrated Photovoltaics (BIPV), with major challenges to be addressed in the coming years [110]. Supported by increasing technological developments, digitization and process innovations, such systems will progressively have to be implemented in the ordinary construction market allowing the achievement of near Zero Energy Buildings. These BIPV products are evolving from only producing energy, towards multifunctional products that can aggregate many features required for the building skin such as thermal and acoustic insulation, solar control, safety in case of fire, etc.

However, to enter the building market, BIPV products have to meet multiple goals including cost-effectiveness as well as compliance with quality, safety and reliability requirements. It is

also essential that product standards, industry standards and specific rules for the type of installation and use in buildings is coordinated. The EN 50583-1:2016 [111] and EN 50583-2:2016 [112] standards made a first step in this direction by defining the properties and the applicable regulatory framework for photovoltaic modules used as construction products. Nevertheless, the current regulatory framework collects norms created for standard PV or, on the other hand, for “non-active” building products, without proposing new testing procedures specifically adapted to BIPV. This topic is also addressed within the work of IEA PVPS Task 15 under Subtask E [113].

Design, composition and format of solar-active surfaces for contemporary architecture, according to requirements of architects and designers, are increasingly emerging. Using validated PV technologies (e.g. crystalline and thin-films), colourful, patterned or printed solutions, texturized pane surfaces, large or small, rectangular or non-normalized dimensional formats are developed. Also, different material compositions of the PV module packaging layers (typically glass-based) are combined with full-integrated constructive solutions for building skin which, in some cases, also include advanced and prefabricated solutions for the buildings market, both in new and renovation. This trend, which is being consolidated today also from a manufacturing perspective, may contribute to a rapid re-configuration and increase in energy efficiency of existing and newly constructed buildings.

Conventional PV modules are subject to the electrotechnical certifications and CE marking in accordance with the IEC standards, IEC 61215-2:2016 [114] and EN IEC 61730:2016 [115]. As a construction product BIPV modules must comply both with electro-technical standards and with the Construction Products Regulation CPR 305/2011 [116], and accordingly all building products should carry the CE-mark-to indicate conformity with essential health and safety requirements set out in the European harmonized standards. Specifically, the EN 50583:2016 [111] provides basic principles for BIPV product qualification and a collection of both electrotechnical and building standards that are relevant for BIPV products depending on their mounting category and their main material. In the case of customized products or PV modules that have undergone, or will undergo modification from their originally assessed design, it is mandatory to retest some relevant performance and safety requirements, according to IEC 61215 [114] and IEC 61730 [115] retesting guidelines, in order to maintain type approval, design and safety qualification.

The discussion below is focused on different customization possibilities considering five main customization strategies (Figure 5) in the definition of a tailor-made BIPV product, as described below, as driver of the architectural integration design in BIPV:

1. New cell features and PV technologies
2. Electrical layout
3. Packaging layer
4. Dimensional customization
5. Constructive solutions

Of primary interest is the energy rating of a customized BIPV module. Measurements are necessary to check the compatibility of custom designs with electrical and thermal performance (e.g. uniformity of transparency on the solar cells, avoiding induced hot spots, control of module temperature, etc.). Standard testing protocols such as IEC 61853-1 and IEC 61853-2 standard [117, 118], for special BIPV/BAPV and bifacial modules is suggested. For each possible customization strategy, the possible implications regarding the building and the solar system are also identified. Customization implies choices and consequences at different levels including architectural functionalities (e.g. improving aesthetic, energy performance improvements, cost benefits, greater energy yields and efficiencies, etc.) and meeting construction

requirements (dimensional flexibility, easy mounting, safety and reliability, thermal stability and comfort, fire security, climate protection, maintenance and durability over time, etc.). The result of different customization options thus implies different consequences on energy output and reliability.

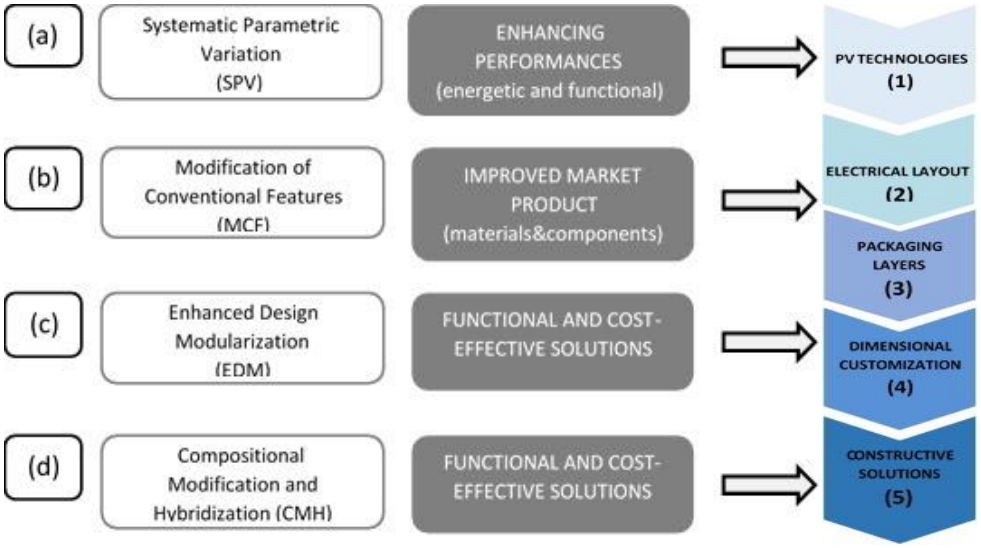

Figure 5: Main customization strategies in the definition of a tailor-made BIPV product.

Architectural functionalities

Architecture design requires special appearance of BIPV modules such as texture, uniformity of surfaces as for example low-recognizable PV, chromatic mimicry, technological mimicry, etc.; aspects related to mounting and framing possibilities (BIPV/BAPV with frame or frameless); aspects related manufacturing and maintenance cost (for example, aspects related to mounting systems, fixings and joints. For example, a different framing or mounting system (e.g. a vertical façade system, with uprights and crosspieces visible, or hidden by the solar cladding system) can have a greater or lesser impact on aspects such as soiling, the accumulation of snow or water, air ventilation, all factors that can affect both the energy production of the system and the aspects related to the costs of maintenance of the building.

Construction requirements

BIPV as a building construction skin system implies developments and qualification approaches linked to construction requirements as specified in the European Construction Product Regulation CPR 305/2011. Among the essential requirements e.g. mechanical stability or structural integrity (rain, snow, wind, hail); fire and sound properties; aspects related degradation or reliability and to energy economy and heat retention (influence on thermal balances, temperature effects) can be considered. All the essential requirements are specified in Annex I of CPR 305/2011 [116] and detailed in the harmonized standards and rules in force for building elements.

3.4.3 New requirements for standardization

The development of standardized tests for qualifying PV module performance and safety started in the seventies (US JPL Block Buys I-V) and early eighties (EU Spec. 501-503), see [119]. The International Electrical Committee (IEC) established the Technical Committee “Solar Photovoltaic Energy Systems” TC 82 in 1981. Because PV is a global market, most of the

PV standards are developed in a top-down fashion, so the TC 82, backed by 43 national committees as full members proposes, develops and issues the vast majority of PV related standards, which then are adopted by supranational and national standardization bodies. More than 500 experts from Asia-Pacific, the Americas and Europe cooperate within TC 82, with industry as well as research groups involved.

The IEC's central office standardization management board states: "It appears that TC 82 has the largest program of work in IEC (in terms of number of projects). TC 82 were observed to be the second highest number of publications sold among all IEC TCs / SCs from July 2018 to June 2019 in IEC CO sales statistic." [120]. August 2020, 150 published PV standards exist, and 75 are currently under development.

Almost half of all PV standards focus on modules, one third of the published, and one quarter of the standards under development focus on component and materials characterization and durability. The high number of active standardization projects - new standards, as well as new editions of already existing ones – indicates that PV, and PV module development is a very active evolving field. In general, PV standards focus on quality and reliability along the whole value chain from cells, materials and components to systems and grid integration, including traceable and reproducible measurement and characterization procedures. Nevertheless, well established, test procedures for PV modules have their shortcomings:

- Tests primarily are able to detect early failure modes (design flaws, infant failures) but are only loosely related to failures that might occur in long-term outdoor applications under different climatic and operating conditions
- Tests were designed to detect failures from known and established materials. New materials may have failures that the test do not detect.
- The tests were initially designed for applications with non-restricted heat dissipation under moderate climatic conditions only [121].
- Changes in module manufacturing, BOM and assembling (e.g. cell interconnect technology) may provoke new failure modes as well, not covered by existing test procedures.

Optimum PV module test design was assumed to have each test procedure specified in a way, that it exactly covers / provokes one distinct failure mode. If new failure modes were observed in field applications, new test procedures shall be designed, and added to the test specifications. In [122] a table lists common module failure modes, and how standard sequential testing routines are able to detect such failures. Table 3 replicates this and expands the list by additional failures and test procedures. From this table it is obvious, that a 1:1 relation between field failures and test procedures is only rarely achieved.

The actual versions of the module type and safety qualification standard series IEC 61215 [114, 123–127] and IEC 61730 [115, 128] were issued in 2016. At that time, mainly the structure was changed to better handle evolution of technologies and test procedures, and to align requirements with horizontal standards, e.g. the insulation coordination IEC 60664-1 [129]. In parallel, new test procedures for materials in the IEC 62788 series [130–138], as well as for known and newly detected module field failure modes, that are not covered by existing standards were developed, e.g. the IEC TS 62804 series [139, 140] for potential induced degradation issues, or a test procedure for dynamic mechanical load stresses, IEC TS 62782 [141].The original intention was that a single PV module design shall be for all purposes and environments, but implicit application was focused on (standard) open rack mount in moderate climates. With a proposed standard series IEC 62892 with four parts a ranking of module designs in different climates was intended, but finally three parts were cancelled and only a single document related to local climate and temperature variations, IEC 62892 *Extended thermal*

cycling of PV modules - Test procedure, was issued, that is practically useful only for thermo-mechanical fatigue of solder bonds [142].

Although modules with non-restricted air flow operate even in very hot climates at temperatures below 85 °C, the test temperature used in many of the module qualification tests, an additional standard for high(er) temperature applications, IEC 63126 *Guidelines for qualifying PV modules, components and materials for operation at high temperatures*, [143], was developed, providing modified test procedures for modules operating at higher temperature levels, Level 1 and 2. These levels are defined by a 98 % quantile operating temperature, i.e. the temperature a module exceeds for 175.2 h per year. If this 98% quantile is not exceeding ≤80 °C, the standard tests are sufficient without modification, Level 1 is for a 98 % quantile up to 80 °C and Level 2 for applications where the 98 % quantile is not exceeding 90 °C.

The system of module type and safety qualification is well established, with the necessary equipment available at test labs and manufacturers. Several "*extended testing*" procedures were proposed from different test houses, manufacturers, reinsurance and engineering companies, see e.g. [144], DuPont [145] and the Product qualification Program of PVEL [146] having both eight parallel test sequences, but different ones.

Currently in development, IEC TS 63209(-1) *Extended-stress testing of photovoltaic modules for risk analysis* [147], aims to standardize the variety of existing extended test protocols, and has (at present) five parallel test sequences for TC, (D)ML, UV, DH and PID. In the mechanical load and UV sequences, also TC and HF are applied to open-up possible cracks and to force delamination by thermo-mechanical stresses, and frost if humidity is able to enter the package.

Part 2, IEC TS 63209-2 *Durability characterization of polymeric component materials and packaging sets* [148], shall support the module (or mini-module) tests by component and coupon level tests, as e.g. UV testing by Xe-arc lamps, as defined in relevant module material standards within the IEC 62788 series, needs very long testing time (2000, 4000, up to 16000 h, i.e. 2 years) to achieve relevant dose when compared to outdoor applications under high irradiation conditions.

Table 3: Sequential module testing procedures and correlation with common failure modes. From [122], updated.

Standard	**IEC 61215-2 Ed2, IEC 61730-2 AMD 1 Ed2**									**61701** **62716**	**62979**	**NP 82** **1771**
Test procedure / failure mode	**TC**	**DH**	**HF**	**UV**	**ML**	**DML**	**Hail**	**BPT**	**62804 PID**	**NaCl NH_3**	**BPR**	**LeTID**
Delamination		×	×	×					×			
Encapsulant adhesion & elasticity		×		×								
J-Box adhesion	×	×	×									
Cell breakage c-Si	×				×	×	×					
Broken interconnects, ribbons	×				×	×						
Glass breakage	×				×	×	×					
Open Connections (potential arcing)	×											
Solder bonds (potential arcing)	×				×	×						
Corrosion (all technologies)		×								×		
Electrochemical corrosion (TF.)		×										
Inadequate edge delamination (TF)		×	×									
Encapsulant & backsheet discoloration				×								
Ground fault due to backsheet degradation				×								
Structural failures					×							
Bypass diode failure								×			×	
BPD overheating degradation of encapsulant & backsheet materials								×			×	
Specific corrosion (deicing, etc.)									×			
LeTID												×
PID									×			
Bifacial coefficient. degradation		×							×			

Both parts of IEC TS 63209 [147, 148] focus only on module designs using crystalline silicon cells and are not intended to use in combination with pass/fail criteria, but all data shall be reported.

In contrast to the extended testing procedures, and the ones for higher operating temperatures, a market for non-standard PV modules exists, where the reliability requirements may differ, and often be lower than for long-term outdoor applications in PV power systems. Therefore, work on a standard for PV consumer products [149] was started, that may ease – depending on applications – some of the module type qualification tests, and add others, e.g. a drop test.

The actual drafts for a new Ed. 2 of the IEC 61215 series Ed. 2 [150–155] and IEC 61730 series Ed. 3 [156, 157], are close to being submitted as final drafts (FDIS) to the IEC central office, therefore publication can be expected in 2021. These drafts now include

- For bifacial modules requirements and test procedures including nameplate specifications based on the IEC TS 60904-1-2 [158] measurement, using a bifacial nameplate irradiance BNPI (1000 W/m² front, 135 W/m² back irradiance), and test levels based on BNPI and a bifacial stress irradiance BSI (1000 W/m² front, 300 W/m² back irradiance)
- A performance test for flexible module designs
- Includes PID and dynamic mechanical load testing
- Adds requirements based on component tests, for junction boxes [159], connectors [160] and for back (and frontsheets), [161].

It was planned also to integrate in the new IEC 61215 a test for Light and elevated Temperature Degradation (LeTID) of PERC [162], but now a separate test procedure using current injection at 75 °C is developed, that possibly will be incorporated in the IEC 61215 test flow by an amendment later.

A shortcoming of the standard and extended test procedures is that tests were performed at single stress levels, and combinations of such, so that it is not possible to derive models how e.g. the degradation rate is depending on the temperature, with the other stressors held constant. Therefore, test chamber performance cannot be extrapolated to outdoor service lifetimes under changing environmental conditions. Performing a whole matrix of tests, as, e.g. done within the European SOPHIA Research Infrastructure project, is extremely elaborate, because many modules have to be moved between different climatic chambers, and many interim measurements have to be performed. The status of PV module service life prediction SLP is matter of the Task 13 Subtask 1.4 [163].

Module BOM and manufacturing technologies are rapidly changing and are brought to market quickly in high quantities. It is questionable to design special tests to provoke distinct and field relevant failures by sequential tests with long test durations, even if they are highly accelerated. With the aim to reduce risk in the application of new designs and technologies, within the International PV Quality Assurance Task Force PVQAT, https://www.pvqat.org/ and the Durable Module Materials Consortium, https://www.duramat.org/ a new approach was developed, combining multiple stress factors of the natural environment in a single test (cabinet) instead of targeting specific failure mechanisms, [164, 165]. A TR was issued giving an overview of 16 approaches of sequential and cyclic sequential test methods used for provoking distinct failure modes, with the same schematic applied to characterize them, and on which levels from materials, coupons, mini or full-size modules the test procedures were used.

The new approach, called Combined and Accelerated Stress Testing, C-AST uses newly developed test equipment, at present for parallel testing of several 2 × 2 cell mini modules. It is based on a modified weathering test chamber, allowing for applying temperature, humidity and light in a wide range: -40 °C to +90 °C, 5 % to >95 % relative humidity, and a 2-sun Xe-arc

irradiance source. The possibility for a water spray on front and back, light reflective troughs underneath the modules, mechanical load and equipment for electrical stresses (1500 V system voltage and reverse bias, resistive load) was added. In-situ measurement equipment for module status monitoring for illuminated and dark I-V curves, power measurement, leakage current monitoring and electroluminescence imaging is implemented.

Test schematics, accounting for specific climates (e.g. tropical, continental, arctic) and all seasons are developed, with the idea of applying multiple stresses in a way that the upper limits of the stresses in natural environment are not exceeded, but applied that C-AST is like a bad day, every day. In comparison to the previously used tests, it is shown that many field relevant failures will be provoked by this “essentially design-agnostic testing philosophy” approach. The idea was to launch as a next step two NPs: *Method for combined-accelerated stress testing – Part 1: Climatic chambers*, to specify the C-AST equipment, and a *Part 2: Stress Tests*, describing test flows aiming for winter, spring, tropical and high desert environment stresses. Although presented results are very promising so far, because such infrastructure is at present only available as a single device, located at NREL, at the (online) 2020 spring meeting of TC82s Module Working group WG2 was discussed that more experience and from different labs would be necessary before going in the direction of Test Specifications (TS) or International Standards (IS) with the C-AST approach.

C-AST demonstrates, that there may be a way to test new designs such that possible failures will be detected before field application. But, because of the very complex changing multi-stress conditions during testing it is not possible to extract parameters useful for degradation modelling by these test procedures. In many industries and applications, a movement is seen in the direction of designing a virtual representation of a device and its manufacturing before it is really built, and to check operational behavior by comparison of monitoring data with such a “digital twin”. So, it is an open question how this can be achieved in the PV industry as well. Digital modelling approaches are necessary in testing, certification, and retesting beyond simple pass/fail statements. Ideas of more flexible certification schemes using man *and* machine-readable documents, e.g. in XML-format, to support industry 4.0 and digitalization in construction are discussed in the IEC Standardization Management Board (SMB) supporting digital transformation and “smart manufacturing”, but these discussions are in a very early stage in PV module standardization.

4 RELIABILITY OF ADVANCED MATERIALS, COMPONENTS AND MODULES

4.1 Frontsheets and coatings

Both crystalline silicon PV modules and most thin film modules are manufactured with a front cover made from tempered soda lime silicate glass - the same material used in buildings as window glass. This front cover is an integrated part of a thin film module constituting either a substrate or superstrate for deposition of the various thin conductive-, transparent-conductive- and semiconducting-layers. When used for crystalline silicon modules, the main function is protection against physical impact (hailstorms) and moisture ingress, while also providing structural stability and rigidity (towards wind and snow loads) and bending strength supporting the encapsulation of the interconnected cells. Usually the front glazing is also equipped with an antireflective or antisoiling coating, in order to increase efficiency or maintain the energy yield.

4.1.1 PV glass

Soda lime silicate glass of the same type as used in the building industry, has been the preferred choice of front cover since mass-fabrication of crystalline silicon PV took off by the beginning of the century. This material was available in sufficient quantities and at competitive prices due to the presence of an existing mature manufacturing value chain including float glass furnaces, jumbo glass sheet cutting, edge grinding, glass tempering and final product quality inspection according to well established industry standards.

As the PV industry matured and glass consumption increased into billions of kilograms, production lines dedicated to only producing PV glass were established. Optimization of these PV glass lines has been focused on:

- The **chemical composition**; in terms of low iron content where specifications down to 100 ppm can be obtained while using only raw natural resources (no special treatment) The aim is to reduce the Fe^{3+} to Fe^{2+} ratio as the ferric-oxide (Fe_2O_3) introduces an unwanted optical absorption.
- The **surface topography**; in terms of macro- or micro-structuring of the surface made by rolling the hot glass between two patterned metallic rollers.
- The **sheet thickness**; that typically lies between 1.6 mm and 3.2 mm which also implies that the corresponding furnace melting volume should not exceed the required output needed (calculated as glass width, glass thickness, extraction speed), as too large melting volumes will be costly in terms of heat loss.
- Introduction of a **clean-room operated coating step** before the tempering, where solvent based chemicals can be applied by roller or spray coating machines to provide an anti-reflective and/or anti-soiling top-surface treatment.
- Glass **tempering** furnaces, in terms of excessive cooling capacity in the quenching step, as this will determine the amount of build-in surface compression over bulk tension that determines the strength of the heat-strengthened or tempered glass.

The most important functional performance parameters of PV glass are impact and bending strength, high transparency also for non-normal incident light (addressed by applying a micro structured surface topography and an antireflective coating) and low weight translated into a typical thickness of 2 mm.

4.1.2 Flexible frontsheets

There are many Photovoltaic (PV) applications, including Building Integrated Photovoltaics (BIPV), buildings with weight limitations, buildings with curved roof surfaces, or other outdoor portable applications, where flexible or conformable PV products would be beneficial. A flexible PV product made of non-rigid packaging materials, allows for easy transport, installation, and ability to conform to a curved-roof but also comes with challenges. Critical to conformable PVs is the flexible frontsheet which is the outermost superstrate facing the sun and has a significant impact to the performance and reliability of flexible panels. The dominant frontsheet materials are Ethylene Tetrafluoroethylene (ETFE) and Fluorinated ethylene propylene (FEP), which are generally high cost and therefore increases the module BOM cost and potentially the overall levelized cost of energy (LCOE) [94, 166, 167]. Different approaches for replacement of the fluoropolymers have been investigated over the years, including polycarbonate (PC) or polymethylen methyacrylate (PMMA) [168–171]. Especially for PC different approaches for light management have been investigated. None of these materials have been adopted by the PV industry due to issues in long term stability, thermo-mechanical behaviour and compatibility with the encapsulant. Up to now, a lower cost frontsheet comparable to PV glass remains critical to reaching sustainably low flexible module costs.

A recent activity investigated 15 frontsheet candidates for PV modules [172]. Monolithic ETFE was chosen as the positive control due to its inherent UV stability, high transmittance, and proven-lifetime in the field. More cost-effective base materials such as Polyvinylidene Fluoride (PVDF), Polyethylene Terephthalate (PET), and Polycarbonate (PC) have also been included in this study. However, these lower-cost material options, especially the non-fluoropolymers, are inherently more prone to photothermal degradation and therefore are specially formulated to improve UV weatherability. Unprotected PET was selected as the negative control in this study (see Figure 6).

	#	Material	Cost
ETFE (Positive control) →	1	ETFE (Monolithic)	High
Non-PET options	14	PVDF (Monolithic)	High-Med
	15	PC + Acrylic-coating 4	High-Med
PET w/ UV filtering layer →	3	PET + Fluorinated layer	Medium
PET w/ UV filtering coating	13	PET + Fluorinated coating 2	Medium
	4	PET + Acrylic-coating 3	Med-Low
	9	PET + Acrylic-coating 1	Med-Low
	11	PET + Acrylic-coating 2	Med-Low
	12	PET + Fluorinated coating 1	Med-Low
PET w/ integrated UV absorbers	6	PET + UV blocker 1 (high)	Med-Low
	8	PET + UV blocker 2 (high)	Med-Low
	5	PET + UV blocker 1 (low)	Low
	7	PET + UV blocker 2 (low)	Low
Non-stabilized PET (Negative control)	2	PET + w/o UV blocker 1	Lowest
	10	PET w/o Acrylic-coating 1	Lowest

Figure 6: Frontsheet material candidates tested in [172].

One of the major reliability concerns of the polymeric frontsheet is its durability under prolonged UV exposure in the field. To study the photothermal degradation kinetics of these frontsheet candidates, xenon-Arc chambers at various UV irradiance and temperature conditions were utilized to age the frontsheet candidates.

Solar Quantum Efficiency Weighted Transmission (SQEWT) was selected to quantify the degree of photothermal degradation resulting from the UV-aging. SQEWT was calculated from the UV-Vis % transmission spectrum of the material, weighted by wavelength, irradiance and the crystalline silicon quantum efficiency profile.

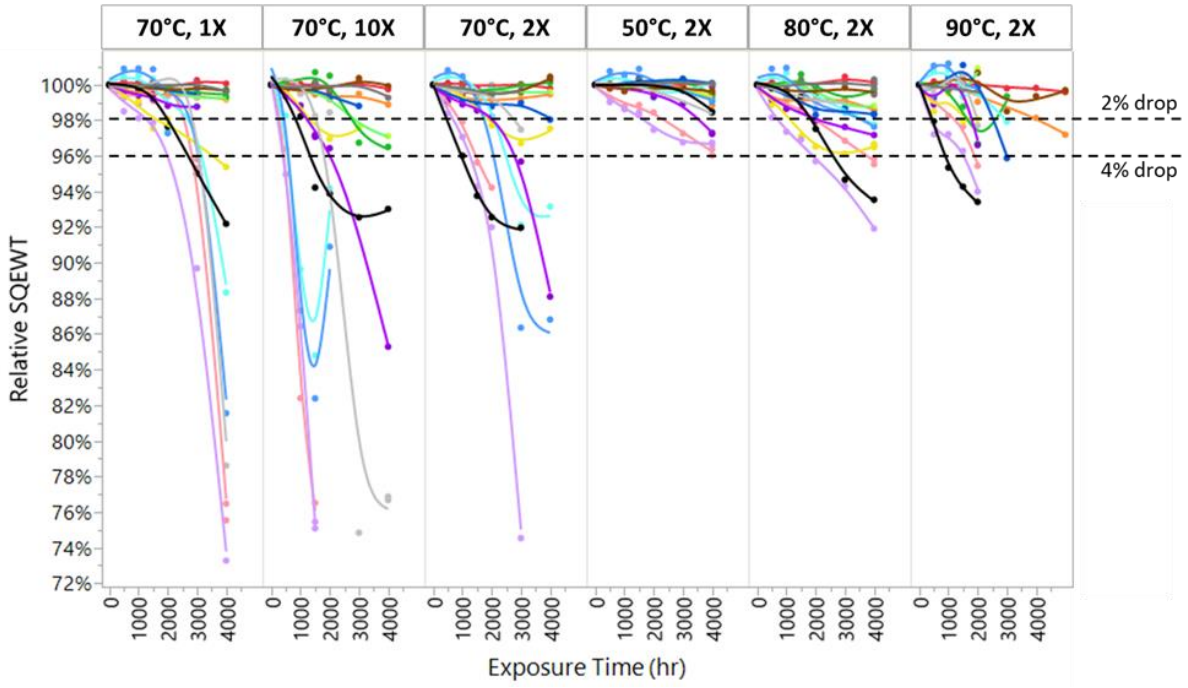

Figure 7: Relative SQEWT drop for all materials over time at different temperatures and UV intensities (1X corresponds to an UV intensity of 0.4 W/m^2 at 340 nm). Dashed lines show specified critical transmission loss ($\Delta SQEWT_{crit}$) of -2 % and -4 %. Each colour represents each frontsheet candidate.

A couple of observations can be made from the relative SQEWT over aging time result. First, the relative SQEWT of most materials decreased along the aging process, resulting from the photo-thermal degradation. Second, the same material degraded at different rates given different UV doses and temperature. Third, the relative SQEWT over time exhibits some other reaction mechanisms, such as decreases in UV absorber concentrations, indicated by the initial increase in Relative SQEWT at the beginning of the aging process for some materials.

These Xenon-Arc experiments provided many insights into how the frontsheet candidates performed in photo-thermal aging and a model to estimate field lifetimes of each material. Two promising frontsheet candidates (Sample #5 & #12, see Figure 6) along with the ETFE control were selected for NREL's Combined-Accelerated Stress Tester (C-AST) [164, 173] to evaluate the durability of the materials under other stresses, such as moisture, thermal cycling, mechanical loading, and voltage biases etc. in a mini-module construction.

In summary, this project demonstrated the difficulties in finding candidates for flexible frontsheets with respect to its UV stability. The durability of the candidate materials still has to be tested within a test module und combined stresses in order to check its suitability.

4.1.3 Abrasion of antireflective and antisoiling coatings

Antireflective (AR) coatings have been commonly used in PV modules since ~2005, and antisoiling (AS) coatings have been explored for use in PV since ~2015. AR and AS coatings provide incremental improvement in performance – after insolation and temperature, soiling is the third most significant natural factor affecting PV module performance. Natural soiling (contamination, including inorganic and organic matter) on the surface of PV modules can gradually reduce performance in the order of 1 %·day^{-1} in the soiling-prone, insolation-rich Middle East and North Africa (MENA) region, whereas sudden power drops as great as 70 % from discrete meteorological events have been recorded worldwide [174, 175]. Cleaning of PV modules, even as frequently as daily, is therefore recommended in soiling prone locations.

While abrasion and delamination are failure modes that can occur for surface coatings, in practice abrasion is presently much more frequently observed. Industry feedback suggests the majority of abrasion results from the cleaning of PV. A wide variety of cleaning equipment and methods are presently applied to PV, including manual and robotic solutions. While the cleaning of the incident surface of modules has been practiced for decades, the cleaning and abrasion of bifacial PV remain to be understood. To compare the durability of coating products, methods of abrasion testing may be applied, including: artificial machine abrasion, falling sand, forced sand impingement [176, 177]. Upon review, existing abrasion standards from other industries are not well suited to PV, e.g., a test resulting in a frosted glass substrate allows little opportunity to examine the durability of coatings. The methods of artificial linear brush abrasion and falling sand abrasion are the most popular in the PV literature, in part because of the ready availability of test equipment. The IEC 62788-7-3 standard [178], covering abrasion methods tailored to PV, is therefore presently in development.

The characteristics of coatings subject to artificial linear abrasion using slurry plus a brush ("slurry" or unspecified) or a wet brush ("wet", where specified) are examined in Figure 8 and Figure 9. Coatings include porous silica (B), a thin polymer film (P), anatase TiO_2 (V), and a stacked (air) $SiO_2/ZrO_2/SiO_2/ ZrO_2$ (substrate) coating [179], in addition to the glass substrate with no coating (J). The characteristics of direct transmittance (representative of a single junction PV device and weighted relative to the solar photon irradiance [180]), yellowness index (YI, taken here to result from the scattering of light rather than specimen discoloration), the surface energy (i.e., water contact angle), and the average surface roughness (for a 148 µm × 112 µm field of view). For specimens B, P, and Z the contact angle is seen to evolve (typically decrease) with abrasion, converging to that of the uncoated glass substrate, J. For the P coating, the reduction in contact angle is seen to degrade at a lower cycle count when abrasive is present (P_{slurry}) relative to when only wet brush bristles are used ($P_{wet\ (no\ abrasive)}$). For specimens V and Z, a change in the transmittance and YI is seen to occur at or before a local peak in the surface roughness.

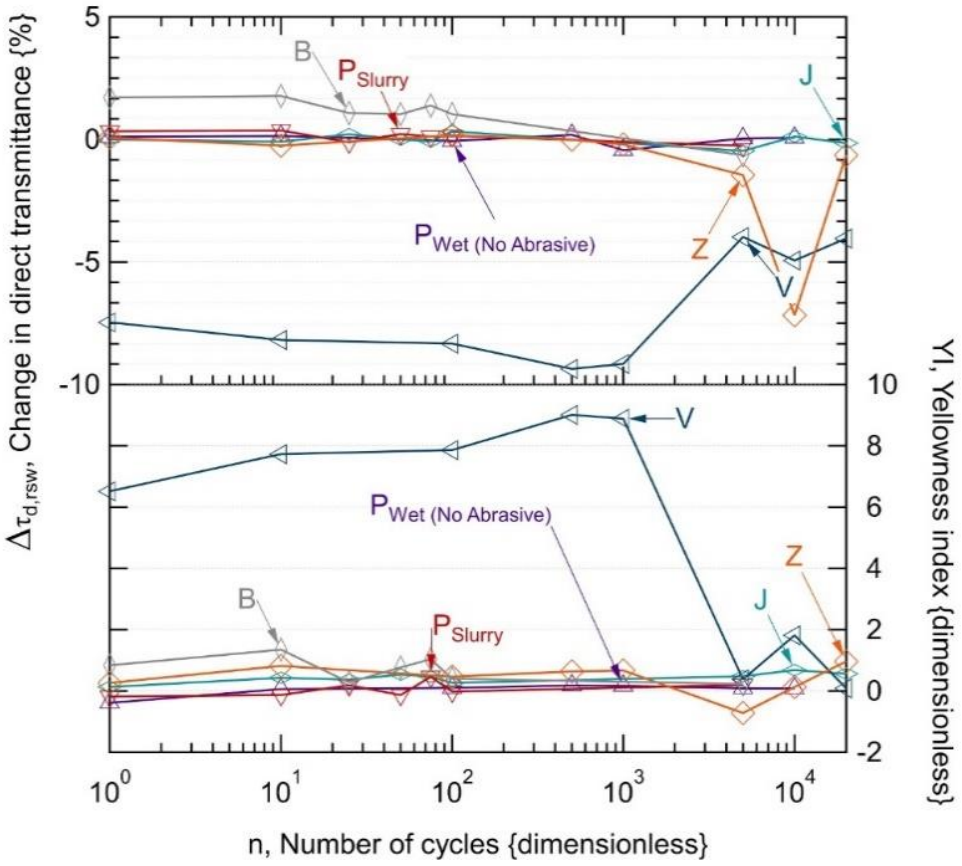

Figure 8: Comparison of the change in direct transmittance (measured without an integrating sphere) and corresponding yellowness index with the brush cycle count (0≤n≤20000) for select experiments for abrasion with slurry ("slurry" or unspecified) or just a wet brush ("wet", where specified).

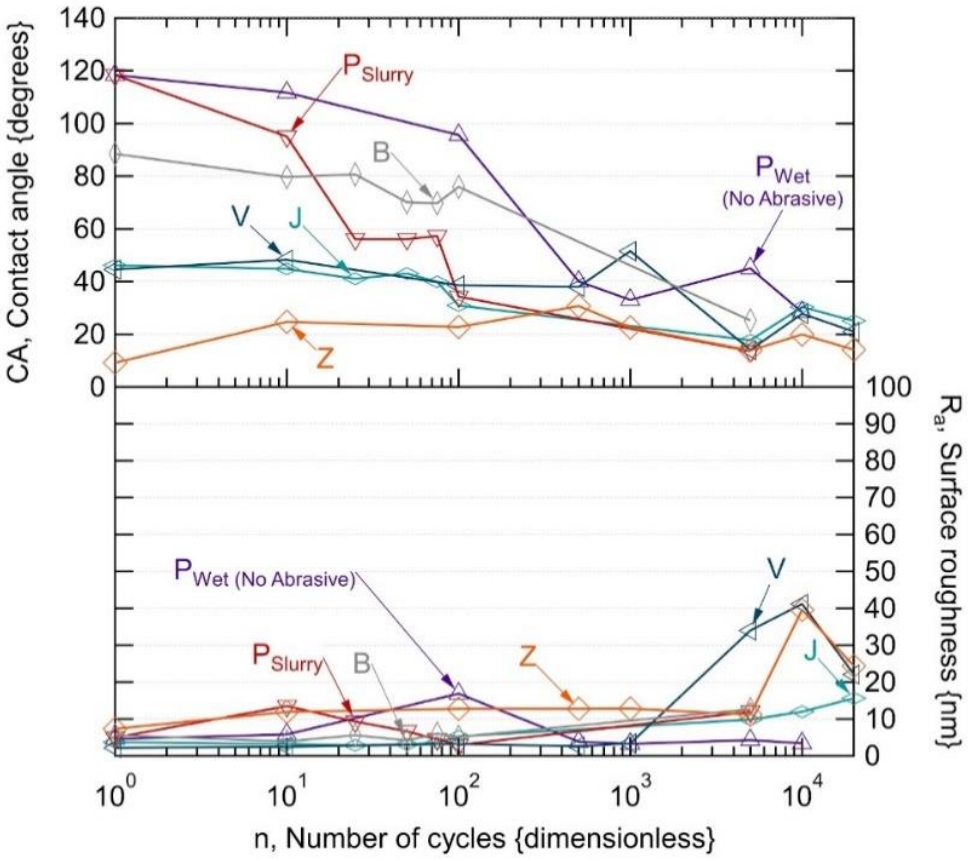

Figure 9: Comparison of the change in surface energy (contact angle) and surface roughness (average) with the brush cycle count (0≤n≤20000) for select experiments for abrasion with slurry or just a wet brush.

A correlation is observed between the characteristics of transmittance, yellowness index, contact angle, and surface roughness. The evolution of the surface energy (towards that of the substrate with no coating, J) as well as a peak in roughness indicate the surface wear of coatings of limited thickness. The coating durability in the figures ranges from 10 to 10000 cycles. The range of coating durability varies with factors including coating material and the presence of abrasive. It remains to be established if the more delicate coatings (polymer-P or porous silica-B) are sufficient for installations requiring infrequent cleaning or if ceramic dielectric coatings (titania-V or stacked dielectric-Z) are economically justified for PV. While only linear abrasion with a polyamide brush is examined in the figures, the cleaning equipment and method may also significantly affect the tribological durability. The experiments in Figure 8 and Figure 9 give an example of the characteristics that might be used to compare coating materials and estimate coating lifetime – if a site-specific acceleration factor can be determined relative to a cleaning method. The characteristics in Figure 8 and Figure 9 may be used to verify and compare coating optical performance as well as for the verification of durability (remaining presence) of coatings subject to accelerated testing. Additional characteristics and methods (e.g., droplet roll-off angle) may prove relevant to the application environment.

4.2 Backsheets

Backsheet development has been an active area of research for many years with new materials and structures introduced recently, driven primarily by cost. Backsheets based on PVF and PET have been used for more than 30 years and have served as good standards for performance and durability in PV applications. Field studies have confirmed its long term performance relative to other backsheet materials [145, 181].

New materials introduced into backsheets have included those based on polyester (PET), polyvinylidene fluoride (PVDF), polyamide (PA), fluoroethylvinylether (FEVE), and polyolefin (PO). The backsheet structure has also evolved from the established PVF/adhesive/PET/adhesive/PVF (aka TPT) to TPX structures where the outer layer has high weatherability and protection of the core layer of the backsheet and the inner layer is designed to have good encapsulant adhesion and protection of the core layer from UV exposure from the front side of the module.

New polyolefin backsheets have been introduced into the market which replace various layers in the backsheet structure including the core PET layer with polyolefin films (blends of polypropylene and polyethylene) [182]. Offerings from different manufacturers have been commercially introduced and claim advantages including a more simplified manufacturing, lower moisture permeability and better hydrolytic stability [40, 183–186]. However, it is difficult to substantiate these advantages without long term accelerated testing that can be correlated with field data. In addition, recent unanticipated backsheet failures including those from a commercial and widely adopted coextruded PA backsheet have highlighted the need for detailed understanding of the possible failure mechanisms associated with new backsheet materials and structures.

4.2.1 Critical backsheet issues of fielded modules

Fielded module evaluations are critical to assessing material degradation and ultimately informing future material design. Indoor accelerated testing is widely conducted but still lacks the ability to accurately portray the results observed in the field. A prime example of this discrepancy is the prevalence of polyamide based backsheet cracking. This material, which passed all indoor accelerated testing has seen large scale failures in the field [6, 38, 187]. In a follow up examination of testing standards, Kempe et al. were unable to replicate the cracking observed in the field after 4000 hours of A3 exposure [138]. Only upon testing using both UV and thermal cycling were cracks reproduced. Lyu et. al., reported that only under the combination of humidity, heat, and light did acetic acid assist in the formation of cracks in polyamide backsheets [6]. These cracks originated in the inner and core layers and propagated through the material to the outside layer [6]. Other materials have also been observed to have field specific failures. Wieser et al. have observed PVDF cracking in field retrieved modules. This failure has been replicated in indoor sequential exposures [145, 187]. This has been associated with a change in phase of the PVDF material. In an indoor exposure test Wang et al. observed a change from the α-phase to the β-phase [188]. However, other studies reported a change from β-phase to the α-phase after damp heat exposure [189]. It is unknown what the mechanism for this phase change is. Regardless of mechanism, it has been shown that this phase change is associated with the loss of ductility in the material.

Fielded module tests are critical to informing new procedures that would replicate the stressors that caused the failure of polyamide base backsheets. Moreover, other types of degradation can only be observed by analysing the field architecture. Fairbrother et al. have observed a spatial dependence of the backside irradiance of modules [190]. This leads to an increase of degradation predictors in the areas of high irradiance. This observation was further expanded

on by Wang et al. in their paper modelling the degradation predictors as a function of their location inside a PV module rack [191]. A statistically significant difference was observed between the degradation predictors between the modules on the rack ends as opposed to those located in the centre of the rack [191]. Additionally the vertical position in the rack also affected the degradation parameters [191]. This macro scale observations of fielded module conditions elucidate effects that materials may not be exposed to during routine indoor testing. To overcome these issues, new test methodologies have been developed within the materials and module test communities and are being adopted within the standards community as an approach to better predict long term performance [173, 192, 193].

4.2.2 Reliability of co-extruded backsheets

In 2010 co-extruded backsheets were introduced into the PV market. The main driving factors for this development were cost reduction and the addition of new features. Co-extrusion allows for thickness optimization in agreement with IEC backsheet and safety standards[REF?]. Moreover, expensive fluoropolymers (PVF, PVDF) are replaced with lower cost polymers (PET, PA, PP, PE derivatives). Additionally, also processing steps are reduced by using co-extrusion.

New materials also allow for new features from co-extruded backsheets. Functional properties like selective permeability, i.e. high acetic acid transmission rates (AATR) and low water vapor transmission rates (WVTR) [39], enhanced optical properties [40], where increased reflectivity leads higher power output via backscattering of light, or increased thermal conductivity have been added to the property profile. The main advantages of co-extruded backsheets are as follows: the full back integration allows for easy material modifications regarding additive formulation, fillers or layer geometry. Also, the backsheet is produced in one step, which also means reduced processing induced material degradation [194]. Also, the likelihood of delamination, which is a major backsheet failure mode, should be significantly reduced.

The first co-extruded backsheet on the market was introduced in 2009/2010 [7, 195] and was based on a symmetrical structure consisting of 3 layers of polyamide but with different filler material in the outer/inner and the core layer. The outer/inner layer was filled with TiO_2 particles to increase the reflectivity, whereas the core layer contained PP and about 20 % of glass spheres for increased mechanical strength [7].

In particular in recent years, an increased occurrence of PV module failures with cracked polyamide (PA)-backsheets have been reported [27,28]. Two main types of polyamide backsheet-cracking were observed: (1) tile-shaped, square cracks (along the intercellular spacing) see Figure 10: PA cracks. Longitudinal and squared cracks of PV modules with PA backsheets [7]. cracks (right) and (2) longitudinal cracks (beneath the busbars of the cells) – see Figure 10: PA cracks. Longitudinal and squared cracks of PV modules with PA backsheets [7]. cracks (left).

Figure 10: PA cracks. Longitudinal and squared cracks of PV modules with PA backsheets [7].

The cracks revealed after several years of field aging have never been observed in forgoing qualification and reliability tests as they are suggested to be the result of a combination of multiple stresses and might also include unexpected material interactions as drivers. Only recently for the first time similar polyamide backsheet cracks have been reproduced by an indoor accelerated aging test utilizing simultaneous combined stresses (UV, humidity, temperature and thermo-mechanical load) [196].

Eder et al. [7] identified the daily and seasonal temperature changes and their corresponding thermo-mechanical loads/stresses due to different thermal expansion coefficients of the different PV module layers as the main driver for crack propagation. The main factor for crack initiation can be found in a physical aging process of PA12 [7][45], which significantly reduces the ability for plastic deformation of the backsheet, visible in the significant decrease of strain-at-break values.

Simulations of tensile stresses building up in standard PV modules yielded a maximum tensile strain of 18 %, occurring between the area of the cells and backsheet [197], which is more or less the strain-at-break value of PA backsheets after aging. Chalking and photo-oxidative degradation of the outermost (only a few µm) PA-layer is caused by outdoor weathering and not related to crack formation. It is assumed that microcracks develop randomly at local notches with slightly higher stress concentrations. But these cracks were found to be very short and only in near surface regions (outer PA layer). Sometimes microcracking is accompanied by a partial delamination of the outer layer. The longitudinal cracks (LC) are directly located below the ribbons (busbars), which usually have a height of around 200 µm. This elevation imposes additional tensile stress in the backsheet, resulting in cracking from the airside of the backsheet into the core. These LC mostly are more pronounced in length and broadness and are always aligned with the busbars (MD). LCs can grow with ageing time and passing through the core layer of the co-extruded backsheet leaving the encapsulant protected by only the inner layer from open contact with the atmosphere.

For the squared cracks (SC), however, a different root cause and appearance has been found. SCs start to grow from the interface encapsulant/ inner PA-layer into the core and outer layer of the backsheet. In this respect it is important to note that SC are exclusively forming in cell interspaces and only in conjunction with certain EVA types/qualities which are prone to show degradation accompanied by significant acetic acid formation. Sun irradiation seems to be one decisive driver for the beginning degradation of the PA-inner layer and the EVA at their joined

interface. An additional environmental stress cracking effect, caused by the formation of acetic acid and the presence of phosphoric additives was suspected by the authors [7].

As the formation of micro- and longitudinal cracks is a two-step process it was not discovered in the predominant single stress tests that were used back in 2010 [7]. Usually the materials and test modules were exposed separately to several thousand hours of damp heat testing, several hundred thermal cycles (according to IEC 61215) and several thousand hours to artificial sunlight weathering (xenon lamps) [114]. After damp heat or prolonged xenon exposure, the decrease in strain-at-break of the backsheet would have been observable, but without combination with crack initiating thermo-mechanical loads, the specific failures like squared cracks and/or longitudinal cracks could not been detected. Furthermore, during thermal cycling, the thermal load seems to have been to too low to induce the physical aging effect of the PA backsheet, which would have induced a reduction in elongation at break.

Also, other companies started to work on co-extruded backsheets in 2010, when the first patents for PP based backsheets were filed [198]. In 2012 a new backsheet, based on cost effective crosslinked polyolefins was developed for solar modules [199]. The coextruded PE based backsheet consists of three polyethylene (PE) layers with different additive contents (the middle layer is a silane crosslinked PE). The crosslinks are built with Si-O-Si bridges with ~5 crosslinks per 1000 C-atoms [200, 201]. It results in a higher thermal stability (120 °C for long-term exposure). Results from artificial weathering on this backsheet revealed a good performance [199, 201]. After 5000 h of damp heat testing and 1500 h of UV and Xenon testing only slight effects of chemical aging have been observed. By IR spectroscopy the formation of carbonyl groups due to oxidation was detected. Also, using UV/Vis/NIR spectroscopy, slight changes in the reflection spectra were observed. Nevertheless, the UV stabilization remained effective, and therefore the ultimate mechanical properties were not affected due to the accelerated aging tests. Especially after the damp heat test at 85 °C physical aging effects have been observed. With tensile test an increase in elastic modulus and yield strength was measured. This can be attributed to post- and re-crystallization of polyethylene, which was revealed by DSC measurements. DMA showed that the damping factor is strongly influenced by exposure to elevated temperatures [202].The polyolefin backsheet also proved to greatly reduces the corrosion by low water vapor transmission and high acetic acid transmission [201]. Another study showed that the PE based backsheet was especially modified for long term durability. This is shown by high temperature aging of up to 170 °C, where an extrapolated lifetime of more than 50 years was calculated [199]. Also, here no yellowing or change in optical properties was observed after 4800 MJ/m² of Xenon lamp exposure and 2600 MJ/m² of UV fluorescence lamp exposure. According the paper this corresponded to more than 50 years of outdoor application in a standard module in Germany and Arizona. However, this backsheet was discontinued a few years after for undisclosed reasons and is not available any more.

A new class of co-extruded backsheet based on different combinations of polyamide and polyolefins have been launched into the market starting around 2015 [185, 186, 198, 203]. This specific composition claims to have lower WVTR and higher acetic acid permeability than PET based backsheet. First reliability studies on this backsheet showed excellent stability against damp heat and UV exposure [185][203]. Another study exposed modules with such backsheets to hot and humid climatic conditions in India. After 18 months of outdoor exposure no visible aging and power degradation was observed [186].

Most recently backsheets based on PP were developed and successfully introduced into the market [40].The material combines the low WVTR of PET based backsheets but provides high permeability of acetic acid but also oxygen. The general material behaviour of these kind of

backsheets is different compared to standard PET based backsheets. Co-extruded PP backsheets have lower stiffness and higher flexibility than laminated backsheets with a PET core layer (see Figure 11: Tensile stress-strain curves of co-extruded PP and laminated PET based backsheets.). Several studies reported excellent stability towards damp heat as well as extensive irradiation exposure [183, 184, 204]. None of the studies showed any significant deterioration of mechanical properties or sensitivity for embrittlement and cracking. Only slight yellowing was observed, mostly depending on the different additives used.

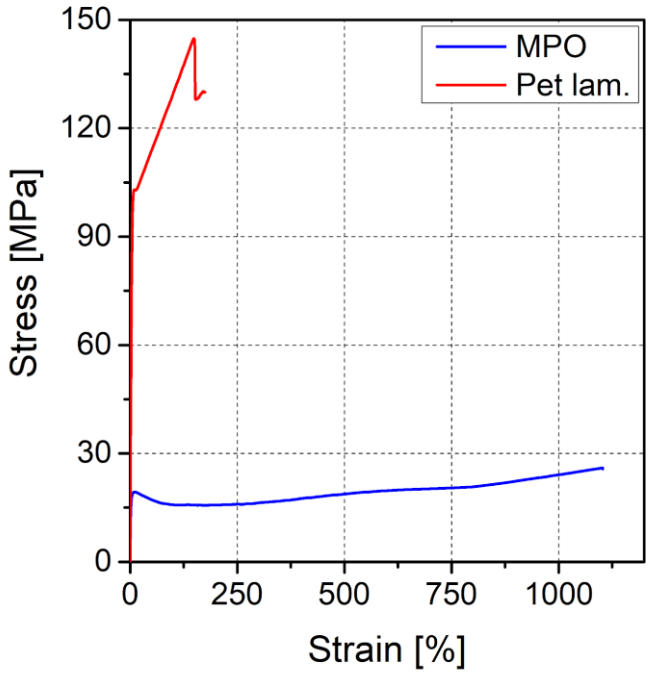

Figure 11: Tensile stress-strain curves of co-extruded PP and laminated PET based backsheets.

4.2.3 Transparent backsheets

Another recent development has been the commercial introduction of transparent backsheets. While transparent backsheets from different manufacturers have been used in the past in building-integrated PV (BIPV) applications [205], the emergence of bifacial cells and modules has driven further development of materials [206, 207]. Transparent backsheets have been commercially adopted by module manufacturers including Jinko and LG and have been deployed into the field.

The requirements for a transparent backsheet are similar to those of white and black backsheets used for over 30 years but with some important differences. In the case of white backsheets, the inner and outer layers of the backsheet include white pigment and UV stabilizers to prevent UV light from damaging the PET core of the backsheet. In the case of transparent backsheets, UV stability and high light transmission is critical to the output power of the bifacial module. Stable optical and mechanical properties are therefore required. From the rear side of the module, the outer layer of the transparent backsheet needs to block damaging UV wavelengths from reaching the PET core while efficiently passing light in the range of the bifacial silicon cell spectral sensitivity. From the front side of the bifacial module, a combination of UV

transmitting and UV absorbing encapsulant reduces the direct UV component to the inner side of the backsheet. This UV exposure can be further reduced by using a white grid patterned on the inner side of the backsheet to block and reflect light from the cell gaps, leading to higher power from internal reflections on the front and back of the bifacial module.

While transparent PVF films have been available from DuPont (designated TUT) for more than 20 years and successfully used in the PV industry in BIPV applications [206], a new PVF film was developed for long term performance. UV light blocking over the course of UV exposure is shown in Figure 12 for the old and new PVF film. The protection of the core PET is critical in this application and UV durability of a transparent backsheet using PVF is shown in Figure 13.

While bifacial modules were first introduced into the market using primarily double glass module structures, the glass/backsheet structure offers several advantages. Double glass modules are much heavier the glass backsheet bifacial modules, typically from ~18 % to 34 % heavier for a 72 cell module for 2 mm / 2 mm and 2.5 mm / 2.5 mm glass respectively. The higher weight has implications on transport, installation and BOS. The greater thermal mass, longer evacuation times, greater bubble entrapment and thicker encapsulant in double glass modules have implications on module production throughput. New lamination equipment is also required to produce double glass modules effectively. Finally, double glass modules have limited field history and delamination has been observed in older double glass modules leading to some reliability concerns. The durability of modules using transparent backsheets was compared to double glass structures under typical accelerated stress conditions including damp heat, UV and thermal cycling with similar performance found in both structures [207]. In comparison with outdoor performance, the GB structure was also found to have lower operating temperature compared to GG modules, consistent with modelling developed by Sandia. This higher performance due to lower temperature has also been reported by Jinko. In addition, better PID performance with transparent backsheet compared to double glass was observed in 60 cell modules produced with identical p-PERC cells and POE encapsulant [206].

The commercial development of transparent backsheets should further the development of polymeric frontsheets as well where similar requirements exist with higher UV durability requirements from direct exposure.

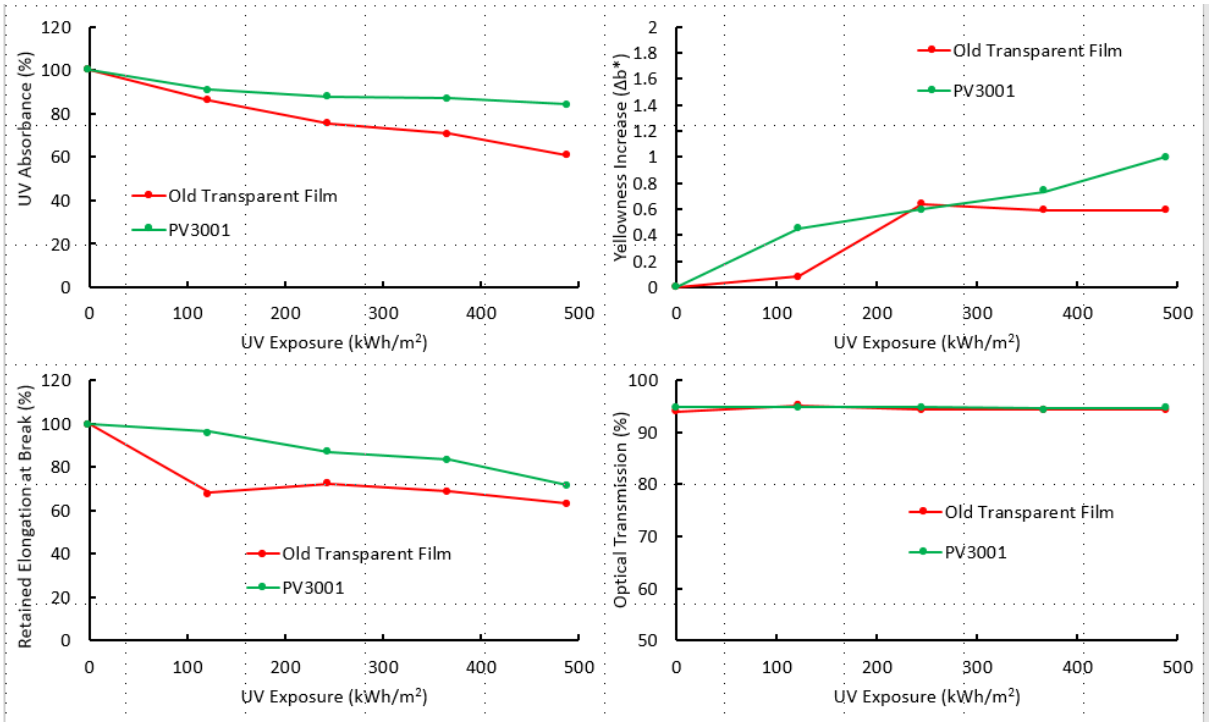

Figure 12: Comparison of the durability old and new PV3001 transparent PVF film for UV absorbance, yellowness, elongation and optical transmission.

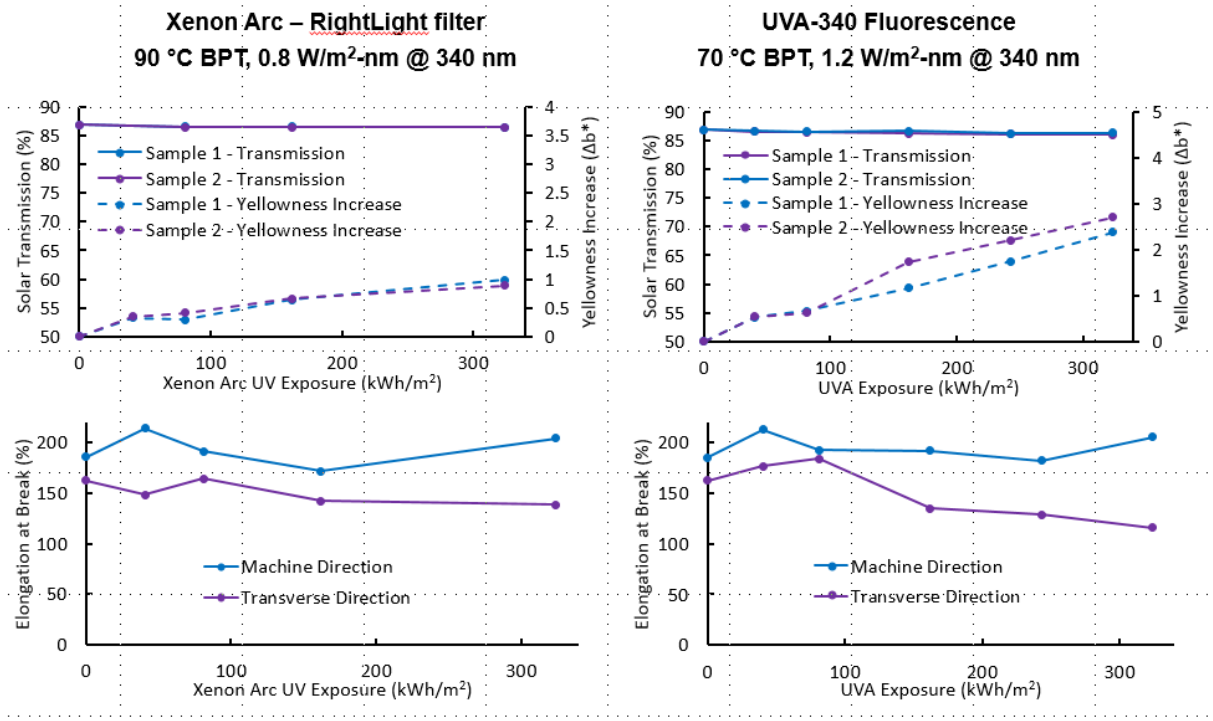

Figure 13: Comparison of the durability of a transparent PVF based backsheet from the rear side under two UV accelerated stress conditions.

4.3 Encapsulants

Polyolefin (PO) materials and silicone encapsulants are presently being explored as an alternative encapsulant material to EVA. The polyolefins used in PV modules share a similar composition with EVA, i.e., a polyethylene-based chemistry, without the vinyl acetate side groups. Silicone encapsulants are based on a -Si-O- or similar backbone structure, rather than a hydrocarbon structure.

4.3.1 Polyolefin encapsulants

Polyolefin elastomers (POE) and thermoplastic polyolefines (TPO) are all polyethylene-based materials. The difference lies in the chemical nature of the side groups attached to the main polyethylene chain, which can be acrylates, acrylic acids or n-alkanes. PO encapsulants generally have similar or higher volume resistivity than EVA and lower WVTR, see Chapter 2 for more about PV encapsulants' properties.

POE is chemically crosslinked via peroxide reaction, as well as EVA, and has the advantage that no acetic acid is produced with aging because no vinyl acetate moieties are present. POEs have been found to be a valid alternative to EVA with the additional advantage that these encapsulants are not prone to develop PID [11, 12].

TPO does not need chemical crosslinking and during the lamination process they simply melt to connect all the PV module's components. TPO has higher melting temperature than EVA and POE, 100 °C to 110 °C compared to 60 °C to 70 °C, but lamination time can be shorter, as no crosslinking reaction has to take place [49]. Nevertheless, the lamination time should be at least long enough to let the material flow and adhere to all of the PV module's layers. TPO showed higher transmittance values and higher thermal stability than EVA [51], less susceptibility to creep [14] and very good adhesion at the glass-encapsulant interface as well as at the glass-backsheet interface.

The optical-performance and optical-durability of polyolefin encapsulants

The same characterization methods for EVA may be used to quantify the optical performance of PO materials. For example, transmittance, spectral bandwidth, yellowness index (*YI*), and UV cut-off wavelength (λ_{cUV}) may be determined using IEC 62788-1-4 [208].

The spectral transmittance, measured using an integrating sphere, is shown for representative thermoplastic TPO and thermoset POE materials in Figure 14. Specimens in the figure are from the International Photovoltaic Quality Assurance Task Force (PVQAT), task group 5 (UV weathering) "Study 2", concerned with the IEC TS 62788-7-2 weathering standard [209]. In Figure 14, unaged specimens (solid line) are compared to artificially weathered specimens (dashed line). The UV transmittance is shown in detail in the inset (left) of the figure.

The optical performance of TPO and POE encapsulants is generally similar to EVA [210, 211]. The transmittance and spectral bandwidth depend on the material formulation, including the UV absorber(s), UV stabilizer(s), and anti-oxidant(s). As in EVA materials, separate UV-transmitting formulations and UV-blocking formulations may be used for the incident-irradiated-surface or the back-surface of the cell, respectively. The UV cut-off wavelengths (10 % transmittance) of 246 nm (for UV-transmitting POE-2), 275 nm (for UV-blocking TPO-1) and 276 nm (for UV-blocking TPO-2) are similar to those of UV-transmitting EVA and UV-blocking EVA formulations. Polyolefins may have higher crystalline content than EVA (typically on the order of 5%) with consequent optical scattering. Crystalline content in EVA is reduced in proportion to vinyl acetate content (Vac), which commonly varies from 28 % today to 33 % for traditional EVA for PV). Reduction in transmittance and rounding of the UV cut-off spectra results from

crystallinity (where TPO-2 has a greater crystallinity than TPO-1) as well as discoloration (from the formation of chromophores for the weathered specimens).

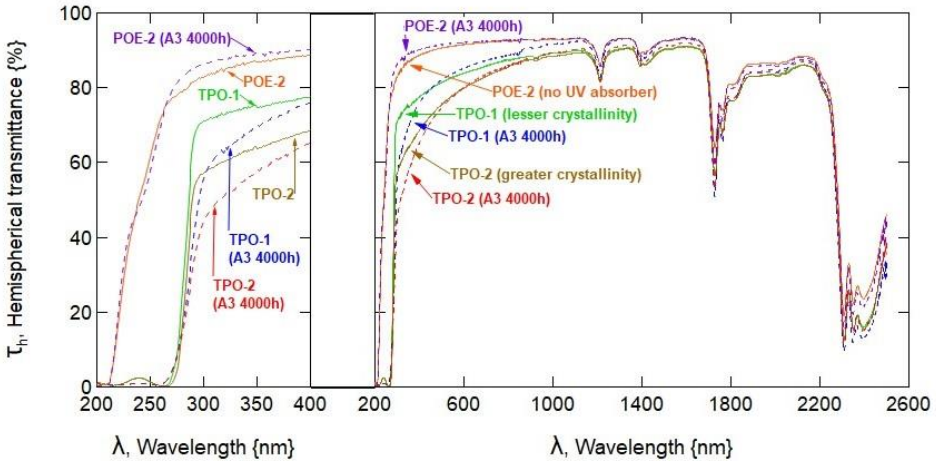

Figure 14: Spectral transmittance of polyolefin encapsulants, including a thermoplastic (POE-2), a thermoset with lesser crystallinity (TPO-1), and a thermoset with greater crystallinity (TPO-2). A solid line is used to indicate the hemispherical transmittance (with an integrating sphere) for unaged specimens; a dashed line is used to indicate the transmittance for specimens after artificial UV weathering (IEC TS 62788-7-2, method A3 for 4000 hours).

The characteristics of haze, *YI*, and λ_{cUV} may be used to further assess the optical performance of encapsulants. Haze (%) may be determined from the difference between the hemispherical transmittance, τ_h (%), and the direct transmittance, τ_d (%), **Fehler! Verweisquelle konnte n icht gefunden werden.**. *Haze* specifically quantifies the optical scattering, where a value of zero would indicate no scatting and a value of 100 would indicate strictly diffuse light. *YI* may be determined from ASTM E313 [212]. *YI* quantifies the discoloration, where a positive value would be perceived by a human observer as yellow and negative value would be perceived as blue. *YI* may be increased by optical scattering in addition to discoloration. A change in λ_{cUV} may signify the loss of a formulation additive (as suspected in [213], no example will be given in the figures in this section).

$$haze = \frac{\tau_k - \tau_d}{\tau_k} \quad (1)$$

The haze and *YI* of the PO materials in Figure 14 are shown as a function of artificial weathering in Figure 15. The effect of weathering is examined in the figure in separate read points up to the cumulative duration of 4000 h. Errors bars are shown in the figure for two standard deviations. The greatest *haze* is seen for TPO-2 (greater crystallinity), then TPO-1 (lesser crystallinity), with the least *haze* for POE-2. The *haze* is seen to slightly decrease with weathering for TPO-2 and TPO-1 (suggesting a loss of crystallinity), whereas *haze* increases slightly with weathering for POE-2 (suggesting an increase or evolution of the structure of the crystalline content). The *YI* is relatively stable through the first 75 MJ m^{-2} of UV exposure, followed by an increase in *YI* for TPO-2 and TPO-1. The *YI* of 10 is modest, being within the range of perception for some human observers without being placed on a white background. The simultaneous increase in *YI* occurring as haze is decreased suggests discoloration of TPO-2 and TPO-1. The *YI* is greatest for TPO-2 throughout the experiment, which may follow from the effect of optical scattering rather than just discoloration. The changes in *haze* and *YI* in are modest, however, the nominal dose in IEC TS 62788-7-2 [138] method A3 simulates in the

order of the first 5 years of field use for PV modules installed in a temperate (e.g., continental or maritime) climate using a modest (e.g., rack or tracker) mounting configuration.

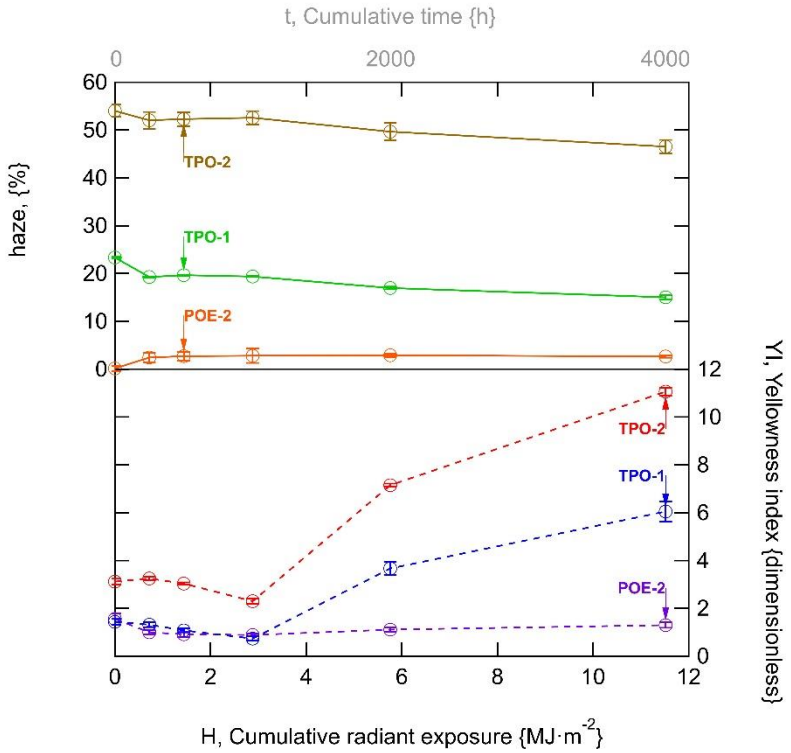

Figure 15: Optical scattering (the haze) and discoloration (YI) for the aforementioned polyolefin encapsulants. Optical performance is distinguished between the materials as well as with the IEC TS 62788-7-2 weathering (method A3), where the cumulative exposure is indicated at 340 nm.

As shown in Figure 14 and in Figure 15, encapsulants can be distinguished by their initial performance and/or the effects of weathering. Optical performance immediately results from the formulation additives, whereas it may require prolonged and/or sequential accelerated tests to identify the effects of weathering. Industry normative methods to examine the interaction between components in a PV module (e.g., the encapsulant and interconnect ribbon) remain to be developed. The effect of weathering is typically observed as the attenuation of transmittance with rounding of the UV cut-off transition, as shown in the inset of Figure 14 for TPO-1 and TPO-2. At least initially, change in *haze*, *YI*, and λ_{cUV} with weathering may result from independent effects. Fortunately, the principle optical performance characteristics and their durability to weathering may be characterized using the same methods used for EVA encapsulant. This should allow for direct comparison between encapsulants using the same test equipment.

4.3.2 Recent studies on reliability of PO encapsulants

French et al. studied minimodules with multicrystalline monofacial Al-BSF, monocrystalline bifacial PERC and multicrystalline bifacial PERC with different back encapsulants exposed under modified damp heat conditions (mDH at 80 °C and 85 % RH). The trend of power loss, see Figure 16, was more evident for white EVA and Al-BSF combination. It was observed that Al-BSF had a power loss of about 50 % with white EVA. Other modules were seen to have a power loss of about 10-30 % with white EVA [214].

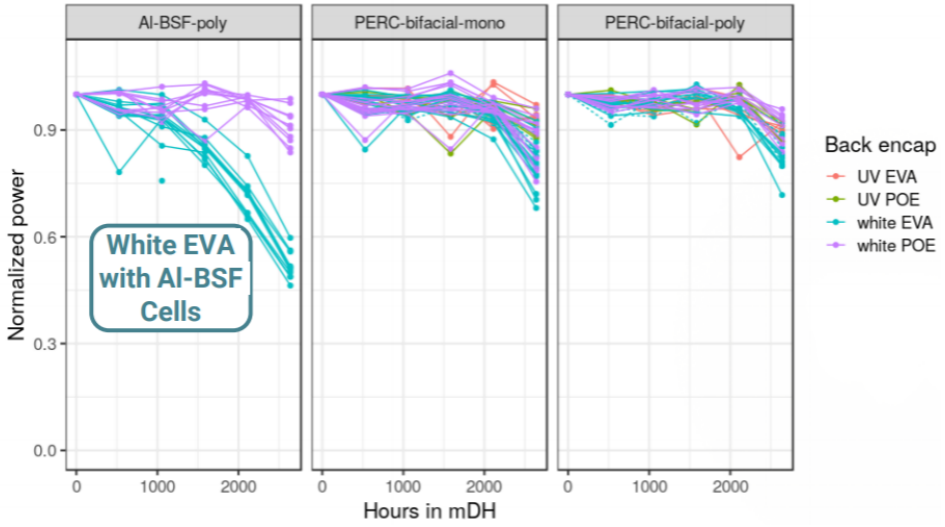

Figure 16: Normalized power trends of multicrystalline monofacial Al-BSF, monocrystalline bifacial PERC and multicrystalline bifacial PERC with different back encapsulants.

Braid et al. [215] used various rear encapsulants (UV-cutoff EVA and white EVA) for fabricating 12 72-cell modules containing either multicrystalline monofacial Al-BSF, monocrystalline monofacial PERC (Gen1) and monocrystalline bifacial PERC (Gen2) cells, the modules were exposed under DH for up to 3000 hours and thermal cycling conditions (alternating between -40 °C and 85 °C for 6 hours in 100 cycle intervals for up to 800 cycles). All Al-BSF modules and Gen1 had UV-cutoff EVA as the rear encapsulant whereas all Gen2 modules made use of white EVA. It was observed that the Gen2 modules (with white EVA as back encapsulant) showed a drastic power loss in comparison to other modules and the encapsulant was disqualified for further analysis. Gen2 was seen to have a greater power loss than Gen1 along with an increase in series resistance (R_{sh}) and decrease in short circuit current (I_{sc}) due to corrosion in the busbar region and degradation of passivation layer (the presence of localized back contacts makes it more vulnerable to corrosion). The degradation continued for Gen2 during dark storage period of 3 months after 2000 hours of DH exposure due to the presence of residual acetic acid. Those that underwent thermal cycling showed considerably lower levels of power drop compared to DH counterparts and an increase in R_{sh}, decrease in FF were seen. One of the reasons for the increased degradation in Gen2 modules was the usage of EVA; the higher level of TiO_2 could have led to the formation of radicals that sped up the degradation process.

UV stability of coupons fabricated by using a TPO encapsulant was studied by Adothu et al. [51]. The performances of coupons laminated with TPO were compared to coupons laminated with a commercially available fast-cure EVA. They reproduced hot and dry conditions by using a 365 nm LED light source with a maximum intensity of about 900 W/m2, at a temperature of 90 °C and 10 ´% to13 % RH. They exposed the samples at the conditions described above up to 50 days. Samples laminated with TPO showed better optical performances after 50 days of UV exposure than samples laminated with EVA. Additionally, they reported a peel adhesion strength of about 200 N/cm at the encapsulant-glass interface, as well as at the encapsulant-backsheet interface, which is higher than what is usually observed for EVA. In a following study [14], 72 cells standard modules were fabricated using EVA and TPO as encapsulation materials and their performances were compared after exposing the modules to 1000 hours of DH

test. Modules produced with TPO showed higher power output (about 3 %) compared to the modules produced with EVA, lower discoloration after 1000 hours of DH test and higher toughness.

Barretta et al. compared degradation behaviour of EVA, TPO and POE films not encapsulated under artificial ageing tests, with a focus on changes in additive composition of the encapsulants and their effects on degradation processes taking place. They observed no relevant changes in chemical, thermal and optical properties after 3300 hours of DH storage. EVA and POE showed a similar behaviour upon UV exposure with signs of photo-oxidation observable only with an applied dose of about 200 kWh/m^2, whereas TPO showed the most extensive damages (yellowing, embrittlement, reduced thermal stability, depletion of stabilizers).

The effect of microclimate on encapsulant degradation was also studied by Ottersböck et al. [216]. They studied the degradation behaviour of single films of TPO and three different types of EVA as well as laminated glass/encapsulant/backsheet samples under artificial ageing conditions (DH and Xenon test) for a total exposure up to 2000 hours. They observed different ageing behaviour according to the different microclimatic conditions. Additionally, under irradiation, they saw evidence of deacetylation reaction for samples laminated with EVA, proved by the increase of crystallization temperature, whereas, for TPO only morphological changes related to reversible processes were detected.

Oreski et al. [52] investigated chemical, optical, thermal and thermo-mechanical properties of TPO and POE and compared their properties to an EVA reference encapsulant. They produced single cell as well as 6-cell framed test modules and exposed them up to 3000 hours of DH test. TPO showed the lowest thermal expansion compared to the other two encapsulants, thus being the most thermo-mechanically stable material (thanks to the higher melting temperature). Modules laminated with TPO and POE are semi-transparent in the UV region, whereas EVA showed a sharp UV cut-off at 375 nm. The test modules showed no relevant power degradation upon DH exposure, only samples with TPO showed some yellowing that disappeared after irradiance. After 3000 hours of DH exposure, samples with EVA encapsulants showed signs of silver grid corrosion, which was not detectable in TPO or POE samples, see Figure 17. The presence of Ag-acetate was detected, due to EVA hydrolysis and formation of acetic acid during DH storage.

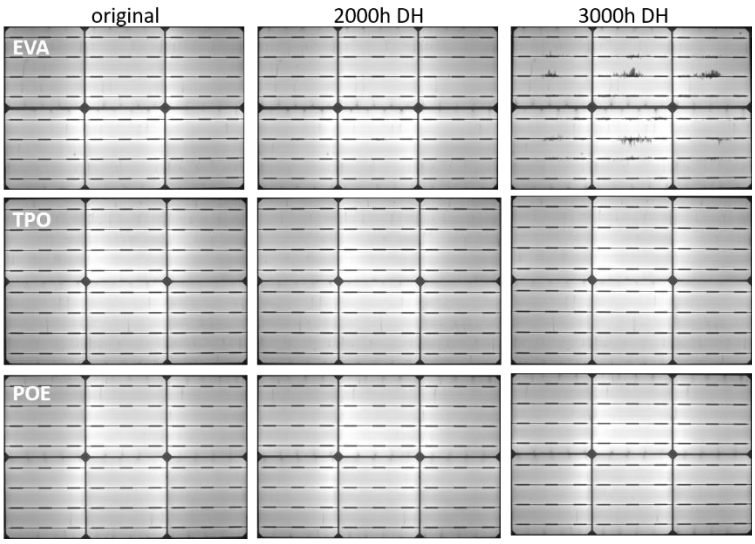

Figure 17: EL images of test modules before and after 2000 h and 3000 h of DH storage [6].

4.3.3 Recent silicone encapsulant developments

Silicone encapsulants - poly-dimethyl siloxane (PDMS) and its derivatives - had been utilized to laminate the PV cells in a PV module before early 1980s [78, 217], because of their notable stability and durability against various kinds of environmental stressors [18]. Lower degradation of the PV modules with silicone encapsulant has been reported [218, 219]. However, the utilization of silicone was limited in the PV market, since the cost for using silicone as a PV encapsulant was much higher than EVA due to material cost and the complexity of applying silicon as a viscous liquid to PV modules during production. [220]. Despite these barriers, silicone has certain technical advantages for the encapsulation of PV cells: corrosion protection and no discoloration following UV exposure [18, 220], PID inhibitive properties [221], and superior optical transmission. The higher UV-transmissivity of silicone can enhance the efficiency of PV modules [220, 221].

Recently a silicone encapsulant-sheet has been developed and launched, which can laminate the PV cells under a conventional vacuum-heat lamination process. In the report on the reliability of PV modules with this silicone encapsulant-sheet, similar features were observed to those of conventional silicone (liquid form) [222]. Modules with this encapsulant did not observe any corrosion in their EL images after DH6000 , unlike the PV modules with EVA (Figure 18). Interestingly, even when this silicone encapsulant-sheet was only utilized as a front-side encapsulant, obvious corrosion was not detected. Also, no PID was found in the PV modules with this silicone encapsulant-sheet, as well as the previous reports on the reliability of those with the conventional silicone encapsulants. Though the details in other properties (including stability and durability against thermo-mechanical / optical-weathering stressors) have not been reported yet, similar reliability to that of PV modules with conventional silicone might be expected. Hence, the utilization of silicone materials is assumed to increase in the future as this development is further tested and validated.

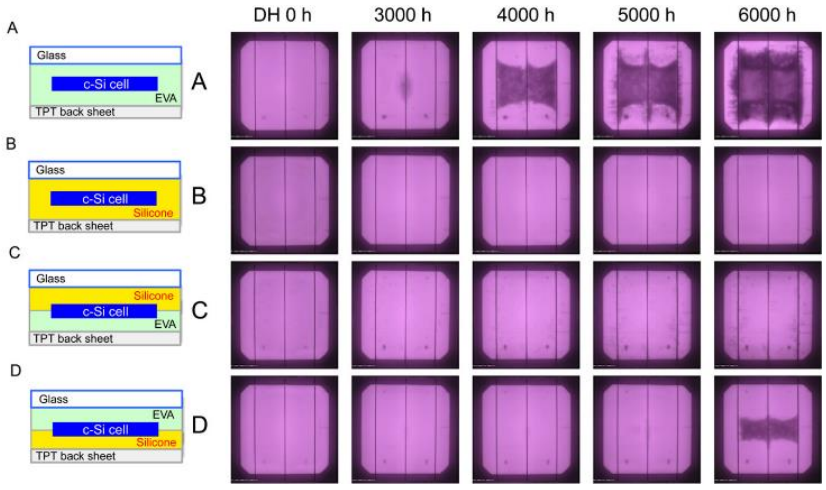

Figure 18: EL images during DH stress test. Configurations of tested PV modules are indicated in the left panels (A to D). Copyright (2018). The Japan Society of Applied Physics.

4.4 Cell interconnection and metallization

As pointed out in section 3, new cell architectures often require new interconnection approaches. In the following sections, the most recent and prominent approaches are presented.

4.4.1 Multiwire and low temperature solders

The current trend in crystalline solar cell interconnection is to increase the number of busbars (BB) in order to reduce the amount of silver (Ag) for the cell metallization and to increase the module efficiency. Following this trend has driven the development of cells that have front metallization fingers but no busbars, referred as busbar-less cells interconnected by means of multi wires [223].

In SCHMID's Multi Busbar concept (MBB), 15 solder coated copper wires are soldered on the cells before lamination by infrared soldering [50]. In SmartWire Connection Technology (SWCT™) , copper wires coated with a thin low melting point solder layer are supported by a polymer foil (Foil Wire Assembly - FWA) and the interconnection is carried out during the module lamination process by the alloy layer that builds up a solder contact to the cell metallization [224], (Figure 19). This approach was initially proposed by Day4 Energy [225] (patented in 2003) and today is mass produced by the Meyer Burger group with automated production [30, 226].

Figure 19: SmartWire Connection Technology (SWCT™).

By carrying out the interconnection during the module lamination, typically at a temperature of about 140 °C to 160 °C, i.e. below soldering temperature used with BB technology, SWCT™ induces less thermo-mechanical stress on the cells. This enables SWCT™ to be well suited for the interconnection also of the new upcoming thin wafer cells. SWCT™ is compatible with all type of cell concepts (both monofacial and bifacial), such as rear emitter passivated cells (PERC), silicon heterojunction (SHJ), metal plating and interdigitated back contact (IBC).

The reason why by increasing the number of interconnection wires, the amount of Ag is reduced, and the module efficiency is increased is due to the fact that the power dissipation losses in the fingers, P_f, is inversely proportional to the square of the number of busbars as where J is the current density, L is the width of the cell, n_f is the number of fingers, R_f is the finger line resistance, n_{BB} is the number of busbars and C is a constant [30][99,100].

$$P_f \propto \frac{J^2 L}{12 n_f} \frac{R_f}{n_{ff}^2} \propto C \frac{R_f}{n_{ff}^2} \tag{2}$$

By increasing the number of wires to 18, like for example in the case of SWCT™ design, the same power loss as for a 5BB design can be achieved for finger line resistance 13 times higher. While fingers with a line resistance of less than 1 Ω/cm should be implemented in 5BB cells to

achieve optimum performance, a multiwire method with 18 wires allows the integration of fingers with a line resistance of up to 10 Ω/cm, to realize similar electrical losses in the fingers. Thinner fingers that use less Ag are possible if higher resistance is acceptable. Furthermore, thinner fingers and a lack of thick busbar ribbons results in more light reaching the cell, which increses efficiency.

Thanks to the low temperature contacting process, SWCT™ has the advantages of reduced consumption of Ag and increased module efficiency and can be used with SHJ cell technology that cannot tolerate high temperatures required for conventional soldering, due to degradation of the passivation properties of the amorphous hydrogenated silicon (a-Si:H) layer. At the cell metallization level, this constraint imposes the use of low-temperature-cured Ag pastes, with curing temperatures typically below 230 °C. These pastes have bulk resistivity about 2 or 3 times higher than standard high-temperature cured Ag paste used for mono-junction solar cells [227]. With a standard BB design, to keep the P_f as low as possible with high bulk resistivity Ag pastes, more Ag and thicker fingers are required to keep R_f as low as possible (see Eq 2). In [228] it is shown that the front side application of low temperature Ag paste for BB soldering interconnection of SHJ is about 145-165 mg per cell depending on the number of BB (Figure 22), this is about 50% to 80% higher than for the high temperature paste used in the case of standard crystalline solar cells. The consumption of Ag jumps to 420-335 mg in the case of bifacial SHJ cells as Ag fingers are printed also at the back side. In addition, soldering on to low temperature cured Ag paste, a minimum BB thickness between 25 and 35 µm is necessary to avoid peeling off the Transparent Conductive Oxide (TCO) surface. All this induces higher silver consumption compared to standard silicon solar cells. As silver costs are ranked 2nd after the silicon wafers, reducing it use is important. Moreover, to reduce the stress between the cell and the ribbon, non-conventional bismuth based solder and dedicated flux are needed. An improvement in the interconnection of SHJ solar cells can be achieved if the ribbons are glued using electrically conductive adhesive (ECA). The constrains on the thickness of the BB are relaxed and the Ag paste mass drops in the range of 245 mg to 175 mg in the case of bifacial SHJ cells. The silver paste savings is may be offset by using ECA that has a similar price and also contains silver. SWCT™ has the advantage that much less Ag paste is required. With 18 wires, SWCT™ requires less than 100 mg of Ag for bifacial SHJ cells due the thinner fingers and no BB. Researchers hope to reduce this to 60 mg with further process optimization (Figure 20).

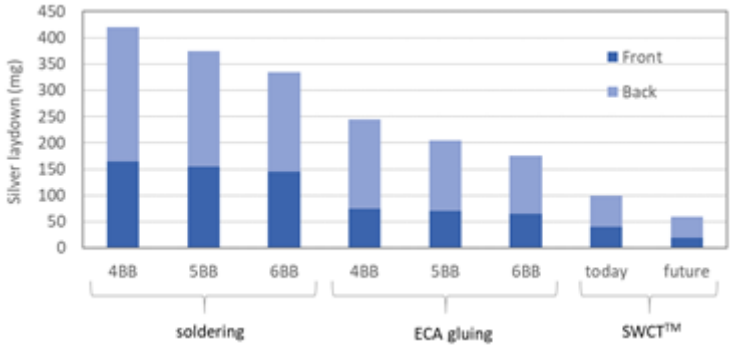

Figure 20: SWCT - Ag laydown - Mass of screen-printed low temperature silver paste deposited at front and backside of SHJ solar cell for three different interconnection technologies: soldering, electrical conductive adhesive (ECA) gluing and SWCT™.

The application of SWCT™ to SHJ has been helped by the recent development in the thin-line printing of low-temperature cured Ag pastes [30, 229]. The possibility of printing low-temperature cured Ag lines with sufficient conductivity using minimum screen openings down to 20 µm has been demonstrated and resulted in approximately 30 µm-wide fingers with a line resistance of 5 Ω/cm, which is sufficient for module integration using SWCT™ without adding electrical losses from the fingers. Printing a line width of just 16 µm on a textured waver coated with ITO has been demonstrated by using a special mesh with zero-angle orientation and a screen opening of only 12 µm as shown in Figure 21 [230].

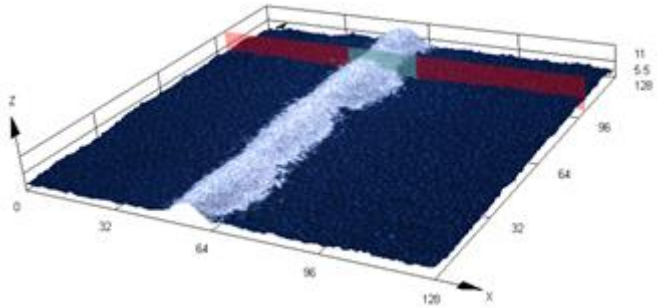

Figure 21: 3D reconstruction using a laser scanning confocal microscope (Olympus LEXT) of a low temperature silver paste printed with a 12µm screen opening (CSEM).

Another advantage of using round wires in multiwire interconnection technologies is the reduction in cell shadingcompared to standard BB technology for an equivalent cross section of copper [223]. The round wire geometry also allows the light to be reflected either back to the glass, where internal reflection occurs (when the angle of incidence is above 42°) or directly toward the solar cell. For example, wires with a diameter of 200 µm employed in SWCT™ exhibit an optical dimension of about 140 µm as a result of the re-collection of part of the light reflected onto the circular wire surface [30, 223]. This allows the transition from standard BB interconnection schemes using five busbars and flat ribbons to interconnections with round multiwire, without increasing the shadowing losses of the interconnections.

Additionally, module with multiwire interconnection appear to be more resistant to cell cracking. Each cell is contacted to the wires by 1000 to 2000 electrical contact points, enabling broken cell pieces to remain connected.

Finally, the use of multiple thin wires instead of fewer large busbars gives modules an aesthetic improvement, with a more homogeneous surface, as can be seen for instance in the facade of CSEM building with bifacial SHJ modules based on SWCT™ (Figure 4).

The design qualification and type approval of SWCT™ was demonstrated for both 60-cells and 72-cells SHJ GG module configuration by obtaining IEC 61215:2016 [114] and IEC 61730:2016 [128] certifications by TÜV Rheinland. In addition, extended reliability tests were done to further validate the ability of SWCT™ to withstand climatic natural environmental stresses. Impressive results were obtained for thermal cycling tests where no degradation was observed after more than 1000 cycles which corresponds to 5 times the IEC norm. Damp-heat tests were also pursued and a degradation of 4 % was measured after 14000 h which corresponds to 14 times the IEC norm (Figure 22).

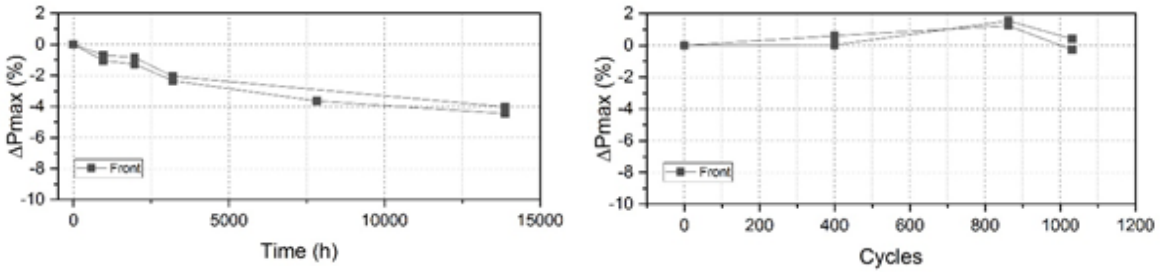

Figure 22: Maximum power variation of full size (72cell) modules SWCT tested in extended DH (left) and TC (right) conditions.

By using the new generation SWCT™ and mono-facial SHJ solar cells with efficiency of 23.4 % manufactured by French Atomic Energy and Alternate Commission (CEA) on Industrial Meyer Burger cell manufacturing equipment, a record 72 cells module with power of 410 Wp was produced in 2018 [231]. More recently, solar modules with 72 bifacial SHJ cells and the new generation SWCT™ cell connection technology has been industrialized by Meyer Burger with a power of 480 Wp (410 Wp monofacial operation). In 2019, REC solar has installed a 600 MWp SWCT™ production line [232] for 120 half-cells glass backsheet modules with a maximum power of 380 Wp [233] proving the full compatibility of this interconnection technology with modern cells designs.

4.4.2 Electrically conductive adhesives

Generally speaking electrically conductive adhesives (ECA) are composite materials based on a conductive filler and an insulating polymeric adhesive. Here, thermosetting as well as thermoplastic resins can be used as the matrix material. Epoxy resins, silicones or polyurethanes are widely used thermosets whereas polyimides are typical examples for thermoplastic resins used in ECAs [70, 234, 235]. Among the conductive fillers silver (Ag) is the most commonly applied. It has the highest electrical conductivity with the ability to retain its high conductivity even when the silver particles are oxidized. But also gold (Au), nickel (Ni), copper (Cu), tin (Sn), SnBi or SnIn coated copper in various sizes and shapes find application as filler materials [29].

Depending on the loading level and type or shape of the electrically conductive filler, ECAs are divided into isotropic conductive adhesives (ICAs), which are usually used to replace the traditional SnPb solder alloys in electronic interconnects, and anisotropic conductive adhesives (ACAs). Due to their high filler content (50 to 80 volume %) ICAs provide an electrical conductivity in all directions throughout the material (x-, y- and z-direction). Here, the resin is generally cured at higher temperatures to provide the shrinkage force to increase the conductivity, adhesion strength and chemical and corrosion resistance [29, 236, 237].

ECAs are currently starting to replace solders for ribbon bonding and have enabled novel cell interconnection technologies such as shingled cells [34, 238, 239].

Ribbon based interconnection based on electrically conductive adhesives

Connecting via print-application of ECA offers several advantages over the conventional solder process for electrical interconnection like the possibility of low temperature processing, potential for higher resolution printing and easier handling [234]. The soldering process requires temperatures of 210 °C for the conventional tin-lead solders or even more for lead-free solders. These high temperatures often cause cell breakage and introduction of micro cracks in the crystalline Si-cells. Therefore, the dominating limitation in the ambitions to reduce the wafer thickness is set by the soldering process. The curing reaction of ECAs usually takes place

below 180 °C and can be tailored by modifying the basic polymeric binder. Thus, switching to an adhesive interconnection technology allows for further reducing the wafer thickness and innovative possibilities in cell design. Another advantage is that the adhesives can be applied by screen printing directly onto the finger grid of the cell without using additional busbars on the front side of the cell.

Compared to lead-based solder alloys, application of ECAs is a more environmentally clean solution for interconnection tasks [234, 240]. By replacing the toxic lead containing solders, the accompanying challenges concerning waste management and recycling can be avoided. Furthermore, the possibility to use non-solderable materials like silver coated ribbons, which are used as light capturing ribbons, opens new possibilities in further cell- and PV module designs [241]. Nevertheless, the replacement of the soldering process by ECAs also has some limitations. A big drawback is the high silver price which is why the highly filled adhesives are much more expensive than solders. This can be partially compensated by reducing the busbars. Another challenge is the ability to withstand harsh environmental conditions in various climate zones, especially cold climates, where some issues with limited impact resistance, weakened mechanical strength, reduced adhesion and increased contact resistance (when choosing non-suitable ribbon coatings) were noticed [234].

Shingled solar cells using ECA

Traditional interconnects such as busbars usually cause optic losses due to cell shading. To reduce the impact of this phenomenon, new module concepts and cell architectures have been developed. Solar cells can be cut into strips and when the strips overlap it is possible to create a string in which there are no empty spaces between the cells. Shingled solar cells thus have lower optical losses and are characterized by higher efficiency [242, 243]. A further advantage of this technology is that curing temperatures of ECAs is typically lower than soldering temperature resulting in lower residual mechanical stresses on solar cells. Additionally, a lower processing temperature would imply a lower energy demand for the whole process [34]

To connect shingled solar cells and to prevent joint failure, it is necessary that the interconnection material is characterized by a low ratio of shear modulus (G) over shear strength ($\tau_{sh.\ str.}$) [243] and ECAs are very good candidates to fulfill these requirements. The main drawback of using this technology is that the series resistance is increased and its extent depends on ECA's curing conditions [242, 243].

Tonini et al. [34] described the main differences and technological challenges along the process chain of a PV module using a shingled architecture compared to a traditional "stringed and tabbed" PV module and identified five critical steps. (1) *Cell layout*, namely the silver grid lines have a longer pathway towards the busbars (BB) because pseudo-BB are located only on the front end or on the back end of the shingles cell. (2) S*ingulation*: the characteristics of the laser used for cutting the cell (power, repetition rate, scanning speed and especially its accuracy) have to be finely tuned to ensure minimum damage to the cells. (3) *ECA printing*: screen printing is preferred with respect to dispensing, as it is considered as a fast, simple and robust process that has been implemented for decades in c-Si PV production. (4) *String assembly*: the overlapping area is a parameter that can be optimized to find the optimum condition between reducing materials cost (small glue area) and improving mechanical stability (big glue area). Additionally, the accuracy of shingle-to-shingle alignment and total string length are fundamental to ensure the desired power output and reliability as well as aesthetic consistency. (5) *ECA curing*: to avoid the occurrence of adhesion issues it is important that the ECA is completely cured. Differential Scanning Calorimetry (DSC) can be used to determine curing temperature and effectiveness of curing process.

Currently the reliability of modules built using shingle interconnections are of great interest in the scientific community, but not many studies have been published and relevant work is ongoing. Additionally, qualification tests for ECAs in PV modules have not yet been developed and implemented [244].

Mesquita et al. [245] proved Scanning Acoustic Microscopy (SAM) to be a powerful tool to non-destructively characterize modules built using ECAs. In their work, the authors could clearly distinguish between defective and non-defective adhesive after accelerated ageing tests. Schiller et al. [246] proposed an accelerated TC test able to give in a reduced time results that are similar to the typical IEC TC test. The proposed test might be useful during material development to reduce testing time. Three ECA formulations have been tested by Pitta Bauermann et al. [247]. Two formulations fulfilled the IEC 61215 criteria in terms of power loss after humidity freeze, DH and TC but none of the formulations showed performances comparable to traditional soldered ribbon, possibly due to the negative interaction between adhesive and water. Additionally, the adhesives showed differences depending on the stress applied, thus showing that a climate-specific application should be considered. Klasen et al. [248] proposed a model able to predict, in comparative studies, mechanical stresses in the joints of shingled solar cells using different geometries.

Thermo-mechanical properties and fatigue behavior

An important property for the application of ECAs in PV modules is the mechanical behaviour and the fracture toughness of the cured resin. With regard to high-efficiency cell concepts and reduced cell thicknesses the consideration of mechanical strain is especially important.

Springer et al. recently investigated the viscoelastic properties of different ECA formulations [238]. Chemical composition and cure conditions had a large influence on visco-elastic material properties. Furthermore, the response to dry and damp heat exposure was investigated. Depending on the ECA type, the observations ranged from no change to significant changes in the visco-elastic properties. Damp heat exposure caused embrittlement to a point, where even small strains imposed during Dynamic Mechanical Analysis caused fracture. Also changes in thermal expansion behaviour were detected after aging. Embrittlement of ECAs have also been reported elsewhere [234].

So far, only a limited number of papers [249–252] dealing with the fatigue behaviour of different types of cell interconnection have been published, and they are giving contradictory values. Pander et al. found that application of ECAs in silicon solar cells resulted in a reduction of strain within the silicon compared to the solder [249]. They were also studying fatigue of solar cell interconnectors and designed the loading profile during the fatigue test in the way to achieve the same strain amplitude in the cell gaps as found in a full size module simulation under ±1000 Pa, which corresponds to IEC testing [250]. Dietrich et al. investigated fatigue of solar cell interconnectors as well and chose the test amplitude in such a way that the failure occurs in less than 10 000 cycles [250]. However, the authors did not give information of the load levels applied in their fatigue test. Zarmai et al. [252] studied thermo-mechanical damage and fatigue life of solar cell solder interconnections and reported calculated values of maximum stress concentration in the solder joint of 21 MPa. This value was obtained within the thermal-cycling test in the temperature range from -40 °C to 85 °C according to IEC 61215 [114].

Oreski et al. investigated the cyclic fatigue behaviour of two different ECA types [70], where a significant difference was found in the fatigue resistance. One explanation lies in the intrinsic fatigue resistance of the materials, but also the influence of sample preparation may influence the worse case fatigue resistance. Regarding the cyclic fatigue behaviour of the investigated ECA types, both S-N curves are either significantly above [250, 251] or in a similar range [252] of mean stress levels that were reported for interconnections in PV modules. Also, the reported

values for number of cycles to failure for soldered bonds are in a similar range. For ECA bonded test modules a slight power loss after thermal cycling, damp heat and irradiance exposure was observed [70]. In this study power loss was attributed not only to failure of the ECA bond but also to additional factors like sample preparation and cell damages that were present from the start.

Interactions with other module components

In the same study [70] the compatibility of different ECA formulations and various encapsulation films and ribbon materials was investigated. No harmful interactions were found between the investigated ECA formulations and the different encapsulant films after lamination and aging tests. The main outgassing products were identified as fragments of the hardener. Also, no migration of silver particles was observed. ECAs were compatible with all tested ribbon types (Cu, Ag, SnAgCu) as no delamination or discoloration after lamination or accelerated aging tests was observed.

4.4.3 Advances in cell metallization

Electrons from/to a crystalline silicon photovoltaic (PV) cell are transferred through the respective contacts on the front and rear surfaces of the PV cell. The electrical performance of the contacts on both sides of the PV cell have been reviewed since 1980s [253, 254] and detailed mechanisms of the formation and current transmission in these contacts is reported [255–257]. As indicated in a recent roadmap on the PV technologies [53], classical screen printing of silver paste remains the preferred choice for cell metallization today and currently comprises over 95 % of the PV cell market. This technology is projected to remain the dominant technology for the next decade (over 85 % market share in 2029) [53]. Therefore, this section reviews the current status of screen-printing technology in relation to the long-term reliability of PV cells/modules.

Screen printing cell metallization based on silver

The electrical contact on the n^+ emitter surface of PV cells is formed with silver paste (silver metal, glass frit, and organic binders) through the “Fire-Through” sequence: (1) screen-printing of the paste, (2) evaporation of the organic binders, and (3) firing (etching of SiNx layer) at high-temperature. Afterwards a thin glass layer (including numerous silver nanoparticles) is formed at the interface between the silver and silicon surface. Silver crystallites embed into the bulk silicon is observed, depending on the firing conditions and the constituents in the paste used. These silver crystallites directly contact with the bulk silver and penetrate through the glass layer in some cases. From these observations, it is supposed that the electrons generated in the PV cell are transferred via three routes in this contact: (1) *direct transfer* from n^+ emitter to the bulk silver (silver crystallites within silicon can contribute this electron transfer route) [258, 259], (2) *tunnelling transfer* via the silver nanoparticles distributed in the glass layer [260, 261], and (3) *percolation transfer* via these silver nanoparticles [262, 263]. For the p^+-surface contact, aluminium is also contained in the silver paste, producing the ohmic contact.

To achieve the high efficiency in a PV cell, the optimization of the electrical properties of these contacts is important. To achieve optimal performance reduction of contact resistance, decrease in line resistance of electrodes, and suppression of carrier recombination occurring around metallization must be addressed. In addition to the optimization of “Fire-Through” conditions, the modifications of additives in the glass frit are also critical. A significant development was the addition of tellurium oxide to the glass frit, which was filed as a series of patents in early 2010s [264]. The tellurium-based paste leads to the reduction in contact resistance and the suppression of carrier recombination, from the reduced viscosity of molten glass generated during the firing process (the lower viscosity causes the uniform etching of SiNx, resulting in a

larger more uniform contact) [265–267]. I has been suggested that the suppression of deep etching with the tellurium-containing pastes (indicating the inhibition of deeper growth of the silver crystallite) results in mitigating the shunting and the carrier recombination [268].

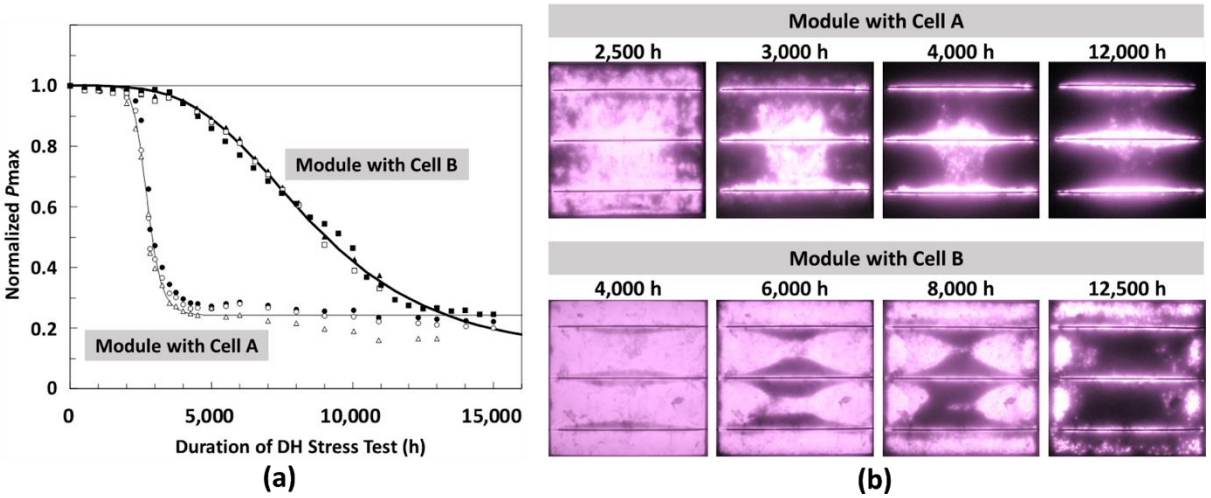

Figure 23: Degradation in P_{max} in PV mini-modules with Cell A (made with an old paste) or Cell B (made with a new paste) during DH stress test. Lines indicate the fitted curves to logistic model (a), and the corresponding EL images (b).

Screen printing cell metallization based on tellurium

Important changes in the reliability of PV modules were recognised simultaneously with the market introduction of tellurium-based paste (around 2012) [269]. Under high-temperature and high-humidity stress conditions, the power-loss in PV modules made with cells using the new paste (post-2012) is less than in those using the old paste (pre-2012). As shown in Figure 23 (a), the time progressions of the degradation in both PV modules are quite different, although they all reach a similar end state degradation of 80 % power-loss after long periods of DH stress. The duration of the initial lag phase in these tests are 2000 h and 4000 h in the PV modules with old and new pastes, respectively (this duration is defined as the time to 5 % reduction in power at STC). The time to reach 50 % power loss for the PV modules with old and new paste is roughly 2800 h and 8500 h, respectively. Modules using the new paste survived at least twice as long in DH testing and exhibited unique patterns in electroluminescence (EL) imaging. In modules with the old paste (Figure 23 (b)), EL following DH testing shows a darkening at the edges of the cell and progresses to darken the entire cell as DH testing progresses. In contrast, modules with the new paste shows degradation starting along the busbars and expanding to the whole cell area. A crucial difference in the moisture penetration into these PV modules seems to be not assumed [270, 271], irrespective of their distinctive evolutions of EL image. Therefore, these observations suggest that the corrosive mechanisms in both PV modules might be slightly different. Under the hygro-thermal stress conditions, it is demonstrated that acetic acid (and other organic acids) liberated from an encapsulant corrodes the metallization, through the dissolution of glass layer located at the interface between the bulk silver and silicon surface [272, 273] and/or the aggregation of organic lead compounds at this interface [274]. This corrosion at this interface induces the spatial non-uniform elevation of contact resistance within the cell surface, depending on the uneven moisture penetration into the PV module. The apparent series resistance observed in an entire PV cell/module is not highly elevated and in one case, could not be detected by the distributed series resistance effect [275]. In addition, it is reported that the rectified contact is formed at this interface within the PV module exposed outdoors for a long duration [276], as well as at that of PV cells under

artificial corrosive stress conditions [277]. In the PV modules with the new paste, galvanic corrosion of glass layer underneath the bulk silver is suggested [278, 279], since the accumulation of tin on the silver metallization around the busbar was observed [280]. Although the chemical reaction-mechanisms have not been determined, it is important to determine what role tin might play in these corrosive reaction(s) because the penetration of tin into the metallization is also observed in some fielded PV modules [281]. Furthermore, since the electrical degradation signatures of both PV modules (with old and new paste) are similar [282], it stands to reason that the essential mechanism(s) may also be similar, although the spatio-temporal evolution of corrosion was not identical.

Advanced composite metallization using multiwalled carbon nanotubes

Cell cracks can eventually propagate through metal gridlines and busbars, leading to module power loss over time [283–285], and can be a root cause of hotspots [286, 287]. Technical approaches to mitigate the impact of cell cracks include improved designs for cell shape, cell wiring, metallization patterns, and module construction [284]. Multi-wire technology [50] has also emerged as a possible solution to the cell-crack-induced module degradation. In this report, we focus on metal matrix composite (MMC) metallization that makes use of surface-functionalized multiwalled carbon nanotubes (MWCNTs) embedded in commercially available silver paste. Figure 24 visually demonstrates this composite engineering strategy, where the CNTs mechanically and electrically bridge the gaps in severed MMC gridlines, providing redundant electrical conduction pathways. The composite metallization imparts unique properties to the metal gridlines and busbars: (1) fracture toughness with increased ductility, (2) electrical bridging of cracks [284] ≥ 50 μm, and (3) “self-healing” after repeated cycles of complete electrical failure under tensile strain and regaining electrical continuity upon crack closure [288–290]. We expect these properties to extend the module lifetime well beyond 25 years of a typical performance warranty.

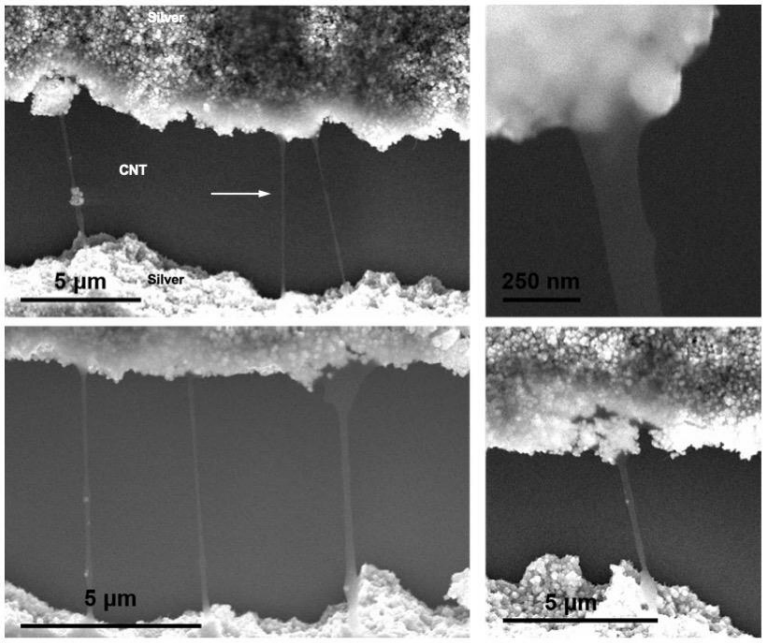

Figure 24: BRIDGECONCEPT – experimental observation of carbon nanotubes bridging cracks.

Figure 25 demonstrates how MWCNT addition to commercial silver paste can increase the modulus of toughness for gridlines screen-printed and fired in a furnace. The modulus of toughness refers to the area under stress (σ) vs. strain (ε) curve in mechanical characterization, which is a key indicator of toughness against fatigue failure, such as strain-induced crack formation. In this particular case, we observe approximately 16 % increase in modulus of toughness and 50 % increase in the critical strain at which the gridline mechanically fails, indicating enhanced ductility. That is, the gridlines can become “stretchy” when a proper amount of functionalized MWCNTs are mixed into the silver paste, electrically bridging cracked cells.

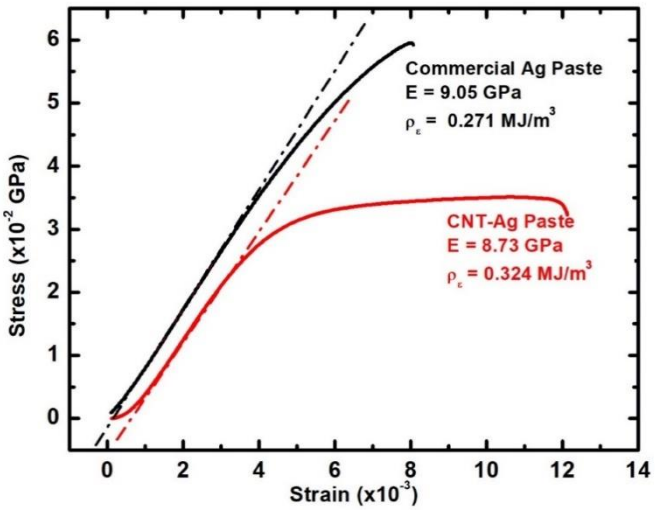

Figure 25: Stress (σ) vs. strain (ε) of commercial silver paste and MMC paste incorporated with functionalized MW-CNTs.

In addition to the increased modulus of toughness and ductility, the MMC gridlines provide exceptional electrical gap bridging capability when the gridlines eventually fracture under extreme strain. Figure 26 shows results from our Resistance Across Cleaves and cracks (RACK) testing setup, where multiple gridlines deposited on a semiconductor substrate are strained to mechanical failure to form cracks, while the resistance along each gridline is measured to record the displacement (i.e., physical gap within the crack) at which the resistance rises to infinity, and thus electrical failure occurs.

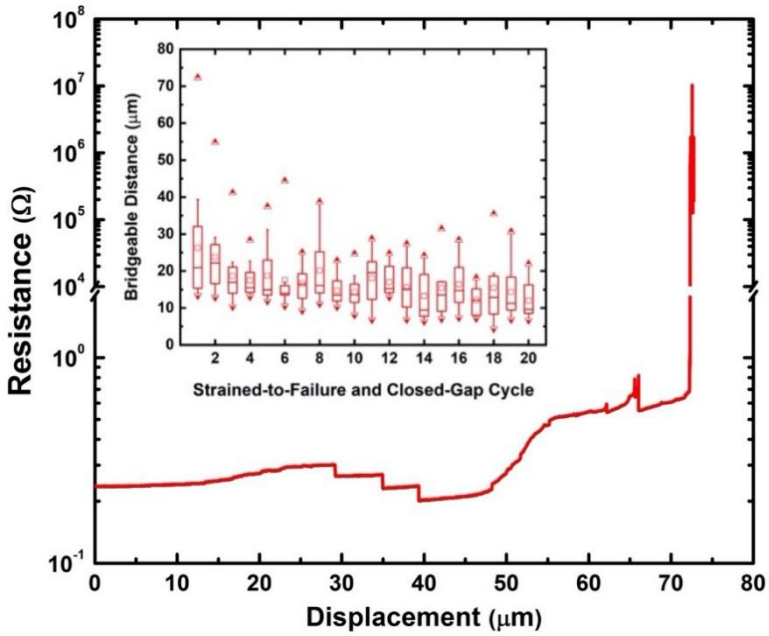

Figure 26: Resistance in MMC gridline as a function of displacement (i.e., gap width in the crack). The inset shows "self-healing" bridgeable gap in the crack.

In Figure 26, we observe that the MMC gridlines can electrically bridge an average of 25 μm displacement (i.e., physical gap width in the crack) for the first strain cycle as well as displacement as large as 70 μm for an outlier case. In comparison, the standard gridlines electrically fail almost immediately and irreversibly after the strain is applied. Silverman *et al.* report that cell cracks observed in mini-modules range from 4 μm to 20 μm in [291]. Haase *et al.* similarly report that cell crack widths observed in full-size modules under mechanical loading can open up to 40 μm [292]. While statistics on crack widths from fielded full-size modules are not readily available, the bridgeable gap by MMC gridlines sufficiently covers the range observed by Silverman *et al.*, suggesting that MMC gridlines may be able to electrically bridge most of the cell cracks appearing in PV modules. Following the approach similar to the work by Hasse et al. [292], we will be working with Sandia National Laboratories to employ Digital Image Correlation (DIC) to analyse cell cracks appearing in fielded and stress-tested full-size modules. This effort will be reported in the near future.

The inset in Figure 26 shows how the electrically failed gridlines after extreme strain >> 70 μm can *"self-heal"* to re-establish electrical continuity, as the gap is closed. Note that the electrical continuity is re-established at approximately 20 μm displacement well before complete crack closure. The "self-healing" is repeatable even after many strained-to-failure and closed-gap cycles. We have speculated that the MWCNTs embedded in silver gridlines would be exposed by fibre pull-out during gridline fracture, as illustrated in Figure 24. These exposed MWCNTs would eventually be severed upon extreme strain, but the tethered MWCNTs may reconnect by Coulombic attraction as the gap is closed. Counter to this speculated electrostatic "self-healing" mechanism, our recent *in situ* SEM strain test suggests that the "self-healing" may originate from high level of asperities at the fracture surface that re-establish electrical connection before complete crack closure occurs.

To ensure that the advantageous electromechanical properties of MMCs do not compromise the cell performance, we compare the performance of Passivated Emitter and Rear Contact (PERC) cells with standard metallization vs. MMC metallization. We observe very little difference in the beginning-of-life cell performance (not shown here for brevity).

To compare how MMC vs. standard gridlines withstand the thermomechanical stress introduced to modules, we measure the busbar-to-busbar resistance through parallel gridlines as a way of monitoring gridline failure. In this case, each mini-module consists of four 156 mm x 156mm cells, and the cells are manually scribed to introduce microcracks prior to encapsulation. Each mini-module is then mounted on a vacuum chuck and flexed by vacuum underneath. The mechanical flexing creates cell cracks, and the following thermal cycling causes cell cracks to propagate. We monitor the change in resistance as the thermal cycling continues. Figure 27 shows that the fractional change in resistance is less pronounced with MMC modules (green data points) after about 100 cycles, compared to that of standard modules (red data points), suggesting that MMC metallization may be able to reduce the fatigue failure of gridlines and busbars.

In summary, we have demonstrated that MMC metallization can provide unique material and electromechanical properties: i.e., enhanced fracture toughness and ductility, electrical gap bridging capability, and “self-healing”. These properties would mitigate the cell-crack-induced degradation of PV modules. We have further demonstrated that MMC metallization does not compromise the beginning-of-life cell performance. The initial mini-module testing using MMC metallization shows promise in reducing the module degradation against thermomechanical stress.

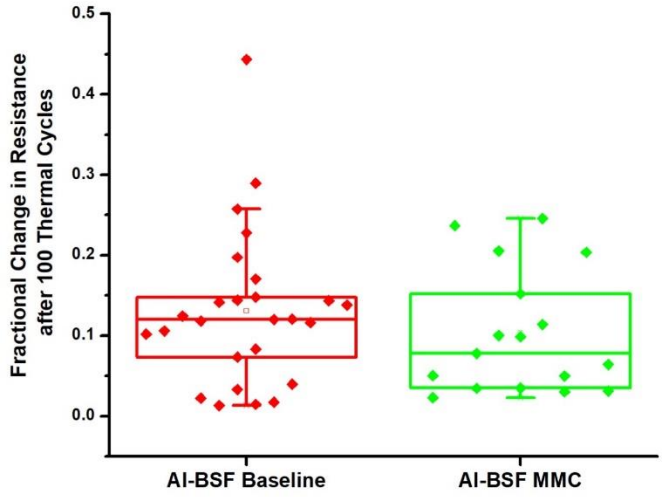

Figure 27: Fractional change in resistance along parallel gridlines used as a measure of gridline failure against thermal cycling.

4.5 Reliability of new module concepts - Lightweight module approaches

A typical c-Si based 60 cell standard module has a weight of about 20 kg and a specific weight of about 12 kg/m^2. Lightweight modules have a lower weight compared to standard modules, but there is no real classification. Most lightweight panels replace glass as the front sheet with other material, which has a major influence on the rigidness and general properties. Another approach is the use thin glass to reduce the weight.

Thin film modules, mostly of the CIGS type, are often lightweight, particularly if thin polymeric materials replace the glass front sheet and/or the substrate, which results in a flexible structure. This approach is most interesting for compound semiconductor based thin film devices, because it does not only provide a flexible structure but should in principle also enable the pro-

duction of modules on a low cost substrate material in a continuous roll to roll production process [293]. Recently, this type of device attained several efficiency records at laboratory scale [294, 295] and for larger modules [296].

There are several examples of companies that offer or offered certified lightweight and flexible thin film solar modules [294, 297–300], with weights down to 2 kg/m^2, not including the bonding material needed for installation.

There are some inherent reliability advantages and disadvantages of glass-free flexible thin film modules. Omitting the fragile c-Si wafer lowers the risks of bending and other mechanical stress, such as hail damage. However thin film compound semiconductor devices are sensitive to humidity and other envorinmental factors [300] and rely on packaging materials to protect the cells. The substrate properties including the semiconductor adhesion and the interfaces of the multi-layer structures are additional issues that can lead to failures and degradation. Lightweight flexible modules are often intended for the application on a solid substrate (e.g., metal or polymer roof), typically bonded with a recommended adhesive. The surface and bonding properties are therefore another factor that may influence the reliability as well as specific installation conditions, e.g. curvature [301, 302]. The reliability of specific lightweight thin film module technologies and material combinations is discussed in several publications [300–302], a review about degradation effects in different layers can be found in [303].

In the c-Si wafer-based module segment a weight reduction compared to the standard module design can be obtained by either using thinner glass or by the use of alternative materials. Using thinner glass allows a conservative module design; the basic concept and the production process of a standard module can be maintained in principle if process parameters are adapted. However, the glass is also a crucial factor for the stiffness of a laminate. Simply reducing the glass thickness leads to a considerable bow or a dishing of the central module area.

Therefore, the standard design for a glass/backsheet module with frame is not suitable for designs with very thin glass. Either the module dimensions have to be lowered or the laminate has to be placed on a supporting structure such as a supporting plate or a structure / grid consisting of several beams.

Supporting plates can be very simple as for example plastic twin-wall sheets or a very lightweight and expensive honeycomb structure [304] as used in experimental solar aircraft. Another approach is to use several beams in a lattice-like structure. In the “U-Light” Solar-era.net project, numerous structures with different beam desings were investigated, with an aim toward minimizing material usage [305]. A 60-cell glass/backsheet module with a weight of only 8.8 kg/m^2 including a sub-construction (racking) that enables a tilt angle variation was constructed [306]. The reason for including the sub-construction is that it is difficult to separate the module and the sub-construction in this concept. Mechanical load and hail tests according to the IEC 61215 were successfully performed. A major obstacle to use very thin solar glass is however the cost and the availability. It is technically difficult to harden solar glass that is thinner than 2 mm by thermal processes. The very thin 0.8 mm solar glass that was used in the experiments was chemically hardened and is currently not available.

Replacing the glass by polymeric material, as already described for thin film devices, is also an option for c-Si modules. Glass-free lightweight modules are available from numerous distributers.. This type of c-Si module, often also semi-rigid, are mostly advertised for mobile applications. Their size is mostly smaller than the one of standard modules, and they are offered in various shapes and designs. The lower weight and smaller size reduce stability issues and they are usually not intended for long-term stationary use. Accordingly, they have lower re-

quirements concerning ambient stress (ageing, hail, mechanical load, etc.) and they are usually not certified. Therefore, no general statement with regard to reliability aspects are possible. The same is true for more expensive or experimental special solutions with curved or 3D-structures that often focus more on design or specific properties than on weight. Examples are modules based on bent polymeric bulk plates (e.g. by Sunovation), devices that are prepared by forming techniques (e.g. FhG innovation cluster “Solar Plastics”) or solar cells that are embedded in vacuum infused resin (e.g. Solarface / Tecnalia). However, there are also several certified products with more conventional layout (incomplete list):

- Giga Solar FPC; ~5 kg/m^2, certified; flush-mounted onto the roof
- DAS; > 2.5 kg/m^2, certified; ETFE front with protective layer beneath
- Solight / cea & edf & Photowatt; 6 kg/m^2, certified (critical tests 2 fold)
- Operasol / cea & 2ca; 4 kg/m^2, certification pre-qualification

Typically, a frontsheet (often ETFE) replaces the glass in these examples. Hail damage is an obvious concern and there are several publications on this topic. Partly however, they show contradictory results, even for comparable set-ups. In one publication a high material volume (front) and a low substrate rigidness is found to be beneficial, while in the other one there are higher losses with more front volume and less rigid substrate [90][307]. A generalization for all glass-free modules is hindered by the differing and rarely revealed device design.

As for the thin film devices, it is also not clear in how far the applied certification test reflects the actual and relevant stress. A good example is the mechanical load test. The described module type is often recommended for the use on flat rooftops. A mechanical load test under these conditions is probably no major hurdle, but a local unevenness of a real surface may obviously pose a risk. There are similar concerns for a prolonged exposure to water accumulation on the surface, especially if the module is scratched or dented. The PV certification is developed for existing technologies, and new or modified test procedures are needed for these new module designs. New layouts will have different weak points; a polymer front layer is surely more prone to ageing effects than glass. Even more than for standard modules, a certification alone is no guarantee. Since the failure rate of actual products follows a bathtub curve it is possible for a manufacturer to identify issues that appear soon after installation but not be aware of longer-term risks.

5 CONCLUSION

In the last decade and longer, photovoltaic module manufacturers have experienced a rapidly growing market along with a dramatic decrease in module prices. Such cost pressures have resulted in a drive to develop and implement new module designs, which either increase performance and/or lifetime of the modules or decrease the cost to produce them. Many of these innovations include the use of new and novel materials in place of more conventional materials or designs. As a result, modules are being produced and sold without a long-term understanding about the performance and reliability of these new materials. This presents a technology risk for the industry.

There are several motivations for investigating new materials for PV modules. Reducing or replacing expensive materials is important for the overall economics of module production. Lamination is typically the slowest step in a module production line and manufacturers are very interested in materials that can speed up this process step. Increasing performance is an obvious motivation for material innovations. The trend to increasing wafer size also leads to performance gains. Making modules more sustainable is another strong motivating factor. Life Cycle Assessment (LCA) is a methodology to quantify the environmental impact of a product. Some manufacturers seek recognition of ecologically responsible material choices by using various labeling standards to identify good sustainability practices.

The process of material innovation for PV is further complicated by the complex interactions within a PV module. The advantage of one material may be outweighed by its interaction with another component. For example, EVA is inexpensive and highly effective for encapsulation, however it degrades to form acetic acid which can cause corrosion of the metallization if it is not allowed to escape the module package due to use of an impermeable backsheet. New materials must work within the whole module package and in concert with the other materials present. Another issue is that module manufacturers do not typically advertise their bill of materials (BOM) and the BOM for a particular module model can vary depending on when and where it was made.

In the worst case new module designs or new module materials lead to unexpected degradation mechanisms several years after field deployment, which were not predicted in laboratory accelerated testing, such as Potential Induced Degradation (PID), Light and elevated Temperature Induced Degradation (LeTID) or backsheet cracking. Therefore, consumers and manufacturers rely on constant adaptation and development of international standards, such as those from Technical Committee “Solar Photovoltaic Energy Systems” TC 82 to ensure that new materials do not result in unexpected performance or reliability problems.

6 REFERENCES

[1] A. Jaeger-Waldau, “PV Status Report 2019,” Publications Office of the European Union, Luxembourg, 2019. Accessed: Jan. 17 2020. [Online]. Available: https://ec.europa.eu/jrc/en/publication/eur-scientific-and-technical-research-reports/pv-status-report-2019

[2] VDMA, Ed., “International Technology Roadmap for Photovoltaic (ITRPV): Results 2018 incldluing maturity report 2019,” Oct. 2019. Accessed: Jul. 23 2020. [Online]. Available: https://itrpv.vdma.org/

[3] S. Pingel *et al.,* “Potential Induced Degradation of solar cells and panels,” in *2010 35th IEEE Photovoltaic Specialists Conference*, Honolulu, HI, USA, Jun. 2010 - Jun. 2010, pp. 2817–2822.

[4] F. Kersten *et al.,* “A new mc-Si degradation effect called LeTID,” in *2015 IEEE 42nd Photovoltaic Specialist Conference (PVSC)*, 2015, pp. 1–5.

[5] M. A. Jensen, A. E. Morishige, J. Hofstetter, D. B. Needleman, and T. Buonassisi, “Evolution of LeTID Defects in p-Type Multicrystalline Silicon during Degradation and Regeneration,” *IEEE J. Photovoltaics*, vol. 7, no. 4, pp. 980–987, 2017, doi: 10.1109/JPHOTOV.2017.2695496.

[6] Y. Lyu *et al.,* “Drivers for the cracking of multilayer polyamide-based backsheets in field photovoltaic modules: In-depth degradation mapping analysis,” *Prog Photovolt Res Appl*, no. 28, pp. 704–716, 2020, doi: 10.1002/pip.3260.

[7] G. C. Eder *et al.,* “Error analysis of aged modules with cracked polyamide backsheets,” *Solar Energy Materials and Solar Cells*, vol. 203, p. 110194, 2019, doi: 10.1016/j.solmat.2019.110194.

[8] A. Goetzberger, B. Voß, and J. Knobloch, *Sonnenenergie: Photovoltaik: Physik und Technologie der Solarzelle,* 2nd ed. Stuttgart: Teubner Verlag, 1997.

[9] A. W. Czanderna and F. J. Pern, “Encapsulation of PV modules using ethylene vinyl acetate copolymer as a pottant: A critical review,” *Solar Energy Materials and Solar Cells*, vol. 43, no. 43, pp. 101–181, 1996, doi: 10.1016/0927-0248(95)00150-6.

[10] M.C.C de Oliveira, A.S.A.C. Diniz, M. M. Viana, L.V.F. Cunha, “The causes and effects of degradation of encapsulant ethylene vinyl acetate copolymer (EVA) in crystalline silicon photovoltaic modules: A review,” *Renewable and Sustainable Energy Reviews*, vol. 81, pp. 2299–2317, 2018, doi: 10.1016/j.rser.2017.06.039.

[11] M. López-Escalante, L. J. Caballero, F. Martín, M. Gabás, A. Cuevas, and J. Ramos-Barrado, “Polyolefin as PID-resistant encapsulant material in 5PV6 modules,” (in af), *Solar Energy Materials and Solar Cells*, vol. 144, pp. 691–699, 2016, doi: 10.1016/j.solmat.2015.10.009.

[12] B. M. Habersberger, P. Hacke, and L. S. Madenjian, “Evaluation of the PID-s susceptibility of modules encapsulated in materials of varying resistivity,” in *IEEE 7th World Conference, 2018*.

[13] K. Nagayama, J. Kapur, and B. A. Morris, “Influence of two-phase behavior of ethylene ionomers on diffusion of water,” *Journal of Applied Polymer Science*, vol. 137, no. 31, p. 48929, 2020, doi: 10.1002/app.48929.

[14] B. Adothu, P. Bhatt, S. Zele, J. Oderkerk, F. R. Costa, and S. Mallick, “Investigation of newly developed thermoplastic polyolefin encapsulant principle properties for the c-Si PV module application,” *Materials Chemistry and Physics*, vol. 243, 2020, doi: 10.1016/j.matchemphys.2020.122660.

[15] C. Peike, I. Häldrich, K.-A. Weiß, and I. Dürr, “Overview of PV module encapsulation materials,” *Photovoltaics International*, no. 19, pp. 85–92, 2013.

[16] C. Carrot, A. Bendaoud, and C. Pillon, “Polyvinyl Butyral,” in *Handbook of Thermoplastics*, pp. 89–137. [Online]. Available: https://www.routledgehandbooks.com/doi/10.1201/b19190-4
[17] V. Chapuis, S. Pélisset, M. Raeis-Barnéoud, H.-Y. Li, C. Ballif, and L.-E. Perret-Aebi, “Compressive-shear adhesion characterization of polyvinyl-butyral and ethylene-vinyl acetate at different curing times before and after exposure to damp-heat conditions,” *Prog. Photovolt: Res. Appl.*, vol. 22, no. 4, pp. 405–414, 2014, doi: 10.1002/pip.2270.
[18] K. R. McIntosh, N. E. Powell, A. W. Norris, J. N. Cotsell, and B. M. Ketola, “The effect of damp-heat and UV aging tests on the optical properties of silicone and EVA encapsulants,” *Prog. Photovolt: Res. Appl.*, vol. 19, no. 3, pp. 294–300, 2011, doi: 10.1002/pip.1025.
[19] J.Lopez, A.Pozza, T.Sample, “Analysis of Crystalline silicon PV modules after 30 years of outdoor exposure,” in *31st European Photovoltaic Solar Energy Conference and Exhibition, Hamburg, 2015.*
[20] I. Fidalgo, R. Merino, and B. Perez, “Lamination Cycle Time Optimization Using New POE Encapsulants,” in *32nd European Photovoltaic Solar Energy Conference and Exhibition*, pp. 183–186.
[21] O. Hasan and A. Arif, “Performance and life prediction model for photovoltaic modules: Effect of encapsulant constitutive behavior,” *Solar Energy Materials and Solar Cells*, vol. 122, pp. 75–87, 2014, doi: 10.1016/j.solmat.2013.11.016.
[22] M. D. Kempe and P. Thapa, “Low Cost, Single Layer Replacement for the Back-sheet and Encapsulant Layers,” in *Proceedings of SPIE*, 70480D-1-12.
[23] M. Jankovec *et al.,* “In-Situ Monitoring of Moisture Ingress in PV Modules with Different Encapsulants,” in *32nd European Photovoltaic Solar Energy Conference and Exhibition*, pp. 2265–2269.
[24] A. J. Beinert, R. Leidl, P. Sommeling, U. Eitner, and J. Atkaa, “FEM-based Development of Novel-Contact PV Modules with Ultra-Thin Solar Cells,” in *33rd European Photovoltaic Solar Energy Conference and Exhibition*, pp. 42–47.
[25] “©Fraunhofer ISE: Photovoltaics Report, updated: 23 June 2020,”
[26] T. D. Lee and A. U. Ebong, “A review of thin film solar cell technologies and challenges,” *Renewable and Sustainable Energy Reviews*, vol. 70, pp. 1286–1297, 2017, doi: 10.1016/j.rser.2016.12.028.
[27] M. B. Hayat, D. Ali, K. C. Monyake, L. Alagha, and N. Ahmed, “Solar energy-A look into power generation, challenges, and a solar-powered future,” *Int J Energy Res*, vol. 43, no. 3, pp. 1049–1067, 2019, doi: 10.1002/er.4252.
[28] A. Blakers, “Development of the PERC Solar Cell,” *IEEE J. Photovoltaics*, vol. 9, no. 3, pp. 629–635, 2019, doi: 10.1109/JPHOTOV.2019.2899460.
[29] M. J. Yim, Y. Li, K. Moon, K. W. Paik, and C. P. Wong, “Review of Recent Advances in Electrically Conductive Adhesive Materials and Technologies in Electronic Packaging,” *Journal of Adhesion Science and Technology*, vol. 22, no. 14, pp. 1593–1630, 2008, doi: 10.1163/156856108X320519.
[30] A. Faes *et al.,* “SmartWire Solar Cell Interconnection Technology,” in *29th European Photovoltaic Solar Energy Conference and Exhibition*, pp. 2555–2561.
[31] P. Papet *et al.,* “New Cell Metallization Patterns for Heterojunction Solar Cells Interconnected by the Smart Wire Connection Technology,” *Energy Procedia*, vol. 67, pp. 203–209, 2015, doi: 10.1016/j.egypro.2015.03.039.
[32] G. G. Untila *et al.,* “Concentrator bifacial Ag-free LGCells,” *Solar Energy*, vol. 106, pp. 88–94, 2014, doi: 10.1016/j.solener.2013.11.034.
[33] G. G. Untila, T. N. Kost, and A. B. Chebotareva, “Multi-wire metallization for solar cells: Contact resistivity of the interface between the wires and In2O3:Sn, In2O3:F, and

ZnO:Al layers," *Solar Energy*, vol. 142, pp. 330–339, 2017, doi: 10.1016/j.solener.2016.12.049.
[34] D. Tonini, G. Cellere, M. Bertazzo, A. Fecchio, L. Cerasti, and M. Galiazzo, "Shingling Technology For Cell Interconnection: Technological Aspects And Process Integration," *Energy Procedia*, vol. 150, pp. 36–43, 2018, doi: 10.1016/j.egypro.2018.09.010.
[35] H. Schulte-Huxel, S. Blankemeyer, A. Morlier, R. Brendel, and M. Köntges, "Interconnect-shingling: Maximizing the active module area with conventional module processes," *Solar Energy Materials and Solar Cells*, vol. 200, p. 109991, 2019, doi: 10.1016/j.solmat.2019.109991.
[36] W. J. Gambogi, "Comparative Performance of Backsheets for Photovoltaic Modules," in *25th European Photovoltaic Solar Energy Conference and Exhibition / 5th World Conference on Photovoltaic Energy Conversion, 6-10 September 2010, Valencia, Spain*, pp. 4079–4083.
[37] P. Y. Yuen, S. L. Moffitt, F. D. Novoa, L. T. Schelhas, and R. H. Dauskardt, "Tearing and reliability of photovoltaic module backsheets," *Prog Photovolt Res Appl*, vol. 27, no. 8, pip.3144-pip.3144, 2019, doi: 10.1002/pip.3144.
[38] Y. Lyu *et al.,* "Impact of environmental variables on the degradation of photovoltaic components and perspectives for the reliability assessment methodology," *Solar Energy*, vol. 199, pp. 425–436, 2020, doi: 10.1016/j.solener.2020.02.020.
[39] G. Oreski, A. Mihaljevic, Y. Voronko, and G. C. Eder, "Acetic acid permeation through photovoltaic backsheets: Influence of the composition on the permeation rate," *Polymer Testing*, vol. 60, pp. 374–380, 2017, doi: 10.1016/j.polymertesting.2017.04.025.
[40] A. Omazic *et al.,* "Increased reliability of modified polyolefin backsheet over commonly used polyester backsheets for crystalline PV modules," *J. Appl. Polym. Sci.*, vol. 2020, no. 137, p. 48899, doi: 10.1002/app.48899.
[41] K. Whitfield, "Degradation Processes and Mechanisms of PV System Adhesives/Sealants and Junction Boxes," in *Durability and Reliability of Polymers and Other Materials in Photovoltaic Modules 2019*, pp. 235–254.
[42] E. J. Schneller *et al.,* "Manufacturing metrology for c-Si module reliability and durability Part III: Module manufacturing," *Renewable and Sustainable Energy Reviews*, vol. 59, pp. 992–1016, 2016, doi: 10.1016/j.rser.2015.12.215.
[43] A. Laugharne and I. Yucel, "Role of Silver in the Green Revolution," Jul. 2018.
[44] L. Maras, "Environmental challenges disposing of backsheets at PV module EOL," in *EU PVSEC, Munich, Germany 2016.*
[45] K. J. Geretschläger, G. M. Wallner, and J. Fischer, "Structure and basic properties of photovoltaic module backsheet films," *Solar Energy Materials and Solar Cells*, vol. 144, pp. 451–456, 2016, doi: 10.1016/j.solmat.2015.09.060.
[46] G. Oreski, A. Rauschenbach, C. Hirschl, M. Kraft, G. C. Eder, and G. Pinter, "Crosslinking and post-crosslinking of ethylene vinyl acetate in photovoltaic modules," *J. Appl. Polym. Sci.*, vol. 134, no. 23, p. 101, 2017, doi: 10.1002/app.44912.
[47] Xue, H.-Y.a b, W.-H. Ruan, M.-Q. Zhang, and M.-Z. Rong, "Fast curing ethylene vinyl acetate films with dual curing agent towards application as encapsulation materials for photovoltaic modules," *Express Polymer Letters*, vol. 8, no. 2, pp. 116–122, 2014, doi: 10.3144/expresspolymlett.2014.14.
[48] M. Bregulla *et al.,* "Degradation mechanisms of ethylene-vinyl-acetate copolymer - New studies including ultra fast cure foils," in *Proceedings of the 22nd European Photovoltaic Solar Energy Conference*, pp. 2704–2707.
[49] A.-J. Steiner, W. Krumlacher, H. Muckenhuber, M. Plank, K. Sundl, and E. Ziegler, "New Thermoplastic, Non-Curing Encapsulation Material for PV Module Applications," in *31st*

European Photovoltaic Solar Energy Conference and Exhibition, September 14-18, 2015 Hamburg, Germany, pp. 2816–2819.
[50] J. Walter, M. Tranitz, M. Volk, C. Ebert, and U. Eitner, “Multi-wire Interconnection of Busbar-free Solar Cells,” *Energy Procedia*, vol. 55, pp. 380–388, 2014, doi: 10.1016/j.egypro.2014.08.109.
[51] B. Adothu *et al.,* “Newly developed thermoplastic polyolefin encapsulant–A potential candidate for crystalline silicon photovoltaic modules encapsulation,” *Solar Energy*, vol. 194, pp. 581–588, 2019, doi: 10.1016/j.solener.2019.11.018.
[52] G. Oreski *et al.,* “Properties and degradation behaviour of polyolefin encapsulants for PV modules,” *Progress in Photovoltaics: Research and Applications*, 2020, doi: 10.1002/pip.3323.
[53] *International Technology Roadmap for Photovoltaic (ITRPV)*.
[54] R. Frischknecht, P. Stolz, G. Heath, M. Raugei, P. Sinha, and M. de wild-Scholten, “Methodology Guidelines on Life Cycle Assessment of Photovoltaic: Report IEA-PVPS T12-18:2020,” International Energy Agency Photovoltaic Power Systems Programme, 2020. Accessed: Sep. 18 2020. [Online]. Available: https://iea-pvps.org/wp-content/uploads/2020/07/IEA_Task12_LCA_Guidelines.pdf
[55] E. D. Dunlop, A. Gracia Amillo, E. Salis, T. Sample, and N. Taylor, “Transitional methods for PV modules, inverters and systems in an ecodesign framework,” Luxembourg, EUR EUR 29513 EN. Accessed: Sep. 18 2020. [Online]. Available: https://ec.europa.eu/jrc/en/publication/transitional-methods-pv-modules-inverters-and-systems-ecodesign-framework
[56] A. Zygierewicz, “The Ecodesign Directive(2009/125/EC): European Implementation Assessment,” European Union, 2017. Accessed: Sep. 18 2020. [Online]. Available: https://op.europa.eu/s/okQ0
[57] A. C. Russo, M. Rossi, M. Germani, and C. Favi, “Energy Label Directive: Current Limitations and Guidelines for the Improvement,” *Procedia CIRP*, vol. 69, pp. 674–679, 2018, doi: 10.1016/j.procir.2017.11.136.
[58] C. Nuttal *et al.,* “Project to Support the Evaluation of the Implementation of the EU Ecolabel Regulation: ENV.A.1/SER/2013/0065r,” European Union, 2015. Accessed: Sep. 18 2020. [Online]. Available: https://op.europa.eu/s/okQ1
[59] J. Bernreuter, “The Polysilicon Market Outlook 2020: Technology • Capacities • Supply • Demand • Prices,” 2020. Accessed: Jul. 21 2020. [Online]. Available: https://www.bernreuter.com/polysilicon/industry-reports/polysilicon-market-outlook-2020/
[60] M. Osborne, “Why are monocrystalline wafers increasing in size?,” in *Photovoltaics International.* Accessed: Jul. 21 2020. [Online]. Available: https://store.pv-tech.org/store/why-are-monocrystalline-wafers-increasing-in-size/
[61] T. Clausen *et al.,* “Thin silicon solar cells fabricated on cost optimized float zone silicon,” in *3rd World Conference onPhotovoltaic Energy Conversion, 2003. Proceedings of*, 2003, 1210-1213 Vol.2.
[62] Arkadeep Kumar and Shreyes N. Melkote, “Diamond Wire Sawing of Solar Silicon Wafers: A Sustainable Manufacturing Alternative to Loose Abrasive Slurry Sawing,” *Procedia Manufacturing*, vol. 21, pp. 549–566, 2018, doi: 10.1016/j.promfg.2018.02.156.
[63] M. Hutchins, “Manufacturing industry seeks unity on wafer size,” in *PV Magazine.* Accessed: Jul. 21 2020. [Online]. Available: https://www.pv-magazine.com/2020/06/25/manufacturing-industry-seeks-unity-on-wafer-size/
[64] RENA Technologies GmbH, *Wafer Wet Chemical Surface Treatment from M0 to M6 & M12.* [Online]. Available: https://www.rena.com/en/products/large-wafer-wet-processing/ (accessed: Dec. 10 2020).

[65] G. Oreski, B. Ottersböck, and A. Omazic, “6 - Degradation Processes and Mechanisms of Encapsulants,” in *Plastics DEsign Library, Durability and Reliability of Polymers and Other Materials in Photovoltaic Modules*, Hsinjin Edwin Yang, Roger H. French, and Laura S. Bruckman, Eds.: William Andrew Publishing, 2019, pp. 135–152. [Online]. Available: http://www.sciencedirect.com/science/article/pii/B9780128115459000069

[66] M. Köntges *et al.,* “Assessment of Photovoltaic Module Failures in the Field: Report IEA-PVPS T13-09:2017,” IEA - International Energy Agency, 2017. Accessed: Jan. 21 2020. [Online]. Available: http://www.iea-pvps.org/index.php?id=435

[67] A. de Rose, D. Erath, T. Geipel, A. Kraft, and U. Eitner, “Low-Temperature Soldering for the Interconnection of Silicon Heterojunction Solar Cells,” in *Proceedings of 33rd European Photovoltaic Solar Energy Conference and Exhibition*, pp. 710–714.

[68] A. Descoeudres *et al.,* “Silicon Heterojunction Solar Cells: Towards Low-cost High-Efficiency Industrial Devices and Application to Low-concentration PV,” *Energy Procedia*, vol. 77, 2015, doi: 10.1016/j.egypro.2015.07.072.

[69] S. de Wolf and M. Kondo, “Nature of doped a-Si:H/c-Si interface recombination,” *J. Appl. Phys.*, vol. 105, no. 10, p. 103707, 2009, doi: 10.1063/1.3129578.

[70] G. Oreski *et al., Reliability of electrically conductive adhesives*, 2019.

[71] A. Faes *et al.,* “Direct Contact to TCO with SmartWire Connection Technology,” *2018 IEEE 7th World Conference on Photovoltaic Energy Conversion, WCPEC 2018 - A Joint Conference of 45th IEEE PVSC, 28th PVSEC and 34th EU PVSEC*, 2018, doi: 10.1109/PVSC.2018.8547406.

[72] T. Meßmer, F. Demiralp, and A. Halm, “Low Cost Semi Automated Assembly Unit for Small Size Back Contact Modules and Low Cost Interconnection Approach,” *Energy Procedia*, vol. 98, 2016, doi: 10.1016/j.egypro.2016.10.085.

[73] A. Halm, E. Lemp, R. Farneda, J. Theobald, and R. Harney, “Method to Counter Warpage due to Stringing for Back Contact Solar Cells,” in *Proceedings of 33rd European Photovoltaic Solar Energy Conference and Exhibition*, pp. 989–991.

[74] K.M. Broek, I.J. Bennett, M.J.H. Kloos, and W. Eerenstein, “Cross Testing Electrically Conductive Adhesives and Conductive Back-sheets for the ECN Back-contact Cell and Module Technology,” *Energy Procedia*, vol. 67, pp. 175–184, 2015, doi: 10.1016/j.egypro.2015.03.301.

[75] Guy Beaucarne *et al.,* “Study of Compatibility of Silicone-based Electrically Conductive Adhesives and Conductive Backsheets for MWT Modules,” *Energy Procedia*, vol. 55, pp. 444–450, 2014, doi: 10.1016/j.egypro.2014.08.007.

[76] M. Koehl, M. Heck, and S. Wiesmeier, “Categorization of weathering stresses for photovoltaic modules,” *Energy Sci Eng*, vol. 6, no. 2, pp. 93–111, 2018, doi: 10.1002/ese3.189.

[77] M. Halwachs *et al.,* “Statistical evaluation of PV system performance and failure data among different climate zones,” *Renewable Energy*, vol. 139, pp. 1040–1060, 2019, doi: 10.1016/j.renene.2019.02.135.

[78] A. Omazic *et al.,* “Relation between degradation of polymeric components in crystalline silicon PV module and climatic conditions: A literature review,” *Solar Energy Materials and Solar Cells*, vol. 192, pp. 123–133, 2019, doi: 10.1016/j.solmat.2018.12.027.

[79] I. Kaaya, M. Koehl, A. P. Mehilli, S. de Cardona Mariano, and K. A. Weiss, “Modeling Outdoor Service Lifetime Prediction of PV Modules: Effects of Combined Climatic Stressors on PV Module Power Degradation,” *IEEE J. Photovoltaics*, vol. 9, no. 4, pp. 1105–1112, 2019, doi: 10.1109/JPHOTOV.2019.2916197.

[80] R. R. Cordero *et al.,* “Effects of soiling on photovoltaic (PV) modules in the Atacama Desert,” *Scientific Reports*, vol. 8, no. 1, p. 13943, 2018, doi: 10.1038/s41598-018-32291-8.

[81] E.Cabrera, A.Schneider, J.Rabanal, P.Ferrada, R.R.Cordero, E.Fuentealba, R.Kopecek, “Advancements in the Development of "AtaMo": a Solar Module Adapted for the Climate Conditions of the Atacama Desert in Chile,” in *31st European Photovoltaic Solar Energy Conference and Exhibition, Hamburg, 2015.*, pp. 1–22.
[82] Julián Ascencio-Vásquez, Kristijan Brecl, and Marko Topič, “Methodology of Köppen-Geiger-Photovoltaic climate classification and implications to worldwide mapping of PV system performance,” *Solar Energy*, vol. 191, pp. 672–685, 2019, doi: 10.1016/j.solener.2019.08.072.
[83] A. Schneider, J. I. Fidalgo Martínez, R. Merino Martínez, A. Halm, J. Rabanal-Arabach, and R. Harney, “Material developments allowing for new applications, increased long term stability and minimized cell to module power losses,” in *31st European Photovoltaic Solar Energy Conference and Exhibition, September 14-18, 2015 Hamburg, Germany*, pp. 153–156.
[84] N. Bosco, T. J. Silverman, and S. Kurtz, “Climate specific thermomechanical fatigue of flat plate photovoltaic module solder joints,” *Microelectronics Reliability*, vol. 62, pp. 124–129, 2016, doi: 10.1016/j.microrel.2016.03.024.
[85] J. Althaus and J. Mooslechner, “The Impact of Ammonia Atmosphere to PV Modules and Test Methods,” in *Proceedings of 25th European Photovoltaic Solar Energy Conference and Exhibition*, pp. 4011–4014.
[86] D. W. Cunningham, “The Effect of Ammonia Ambient On PV Module Performance and Longevity,” in *Proceedings of 26th European Photovoltaic Solar Energy Conference and Exhibition*, pp. 3088–3092.
[87] U. Weber, T. Sögding, W. Huschke, H. Engelmann, and U. Fliedner, “Evaluation of Ammonia Resistance of PV Modules,” *Proceedings of 25th European Photovoltaic Solar Energy Conference and Exhibition*, pp. 4007–4010, 2010, doi: 10.4229/25thEUPVSEC2010-4AV.3.14.
[88] A. Sahu, N. Yadav, and K. Sudhakar, “Floating photovoltaic power plant: A review,” *Renewable and Sustainable Energy Reviews*, vol. 66, pp. 815–824, 2016, doi: 10.1016/j.rser.2016.08.051.
[89] G. Eder *et al.,* “COLOURED BIPV - Market, Research and Development: Report IEA-PVPS T15-07: 2019,” IEA - International Energy Agency, 2019. Accessed: Sep. 27 2020. [Online]. Available: http://iea-pvps.org/index.php?id=task15
[90] A. C. Oliveira Martins, V. Chapuis, A. Virtuani, L.-E. Perret-Aebi, and C. Ballif, “Hail Resistance of Composite-Based Glass-Free Lightweight Modules for Building Integrated Photovoltaics Applications,” in.
[91] H. Nussbaumer, M. Klenk, N. Keller, P. Ammann, and J. Thurnheer, “Record-Light Weight c-Si Modules Based on the Small Unit Compound Approach – Mechanical Load Tests and General Results,” in *Proceedings of 33rd European Photovoltaic Solar Energy Conference and Exhibition*, pp. 146–150.
[92] A. C. Martins, V. Chapuis, A. Virtuani, H.-Y. Li, L.-E. Perret-Aebi, and C. Ballif, “Thermo-mechanical stability of lightweight glass-free photovoltaic modules based on a composite substrate,” *Solar Energy Materials and Solar Cells*, vol. 187, pp. 82–90, 2018, doi: 10.1016/j.solmat.2018.07.015.
[93] A. C. Martins, V. Chapuis, A. Virtuani, and C. Ballif, “Robust Glass-Free Lightweight Photovoltaic Modules with Improved Resistance to Mechanical Loads and Impact,” *IEEE J. Photovoltaics*, vol. 9, no. 1, pp. 245–251, 2019, doi: 10.1109/JPHOTOV.2018.2876934.
[94] A. C. Martins, V. Chapuis, F. Sculati-Meillaud, A. Virtuani, and C. Ballif, “Light and durable: Composite structures for building-integrated photovoltaic modules,” *Prog Photovolt Res Appl*, vol. 26, no. 9, pp. 718–729, 2018, doi: 10.1002/pip.3009.

[95] N. Yurrita *et al.,* “Multifunctional Coated Composite Material for Encapsulation of Photovoltaic Devices,” in *Proceedings of 36th European Photovoltaic Solar Energy Conference and Exhibition*, pp. 87–89.
[96] J. M. Vega De Seoane *et al.,* “Versatile & Lightweight Transparent Composite Technology for Advanced BIPV Architectural Solutions,” in *Proceedings of 35th European Photovoltaic Solar Energy Conference and Exhibition*, pp. 1452–1457.
[97] S. Kristensen, H. de Moor, M. Driesser, E. Geldof, and K. Spee, “Integration of Flexible Solar Cells in Plastic and Composite Materials,” in *Proceedings of 35th European Photovoltaic Solar Energy Conference and Exhibition*, pp. 192–196.
[98] O. Zubillaga *et al.,* “Glass-Free PV Module Encapsulation with Aluminium and Transparent Fibre Reinforced Organic Matrix Composite Material,” in *Proceedings of 27th European Photovoltaic Solar Energy Conference and Exhibition*, pp. 430–432.
[99] Y. Voronko, G. Eder, M. Edler, G. Oreski, and W. Mühleisen, “Analysis of the triggers for the yellowing of PV materials during artificial ageing,” in *9th European Weathering Symposium EWS “Natural and Artificial Ageing of Polymers”, September 18-20, 2019, Basel, Switzerland*.
[100] A. Jentsch, K.-J. Eichhorn, and B. Voit, “Influence of typical stabilizers on the aging behavior of EVA foils for photovoltaic applications during artificial UV-weathering,” *Polymer Testing*, vol. 44, pp. 242–247, 2015, doi: 10.1016/j.polymertesting.2015.03.022.
[101] G. C. Eder *et al.,* “Climate specific accelerated ageing tests and evaluation of ageing induced electrical, physical, and chemical changes,” *Prog Photovolt Res Appl*, vol. 27, no. 11, pp. 934–949, 2019, doi: 10.1002/pip.3090.
[102] G. C. Eder, Y. Lin, Y. Voronko, and L. Spoljaric-Lukacic, “On-site identification of the material composition of PV modules with mobile spectroscopic devices,” *Energies*, vol. 13, no. 8, 2020, doi: 10.3390/en13081903.
[103] M. Köntges, A. Morlier, G. Eder, E. Fleis, B. Kubicek, and J. Lin, “Review: Ultraviolet Fluorescence as Assessment Tool for Photovoltaic Modules,” *IEEE J. Photovoltaics*, vol. 10, no. 2, pp. 616–633, 2020, doi: 10.1109/JPHOTOV.2019.2961781.
[104] W. Mühleisen *et al.,* “Scientific and economic comparison of outdoor characterisation methods for photovoltaic power plants,” *Renewable Energy*, vol. 134, pp. 321–329, 2019, doi: 10.1016/j.renene.2018.11.044.
[105] W. Gambogi *et al.,* “A comparison of key PV backsheet and module performance from fielded module exposures and accelerated tests,” *IEEE J. Photovoltaics*, vol. 4, no. 3, pp. 935–941, 2014, doi: 10.1109/JPHOTOV.2014.2305472.
[106] J. Tracy *et al.,* “Survey of Material Degradation in Globally Fielded PV Modules,” *Conference Record of the IEEE Photovoltaic Specialists Conference*, 2019, doi: 10.1109/PVSC40753.2019.8981140.
[107] *Photovoltaics in buildings - Part 1: Requirements for building-integrated photovoltaic modules*, 63092-1:2020, IEC, 2020. [Online]. Available: https://webstore.iec.ch/publication/32158
[108] *Photovoltaic (PV) modules - Type approval, design and safety qualification - Retesting*, 62915:2018. [Online]. Available: https://webstore.iec.ch/publication/31110
[109] H. R. Wilson and F. Frontini, Eds., “Multifunctional Characterisation of BIPV: Proposed Topics for Future International Standardisation Activities,” IEA PVPS Task 15, 2020. Accessed: Sep. 10 2020. [Online]. Available: https://iea-pvps.org/wp-content/uploads/2020/04/IEA-PVPS_T15_R11_Multifunctional_Characterisation_BIPV_report.pdf
[110] P. Bonomo *et al.,* “Standardization, performance risks and identification of related gaps for a performance-based qualification in BIPV,” 2019. Accessed: Jul. 21 2020. [Online]. Available: https://bipvboost.eu/public-reports/

[111] *Photovoltaics in buildings - Part 1: BIPV modules*, EN 50583-1:2016, 2016. [Online]. Available: https://infostore.saiglobal.com/en-us/Standards/EN-50583-1-2016-352938_SAIG_CENELEC_CENELEC_805189/

[112] *Photovoltaics in buildings - Part 2: BIPV systems*, EN 50583-2:2016, 2016. [Online]. Available: https://infostore.saiglobal.com/en-us/standards/en-50583-2-2016-352939_SAIG_CENELEC_CENELEC_805191/

[113] IEA PVPS Task 15, *BIPV Research Teams and BIPV RD Facilities. An International Mapping.* [Online]. Available: (https://iea-pvps.org/key-topics/bipv-research-teams-and-bipv-rd-facilities-an-international-mapping-by-task-15/ (accessed: Feb. 23 2021).

[114] *Terrestrial photovoltaic (PV) modules - Design qualification and type approval - Part 1-1: Special requirements for testing of crystalline silicon photovoltaic (PV) modules*, IEC 61215-1-1:2016., IEC, 2016. [Online]. Available: https://webstore.iec.ch/publication/24313

[115] *Photovoltaic (PV) module safety qualification - Part 1: Requirements for construction: Photovoltaic (PV) module safety qualification - Part 1: Requirements for construction*, IEC 61730-1:2016, IEC, 2016. [Online]. Available: https://webstore.iec.ch/publication/25674

[116] *Construction Products Regulation (CPR): Regulation (EU) No 305/2011*, 2011.

[117] *Photovoltaic (PV) module performance testing and energy rating - Part 1: Irradiance and temperature performance measurements and power rating*, IEC 61853-1:2011, IEC, Jan. 2011. [Online]. Available: https://webstore.iec.ch/publication/6035

[118] *Photovoltaic (PV) module performance testing and energy rating - Part 2: Spectral responsivity, incidence angle and module operating temperature measurements*, IEC 61853-2:2016, IEC, Sep. 2016. [Online]. Available: https://webstore.iec.ch/publication/25811

[119] John Wohlgemuth, “History of IEC qualification standards,” Jul. 15 2011. Accessed: Sep. 10 2020. [Online]. Available: https://www.nrel.gov/docs/fy11osti/52246.pdf

[120] IEC Standardization Management Board (SMB), “Circular from virtual SMB meeting May 2020, Geneva. Report of IEC TC82 following its (virtual) Spring 2020 meeting,” in.

[121] U. Jahn, M. Herz, M. Koentges, D. Parlevliet, and M. Paggi, “Review on Infrared and Electroluminescence Imaging for PV Field Applications,” Report IEA-PVPS T13-10:2018, IEA-PVPS Task 13, 2018. [Online]. Available: https://iea-pvps.org/key-topics/review-on-ir-and-el-imaging-for-pv-field-applications/

[122] M. van Iseghem, “PV module test protocols at EDF,” Freiburg im Breisgau, June 2014.

[123] *Terrestrial photovoltaic (PV) modules - Design qualification and type approval - Part 1: Test requirements: Terrestrial photovoltaic (PV) modules - Design qualification and type approval - Part 1: Test requirements*, IEC 61215-1:2016, IEC, 2016. [Online]. Available: https://webstore.iec.ch/publication/24312

[124] *Terrestrial photovoltaic (PV) modules - Design qualification and type approval - Part 1-2: Special requirements for testing of thin-film Cadmium Telluride (CdTe) based photovoltaic (PV) modules: Terrestrial photovoltaic (PV) modules - Design qualification and type approval - Part 1-2: Special requirements for testing of thin-film Cadmium Telluride (CdTe) based photovoltaic (PV) modules*, IEC 61215-1-2:2016, IEC, 2016. [Online]. Available: https://webstore.iec.ch/publication/26860

[125] *Terrestrial photovoltaic (PV) modules - Design qualification and type approval - Part 1-3: Special requirements for testing of thin-film amorphous silicon based photovoltaic (PV) modules: Terrestrial photovoltaic (PV) modules - Design qualification and type approval - Part 1-3: Special requirements for testing of thin-film amorphous silicon based*

photovoltaic (PV) modules, IEC 61215-1-3:2016, IEC, 2016. [Online]. Available: https://webstore.iec.ch/publication/29787

[126] *Terrestrial photovoltaic (PV) modules - Design qualification and type approval - Part 1-4: Special requirements for testing of thin-film Cu(In,GA)(S,Se)2 based photovoltaic (PV) modules: Terrestrial photovoltaic (PV) modules - Design qualification and type approval - Part 1-4: Special requirements for testing of thin-film Cu(In,GA)(S,Se)2 based photovoltaic (PV) modules*, IEC 61215-1-4:2016, IEC, 2016. [Online]. Available: https://webstore.iec.ch/publication/27848

[127] *Terrestrial photovoltaic (PV) modules - Design qualification and type approval - Part 2: Test procedures: Terrestrial photovoltaic (PV) modules - Design qualification and type approval - Part 2: Test procedures*, IEC 61215-2:2016, IEC, 2016. [Online]. Available: https://webstore.iec.ch/publication/24311

[128] *Photovoltaic (PV) module safety qualification - Part 2: Requirements for testing: Photovoltaic (PV) module safety qualification - Part 2: Requirements for testing*, IEC 61730-2:2016, IEC, 2016. [Online]. Available: https://webstore.iec.ch/publication/25680

[129] *Insulation coordination for equipment within low-voltage supply systems - Part 1: Principles, requirements and tests*, IEC 60664-1:2020, IEC. [Online]. Available: https://webstore.iec.ch/publication/59671

[130] *Measurement procedures for materials used in photovoltaic modules - Part 1-2: Encapsulants - Measurement of volume resistivity of photovoltaic encapsulants and other polymeric materials: Measurement procedures for materials used in photovoltaic modules - Part 1-2: Encapsulants - Measurement of volume resistivity of photovoltaic encapsulants and other polymeric materials*, IEC 62788-1-2:2016, IEC, 2016. [Online]. Available: https://webstore.iec.ch/publication/24790

[131] *Measurement procedures for materials used in photovoltaic modules - Part 1-4: Encapsulants - Measurement of optical transmittance and calculation of the solar-weighted photon transmittance, yellowness index, and UV cut-off wavelength*, IEC 62788-1-4:2016, IEC, 2016.

[132] *Measurement procedures for materials used in photovoltaic modules - Part 1-5: Encapsulants - Measurement of change in linear dimensions of sheet encapsulation material resulting from applied thermal conditions: Measurement procedures for materials used in photovoltaic modules - Part 1-5: Encapsulants - Measurement of change in linear dimensions of sheet encapsulation material resulting from applied thermal conditions*, IEC 62788-1-5:2016, IEC, 2016. [Online]. Available: https://webstore.iec.ch/publication/25264

[133] *Measurement procedures for materials used in photovoltaic modules - Part 1-6: Encapsulants - Test methods for determining the degree of cure in Ethylene-Vinyl Acetate: Measurement procedures for materials used in photovoltaic modules - Part 1-6: Encapsulants - Test methods for determining the degree of cure in Ethylene-Vinyl Acetate*, IEC 62788-1-6:2017+AMD1:2020 CSV Consolidated version, IEC, 2016. [Online]. Available: https://webstore.iec.ch/publication/67103

[134] *Measurement procedures for materials used in photovoltaic modules - Part 1-7: Encapsulants - Test procedure of optical durability*, IEC 62788-1-7:2020, IEC, 2016. [Online]. Available: https://webstore.iec.ch/publication/26676

[135] *Measurement procedures for materials used in photovoltaic modules - Part 5-1: Edge seals - Suggested test methods for use with edge seal materials*, IEC 62788-5-1:2020, IEC, 2016. [Online]. Available: https://webstore.iec.ch/publication/32720

[136] *Measurement procedures for materials used in photovoltaic modules - Part 6-2: General tests - Moisture permeation testing of polymeric materials*, IEC 62788-6-2:2020, IEC, 2016. [Online]. Available: https://webstore.iec.ch/publication/28498

[137] *Measurement procedures for materials used in photovoltaic modules - Part 2: Polymeric materials - Frontsheets and backsheets*, IEC TS 62788-2:2017, IEC, 2017. [Online]. Available: https://webstore.iec.ch/publication/26617

[138] *Measurement procedures for materials used in photovoltaic modules - Part 7-2: Environmental exposures - Accelerated weathering tests of polymeric materials*, IEC TS 62788-7-2:2017, IEC, Sep. 2017. [Online]. Available: https://webstore.iec.ch/publication/33675

[139] *Photovoltaic (PV) modules - Test methods for the detection of potential-induced degradation - Part 1: Crystalline silicon*, IEC TS 62804-1:2015, IEC, 2015. [Online]. Available: https://webstore.iec.ch/publication/23071

[140] *Photovoltaic (PV) modules - Test methods for the detection of potential-induced degradation - Part 1-1: Crystalline silicon - Delamination*, IEC TS 62804-1-1:2020, IEC, 2020.

[141] *Photovoltaic (PV) modules - Cyclic (dynamic) mechanical load testing*, IEC TS 62782:2016, IEC, 2016. [Online]. Available: https://webstore.iec.ch/publication/24310

[142] *Extended thermal cycling of PV modules - Test procedure*, IEC 62892:2019, IEC. [Online]. Available: https://webstore.iec.ch/publication/29329

[143] *Guidelines for qualifying PV modules, components and materials for operation at high temperatures*, IEC TS 63126:2020, IEC. [Online]. Available: https://webstore.iec.ch/publication/59551

[144] J. Li and E. Hsi, *Solar Panel Code of Practice: International guideline on the risk management and sustainability of solar panel warranty insurance.* [Online]. Available: https://www.swissre.com/Library/solar-panel-code-of-practice-en1.html (accessed: Sep. 10 2020).

[145] W. Gambogi *et al.,* "Multi-stress durability testing to better predict outdoor performance of PV modules," in *2015 IEEE 42nd Photovoltaic Specialist Conference (PVSC)*, 2015, pp. 1–5.

[146] T. Doyle, R. Desharnais, and T. Erion-Lorico, *2020 PV Module Reliability Scorecard.* [Online]. Available: https://www.pvel.com/pv-scorecard/ (accessed: Sep. 10 2020).

[147] *Extended-stress testing of photovoltaic modules for risk analysis*, IEC TS 63209 ED1, Approved for Draft Technical Specification, IEC, Oct. 2021. [Online]. Available: https://www.iec.ch/dyn/www/f?p=103:38:8143449863034:::FSP_ORG_ID,FSP_APEX_PAGE,FSP_PROJECT_ID:1276,23,102121

[148] *Extended-stress testing of photovoltaic modules for risk analysis – Part 2: Durability characterization of polymeric component materials and packaging sets*, IEC TS 63209-2 ED1, Approved for Committee Draft, IEC, Dec. 2021. [Online]. Available: https://www.iec.ch/dyn/www/f?p=103:38:5971347928768:::FSP_ORG_ID,FSP_APEX_PAGE,FSP_PROJECT_ID:1276,23,103328

[149] *Terrestrial photovoltaic (PV) modules for consumer products - Design qualification and type approval*, IEC 63163 ED1, Preparation of Compilation of Comments, IEC, Oct. 2021. [Online]. Available: https://www.iec.ch/dyn/www/f?p=103:38:8143449863034:::FSP_ORG_ID,FSP_APEX_PAGE,FSP_PROJECT_ID:1276,23,101098

[150] *Terrestrial photovoltaic (PV) modules - Design qualification and type approval - Part 2: Test procedures*, IEC 61215-2 ED2, Approved for Final Draft International Standard, IEC, Apr. 2021. [Online]. Available: https://www.iec.ch/dyn/www/f?p=103:38:0:::FSP_ORG_ID,FSP_APEX_PAGE,FSP_PROJECT_ID:1276,23,101269

[151] *Terrestrial photovoltaic (PV) modules - Design qualification and type approval - Part 1-2: Special requirements for testing of thin-film Cadmium Telluride (CdTe) based photovoltaic (PV) modules*, IEC 61215-1-2 ED2, Approved for Final Draft International Standard, IEC, Apr. 2021. [Online]. Available: https://www.iec.ch/dyn/www/f?p=103:38:5657246992529::::FSP_ORG_ID,FSP_APEX_PAGE,FSP_PROJECT_ID:1276,23,101266

[152] *Terrestrial photovoltaic (PV) modules - Design qualification and type approval - Part 1: Test requirements*, IEC 61215-1 ED2, Approved for Final Draft International Standard, IEC, Apr. 2021. [Online]. Available: https://www.iec.ch/dyn/www/f?p=103:38:5657246992529::::FSP_ORG_ID,FSP_APEX_PAGE,FSP_PROJECT_ID:1276,23,101264

[153] *Terrestrial photovoltaic (PV) modules - Design qualification and type approval - Part 1-1: Special requirements for testing of crystalline silicon photovoltaic (PV) modules*, IEC 61215-1-1 ED2, Approved for Final Draft International Standard, IEC, Apr. 2021. [Online]. Available: https://www.iec.ch/dyn/www/f?p=103:38:5657246992529::::FSP_ORG_ID,FSP_APEX_PAGE,FSP_PROJECT_ID:1276,23,101265

[154] *Terrestrial photovoltaic (PV) modules - Design qualification and type approval - Part 1-3: Special requirements for testing of thin-film amorphous silicon based photovoltaic (PV) modules*, IEC 61215-1-3 ED2, Approved for Final Draft International Standard, IEC, Apr. 2021. [Online]. Available: https://www.iec.ch/dyn/www/f?p=103:38:5657246992529::::FSP_ORG_ID,FSP_APEX_PAGE,FSP_PROJECT_ID:1276,23,101267

[155] *Terrestrial photovoltaic (PV) modules - Design qualification and type approval - Part 1-4: Special requirements for testing of thin-film Cu(In,GA)(S,Se)2 based photovoltaic (PV) modules*, IEC 61215-1-4 ED2, Approved for Final Draft International Standard, IEC, Apr. 2021. [Online]. Available: https://www.iec.ch/dyn/www/f?p=103:38:5657246992529::::FSP_ORG_ID,FSP_APEX_PAGE,FSP_PROJECT_ID:1276,23,101268

[156] *Amendment 1 - Photovoltaic (PV) module safety qualification - Part 2: Requirements for testing*, IEC 61730-2/AMD1 ED2, Approved for Committee Draft for Vote, IEC, Dec. 2021. [Online]. Available: https://www.iec.ch/dyn/www/f?p=103:38:5657246992529::::FSP_ORG_ID,FSP_APEX_PAGE,FSP_PROJECT_ID:1276,23,102561

[157] *Amendment 1 - Photovoltaic (PV) module safety qualification - Part 1: Requirements for construction*, IEC 61730-1/AMD1 ED2, Approved for Committee Draft for Vote, IEC, Jan. 2022. [Online]. Available: https://www.iec.ch/dyn/www/f?p=103:38:5657246992529::::FSP_ORG_ID,FSP_APEX_PAGE,FSP_PROJECT_ID:1276,23,100245

[158] *Photovoltaic devices - Part 1-2: Measurement of current-voltage characteristics of bifacial photovoltaic (PV) devices*, IEC TS 60904-1-2:2019, IEC, 2019. [Online]. Available: https://webstore.iec.ch/publication/34357

[159] *Junction boxes for photovoltaic modules - Safety requirements and tests*, IEC 62790:2020 RLV Redline version, IEC, 2020. [Online]. Available: https://webstore.iec.ch/publication/67338

[160] *Connectors for DC-application in photovoltaic systems - Safety requirements and tests*, IEC 62852:2014+AMD1:2020 CSV Consolidated version, IEC, 2020. [Online]. Available: https://webstore.iec.ch/publication/66763

[161] *Measurement procedures for materials used in photovoltaic modules - Part 2-1: Polymeric materials - Frontsheet and backsheet - Safety requirements*, IEC 62788-2-1 ED1,

Approved for Committee Draft for Vote, IEC, Nov. 2021. [Online]. Available: https://www.iec.ch/dyn/www/f?p=103:38:5657246992529::::FSP_ORG_ID,FSP_APEX_PAGE,FSP_PROJECT_ID:1276,23,102804

[162] K. Ramspeck *et al.,* "Light induced degradation of rear passivated mc-Si solar cells," in *27th European Photovoltaic Solar Energy Conference and Exhibition*, pp. 861–865.

[163] K. A. Berger, "Combined Stress Testing on PV modules - A collaborative research within the European photovoltaic infrastructure research project SOPHIA," in *5th Sophia PV Module Reliability Workshop*.

[164] M. Owen-Bellini *et al.,* "Advancing reliability assessments of photovoltaic modules and materials using combined-accelerated stress testing," *Prog Photovolt Res Appl*, 2020, doi: 10.1002/pip.3342.

[165] K. Hartman *et al.,* "Validation of Advanced Photovoltaic Module Materials and Processes by Combined-Accelerated Stress Testing (C-AST)," in 2019, pp. 2243–2248. [Online]. Available: https://www.scopus.com/inward/record.uri?eid=2-s2.0-85081568169&doi=10.1109%2fPVSC40753.2019.8980545&partnerID=40&md5=0d1c087843c6abd7f06912c2bdc418b1

[166] S. L. Samuels, N. J. Glassmaker, G. A. Andrews, M. J. Brown, and M. E. Lewittes, "Teflon® FEP frontsheets for photovoltaic modules: Improved optics leading to higher module efficiency," in *2010 35th IEEE Photovoltaic Specialists Conference*, 2010, pp. 2788–2790.

[167] N. G. Dhere, "Flexible packaging for PV modules," *Proceedings of SPIE - The International Society for Optical Engineering*, vol. 7048, 2008, doi: 10.1117/12.795718.

[168] E. Bittmann, O. Mayer, M. Zettl, and O. Stern, "Low Concentration PV With Polycarbonate," in *23rd European Photovoltaic Solar Energy Conference and Exhibition*, pp. 537–539.

[169] C. Schmid *et al.,* "Angle of Incidence Performance Study of PV Modules with Patterned Polycarbonate Front Sheets," in *Proceedings of 28th European Photovoltaic Solar Energy Conference and Exhibition*, pp. 3090–3092.

[170] A. Backes, N. Adamovic, and U. Schmid, "New Light Management Concepts for Standard Si Solar Cells Fabricated by Embossing of Polycarbonate Front & Back Sheets," in *28th European Photovoltaic Solar Energy Conference and Exhibition*, pp. 3096–3098.

[171] K. Drabczyk, P. Sobik, Z. Starowicz, K. Gawlińska, A. Pluta, and B. Drabczyk, "Study of lamination quality of solar modules with PMMA front layer," *MI*, vol. 36, no. 3, pp. 100–103, 2019, doi: 10.1108/MI-12-2018-0087.

[172] H. Ng *et al.,* "25 Year Low Cost Flexible Frontsheet - Lifetime Prediction," in *NREL PV Reliability Workshop 2020*, pp. 1–16. Accessed: Oct. 16 2020. [Online]. Available: https://www.nrel.gov/pv/pvrw.html

[173] M. Owen-Bellini *et al.,* "Correlation of advanced accelerated stress testing with polyamide-based photovoltaic backsheet field-failures," in *2019 IEEE 46th Photovoltaic Specialists Conference (PVSC)*, 2019, pp. 1995–1999.

[174] T. Sarver, A. Al-Qaraghuli, and L. L. Kazmerski, "A comprehensive review of the impact of dust on the use of solar energy: History, investigations, results, literature, and mitigation approaches," *Renewable and Sustainable Energy Reviews*, vol. 22, pp. 698–733, 2013, doi: 10.1016/j.rser.2012.12.065.

[175] J. M. Freese, "Effects of outdoor exposure on the solar reflectance properties of silvered glass mirrors," in *Sun II*, pp. 1340–1344.

[176] D. C. Miller, M. T. Muller, and L. J. Simpson, "Review of Artificial Abrasion Test Methods for PV Module Technology," Denver, CO, 2016. Accessed: Feb. 23 2021. [Online].

Available: https://www.osti.gov/biblio/1295389-review-artificial-abrasion-test-methods-pv-module-technology
[177] J. M. Newkirk *et al.,* "Artificial linear brush abrasion of coatings for photovoltaic module first-surfaces," *Solar Energy Materials and Solar Cells*, vol. 219, p. 110757, 2021, doi: 10.1016/j.solmat.2020.110757.
[178] *Measurement procedures for materials used in photovoltaic modules - Part 7-3: Environmental exposures - Accelerated abrasion tests of PV module external surfaces*, IEC 62788-7-3 ED1, Approved for Committee Draft for Vote, IEC, Dec. 2021. [Online]. Available: https://www.iec.ch/dyn/www/f?p=103:38:5657246992529::::FSP_ORG_ID,FSP_APEX_PAGE,FSP_PROJECT_ID:1276,23,101467
[179] P. M. Kaminski, G. Womack, and J. M. Walls, "Broadband anti-reflection coatings for thin film photovoltaics," in pp. 2778–2783.
[180] D. C. Miller *et al.,* "Examination of an optical transmittance test for photovoltaic encapsulation materials," p. 882509, doi: 10.1117/12.2024372.
[181] J. Tracy *et al.,* "Survey of Material Degradation in Globally Fielded PV Modules," in *IEEE 46th Photovoltaic Specialists Conference (PVSC)*, pp. 874–879.
[182] Sraisth, *EU PVSEC: New polyolefin-based backsheet challenges traditional PET-based backsheet*, 2017. [Online]. Available: https://www.pv-magazine.com/2017/10/03/eu-pvsec-new-polyolefin-based-backsheet-challenges-traditional-pet-based-backsheets/
[183] P. Gebhardt, D. Philipp, and P. Hülsmann, "Qualification of Polyolefin Backsheet for PV Modules," in *36th European Photovoltaic Solar Energy Conference and Exhibition*.
[184] F. Rummens, P. Gebhardt, and D. Phillipp, "Impact of Highly Breathable Polyolefin Backsheet on EVA Yellowing," in *36th European Photovoltaic Solar Energy Conference and Exhibition*.
[185] C. Thellen, "Co-Extrusion of a Novel Multilayer Photovoltaic Backsheet Based on Polyamide-Ionomer Alloy Skin Layers," in *33rd EU-PVSEC*.
[186] M. Mrcarica, P. Tummers, K. v. Durme, P. Pathak, and I. Goudswaard, "DSM Innovative Endurance Backsheet Outdoor Validation in Hot and Humid Climate," in *2018 IEEE 7th World Conference on Photovoltaic Energy Conversion (WCPEC) (A Joint Conference of 45th IEEE PVSC, 28th PVSEC 34th EU PVSEC)*, 2018, pp. 548–550.
[187] M. D. Kempe, T. Lockman, and J. Morse, "Development of Testing Methods to Predict Cracking in Photovoltaic Backsheets," in *2019 IEEE 46th Photovoltaic Specialists Conference (PVSC)*, 2019, pp. 2411–2416.
[188] M. Wang, "Degradation of PERC and Al-BSF Photovoltaic Cells with Differentiated Minimodule Packaging Under Damp Heat Exposure," in *IEEE PVSC 46*.
[189] G. Oreski and G. M. Wallner, "Aging mechanisms of polymeric films for PV encapsulation," *Solar Energy*, vol. 79, no. 6, pp. 612–617, 2005, doi: 10.1016/j.solener.2005.02.008.
[190] A. Fairbrother *et al.,* "Differential degradation patterns of photovoltaic backsheets at the array level," *Solar Energy*, vol. 163, pp. 62–69, 2018, doi: 10.1016/j.solener.2018.01.072.
[191] Y. Wang *et al.,* "Generalized Spatio-Temporal Model of Backsheet Degradation from Field Surveys of Photovoltaic Modules," *IEEE J. Photovoltaics*, vol. 9, no. 5, pp. 1374–1381, 2019, doi: 10.1109/JPHOTOV.2019.2928700.
[192] W. Gambogi *et al.,* "Sequential Stress Testing to Predict Photovoltaic Module Durability," in *2018 IEEE 7th World Conference on Photovoltaic Energy Conversion (WCPEC) (A Joint Conference of 45th IEEE PVSC, 28th PVSEC 34th EU PVSEC)*, 2018, pp. 1593–1596.

[193] S. Spataru, P. Hacke, and M. Owen-Bellini, “Combined-Accelerated Stress Testing System for Photovoltaic Modules,” in *2018 IEEE 7th World Conference on Photovoltaic Energy Conversion (WCPEC) (A Joint Conference of 45th IEEE PVSC, 28th PVSEC 34th EU PVSEC)*, 2018, pp. 3943–3948.
[194] G. W. Ehrenstein and S. Pongratz, *Resistance and stability of polymers*. Munich: Hanser Publishers, 2013.
[195] C. Schinagl, A. K. Plessing, E. Url, A. Nigg, H. Muckenhuber, and W. Krumlacher, “Flexible Encapsulation with Backsheets and Frontsheets for PV Applications,” in *Proceedings 27th European Photovoltaic Solar Energy Conference and Exhibition*, pp. 2985–2987.
[196] M. Owen-Bellini, P. Hacke, S. V. Spataru, D. C. Miller, S. Spataru, and M. Kempe, Eds., *Combined-Accelerated Stress Testing for Advanced Reliability Assessment of Photovoltaic Modules*, 2018.
[197] U. Eitner, M. Pander, S. Kajari-Schröder, M. Köntges, and H. Altenbach, “Thermomechanics of PV Modules Including the Viscoelasticity of EVA,” in *26th European Photovoltaic Solar Energy*.
[198] F. Rummens, “PHOTOVOLTAIC MODULES WITH POLYPROPYLENE BASED BACKSHEET,” WO 2011/009568 A1, Jan 27, 2011.
[199] G. Stollwerck, “Polyolefin Backsheet and New Encapsulant Supress Cell Degradation in the Module,” in *28th EU-PVSEC*.
[200] E. Baur, J. G. Brinkman, T. A. Osswald, and E. Schmachtenberg, Eds., *Saechtling Kunststoff Taschenbuch*: Carl Hanser Verlag GmbH & Co. KG, 2007.
[201] G. Stollwerck, “Polyolefin Backsheet Protects Solar Modules for a Life Time,” in *28th EU-PVSEC*.
[202] G. Oreski and W. Schöppel, “Degradation behavior and reliability of a novel multilayer polyolefin backsheet film for PV encapsulation,” in *27th European Photovoltaic Solar Energy Conference*.
[203] F. Rummens, “Long Term Accelerated Weathering Tests on “Coupons” to Develop New Classes of Backsheets,” *in Proc: 31st European Photovoltaic Solar Energy Conference and Exhibition*, pp. 2478–2481, 2015, doi: 10.4229/EUPVSEC20152015-5CV.2.8.
[204] L. Castillon, J. Ascencio-Vásquez, A. Mehilli, G. Oreski, M. Topic, and K.-A. Weiß, “Parallel Natural Weathering of Backsheets across Europe,” in *36th European Photovoltaic Solar Energy Conference and Exhibition*.
[205] W. Gambogi, “Reliability of transparent polymeric backsheets under accelerated aging for bifacial modules,” in *NREL PVRW*.
[206] W. Gambogi *et al., Eds., Performance and Reliability of Bifacial Modules Using a Transparent Backsheet*, 2019.
[207] K. Arihara *et al.,* “Reliability and long term durability of bifacial photovoltaic modules using transparent backsheet,” *Japanese Journal of Applied Physics*, vol. 57, 08RG15, 2018, doi: 10.7567/JJAP.57.08RG15.
[208] *Measurement procedures for materials used in photovoltaic modules.: Part 1-4: Encapsulants - Measurement of optical transmittance and calculation of the solar-weighted photon transmittance, yellowness index, and UV cut-off wavelength*, IEC 62788-1-4, International Electrotechnical Commission, 2016. [Online]. Available: https://webstore.iec.ch/publication/25942
[209] *IEC TS 62788 Measurements procedures for materials used in photovoltaic modules-Part 7-2: Environmental exposures - Accelerated weathering tests of polymeric materials*.
[210] D. C. Miller *et al., Eds., Degradation in PV Encapsulant Transmittance: Results of the First PVQAT TG5 Study*, 2019.

[211] D. Miller, M. Kempe, C. Kennedy, and S. Kurtz, “Analysis of transmitted optical spectrum enabling accelerated testing of multi-junction CPV designs,” *Optical Engineering - OPT ENG*, vol. 50, 2011, doi: 10.1117/1.3530092.
[212] *Standard Practice for Calculating Yellowness and Whiteness Indices from Instrumentally Measured Color Coordinates*, ASTM E313 - 05, ASTM International. [Online]. Available: http://www.astm.org/cgi-bin/resolver.cgi?E313-05
[213] D. C. Miller *et al.,* “Degradation in photovoltaic encapsulation strength of attachment: Results of the first PVQAT TG5 artificial weathering study,” *Prog Photovolt Res Appl*, vol. 28, no. 7, pp. 639–658, 2020, doi: 10.1002/pip.3255.
[214] Roger H. French, “Degradation of PERC & Al-BSF Photovoltaic Cells with Differentiated Minimodule Packaging Materials,” 2019. Accessed: Aug. 12 2020. [Online]. Available: https://www.nist.gov/system/files/documents/2020/01/15/French.pdf
[215] J. L. Braid *et al.,* “EL and I-V Correlation for Degradation of PERC vs. Al-BSF Commercial Modules in Accelerated Exposures,” in *2018 IEEE 7th World Conference on Photovoltaic Energy Conversion (WCPEC) (A Joint Conference of 45th IEEE PVSC, 28th PVSEC & 34th EU PVSEC)*.
[216] B. Ottersböck, G. Oreski, and G. Pinter, “Comparison of different microclimate effects on the aging behavior of encapsulation materials used in photovoltaic modules,” *Polymer Degradation and Stability*, pp. 182–191, 2017, doi: 10.1016/j.polymdegradstab.2017.03.010.
[217] M. A. Green, “Silicon Photovoltaic Modules: A Brief History of the First 50 Years,” *Prog. Photovolt: Res. Appl.*, vol. 13, no. 5, pp. 447–455, 2005, doi: 10.1002/pip.612.
[218] D. C. Jordan and S. R. Kurtz, “Photovoltaic Degradation Rates-an Analytical Review,” *Prog. Photovolt: Res. Appl.*, vol. 21, no. 1, pp. 12–29, 2013, doi: 10.1002/pip.1182.
[219] S. Chattopadhyay *et al.,* “Visual degradation in field-aged crystalline silicon PV modules in India and correlation with electrical degradation,” *IEEE J. Photovoltaics*, vol. 4, no. 6, pp. 1470–1476, 2014, doi: 10.1109/JPHOTOV.2014.2356717.
[220] V. Poulek, D. S. Strebkov, I. S. Persic, and M. Libra, “Towards 50years lifetime of PV panels laminated with silicone gel technology,” *Solar Energy*, vol. 86, no. 10, pp. 3103–3108, 2012, doi: 10.1016/j.solener.2012.07.013.
[221] W. Luo *et al.,* “Potential-induced degradation in photovoltaic modules: a critical review,” *Energy Environ. Sci.*, vol. 10, no. 1, pp. 43–68, 2017, doi: 10.1039/C6EE02271E.
[222] K. Hara, H. Ohwada, T. Furihata, and A. Masuda, “Durable crystalline Si photovoltaic modules based on silicone-sheet encapsulants,” *Jpn. J. Appl. Phys.*, vol. 57, no. 2, p. 27101, 2018, doi: 10.7567/JJAP.57.027101.
[223] S. Braun, G. Hahn, R. Nissler, C. Pönisch, and D. Habermann, “Multi-busbar Solar Cells and Modules: High Efficiencies and Low Silver Consumption,” *Energy Procedia*, vol. 38, pp. 334–339, 2013, doi: 10.1016/j.egypro.2013.07.286.
[224] T. Söderström, “Smart Wire Connection Technology,” in *28th EU-PVSEC*.
[225] A. Schneider, “Solar cell improvement by new metallization techniques,” in *4th WCPEC*.
[226] P. Papet, “Metallization schemes dedicated to smartwire connection technology for heterojunction solar cells,” in.
[227] J. Geissbühler, “Metallization techniques and interconnection scheme for high efficiency silicon heterojunction photovoltaics,” in *Photovoltaics International*.
[228] A. Faes *et al.,* “Metallization and interconnection for high-efficiency bifacial silicon heterojunction solar cells and modules,” *Photovoltaics International*, vol. 2018, no. 41, pp. 65–76.
[229] Y. Yao *et al., Module integration of solar cells with diverse metallization schemes enabled by SmartWire Connection Technology*, 2015.

[230] A. Faes, “Screen-printing for high efficiency solar cells,” in *Asada Mesh Advanced Screen Printing Workshop*.
[231] Meyer Burger, *Record 410 watt module with heterojunction solar cell technology*, 2018. [Online]. Available: https://www.meyerburger.com/en/company/media-center/news/record-410-watt-module-with-heterojunction-solar-cell-technology/
[232] Meyer Burger, *Meyer Burger plans to adapt business model and enter strategic collaboration with REC.* [Online]. Available: https://www.meyerburger.com/en/company/media-center/news/meyer-burger-plans-to-adapt-business-model-and-enter-strategic-collaboration-with-rec/
[233] REC, *REC Alpha Serie.* [Online]. Available: https://www.recgroup.com/en/alpha?parent=81&type=product
[234] U. Eitner, T. Geipel, S. -N. Holtschke, and M. Tranitz, “Characterization of Electrically Conductive Adhesives,” *Energy Procedia*, vol. 27, pp. 676–679, 2012, doi: 10.1016/j.egypro.2012.07.128.
[235] K. Nagarkar, “Reliability of compliant electrically conductive adhesives for flexible PV modules,” in *2016 15th IEEE Intersociety Conference on Thermal and Thermomechanical Phenomena in Electronic Systems (ITherm)*, 2016, pp. 898–905.
[236] Z. Li, K. Hansen, Y. Yao, Y. Ma, K. Moon, and C. P. Wong, “The conduction development mechanism of silicone-based electrically conductive adhesives,” *J. Mater. Chem. C*, vol. 1, no. 28, p. 4368, 2013, doi: 10.1039/c3tc30612g.
[237] R. Gomatam and Kash L. Mittal, *Electrically Conductive Adhesives*.
[238] M. Springer and N. Bosco, “Linear viscoelastic characterization of electrically conductive adhesives used as interconnect in photovoltaic modules,” *Prog Photovolt Res Appl*, vol. 28, no. 7, pp. 659–681, 2020, doi: 10.1002/pip.3257.
[239] L. Theunissen, B. Willems, J. Burke, D. Tonini, M. Galiazzo, and A. Henckens, “Electrically conductive adhesives as cell interconnection material in shingled module technology,” *AIP Conference Proceedings*, vol. 1999, no. 1, p. 80003, 2018, doi: 10.1063/1.5049305.
[240] Y. C. Lin and J. Zhong, “A review of the influencing factors on anisotropic conductive adhesives joining technology in electrical applications,” *J Mater Sci*, vol. 43, no. 9, pp. 3072–3093, 2008, doi: 10.1007/s10853-007-2320-4.
[241] M. Schwark, W. Mühleisen, L. Neumaier, and C. Hirschl, “Low silver content, lead free modules with light capturing ribbons,” in *2017 6th International Conference on Clean Electrical Power (ICCEP)*, 2017, pp. 158–162.
[242] J. Park, W. Oh, H. Park, C. Jeong, B. Choi, and J. Lee, “Analysis of solar cells interconnected by electrically conductive adhesives for high-density photovoltaic modules,” *Applied Surface Science*, vol. 484, pp. 732–739, 2019, doi: 10.1016/j.apsusc.2019.03.307.
[243] G. Beaucarne, “Materials Challenge for Shingled Cells Interconnection,” *Energy Procedia*, vol. 98, pp. 115–124, 2016, doi: 10.1016/j.egypro.2016.10.087.
[244] Y. Hu and R. H. French, “5 - Degradation and Failure Mechanisms of PV Module Interconnects,” in *Durability and Reliability of Polymers and Other Materials in Photovoltaic Modules*, pp. 119–134.
[245] L. V. Mesquita, N. Klasen, E. Fokuhl, D. Philipp, and L. P. Bauermann, “Analysis of shingle interconnections in solar modules by scanning acoustic microscopy,” in *AIP Conference Proceedings 2147*.
[246] C. H. Schiller, L. C. Rendler, G. Mülhöfer, A. Kraft, and H. N. Dirk, “Accelerated TC Test in Comparison with Standard TC Test for PV Modules with Ribbon, Wire and Shingle Interconnection,” in *36th European Photovoltaic Solar Energy Conference and Exhibition*, pp. 995–999.

[247] L. P. Bauermann *et al.,* "Qualification of conductive adhesives for photovoltaic application - accelerated ageing tests," *Energy Procedia*, vol. 124, pp. 554–559, 2017, doi: 10.1016/j.egypro.2017.09.266.
[248] N. Klasen, P. Romer, A. Beinert, and A. Kraft, "FEM simulation of deformations in strings of shingled solar cells subjected to mechanical reliability testing," in *AIP Conference Proceedings 2156, 020016 (2019)*, p. 20016.
[249] M. Pander, S. Schulze, and M. Ebert, "Mechanical Modelling of Electrically Conductive Adhesives for Photovoltaic Applications," 2014, doi: 10.4229/EUPVSEC20142014-5DV.3.39.
[250] R. Meier, M. Pander, S. Großer, and S. Dietrich, "Microstructural Optimization Approach of Solar Cell Interconnectors Fatigue Behavior for Enhanced Module Lifetime in Extreme Climates," *Energy Procedia*, vol. 92, pp. 560–568, 2016, doi: 10.1016/j.egypro.2016.07.020.
[251] M. Pander, R. Meier, M. Sander, S. Dietrich, and M. Ebert, "Lifetime Estimation for Solar Cell Interconnectors," 2013, doi: 10.4229/28THEUPVSEC2013-4CO.10.3.
[252] M. T. Zarmai, N. N. Ekere, C. F. Oduoza, and E. H. Amalu, "Evaluation of thermo-mechanical damage and fatigue life of solar cell solder interconnections," *Robotics and Computer-Integrated Manufacturing*, vol. 47, pp. 37–43, 2017, doi: 10.1016/j.rcim.2016.12.008.
[253] D. K. Schroder and D. L. Meier, "Solar cell contact resistance—A review," *IEEE Trans. Electron Devices*, vol. 31, no. 5, pp. 637–647, 1984, doi: 10.1109/T-ED.1984.21583.
[254] S. Riegel, F. Mutter, T. Lauermann, B. Terheiden, and G. Hahn, "Review on screen printed metallization on p-type silicon," *Energy Procedia*, vol. 21, pp. 14–23, 2012, doi: 10.1016/j.egypro.2012.05.003.
[255] G. Schubert, F. Huster, and P. Fath, "Physical understanding of printed thick-film front contacts of crystalline Si solar cells—Review of existing models and recent developments," *Solar Energy Materials and Solar Cells*, vol. 90, 18-19, pp. 3399–3406, 2006, doi: 10.1016/j.solmat.2006.03.040.
[256] R. Hönig, "Evaluation and microstructure analysis of thick film contacts for industrial silicon solar cells,"
[257] J. D. Fields *et al.,* "The formation mechanism for printed silver-contacts for silicon solar cells," *Nature communications*, vol. 7, p. 11143, 2016, doi: 10.1038/ncomms11143.
[258] C. Ballif, D. Huljic, G. Willeke, and A. Hessler-Wyser, "Silver Thick-Film Contacts on Highly Doped n-Type Silicon Emitters: Structural and Electronic Properties of the Interface," *Appl. Phys. Lett.*, vol. 82, pp. 1878–1880, 2003, doi: 10.1063/1.1562338.
[259] E. Cabrera, S. Olibet, J. Glatz-Reichenbach, R. Kopecek, D. Reinke, and G. Schubert, "Experimental evidence of direct contact formation for the current transport in silver thick film metallized silicon emitters," *J. Appl. Phys.*, vol. 110, 2011, doi: 10.1063/1.3665718.
[260] Z. G. Li, L. Liang, and L. K. Cheng, "Electron microscopy study of front-side Ag contact in crystalline Si solar cells," *J. Appl. Phys.*, vol. 105, p. 66102, 2009, doi: 10.1063/1.3086663.
[261] Z. G. Li *et al.,* "Microstructural comparison of silicon solar cells' front-side Ag contact and the evolution of current conduction mechanisms," *J. Appl. Phys.*, vol. 110, p. 74304, 2011, doi: 10.1063/1.3642956.
[262] M. Pfeffer, P. Kumar, and O. Eibl, "High-Efficiency Crystalline-Si Solar Cells with Screen-Printed Front-Side Metallization: A Percolation Model to Explain the Current Path," *Journal of Elec Materi*, vol. 45, no. 11, pp. 5764–5772, 2016, doi: 10.1007/s11664-016-4818-5.

[263] P. Kumar, Z. Aabdin, M. Pfeffer, and O. Eibl, “High-efficiency, single-crystalline, p- and n-type Si solar cells: Microstructure and chemical analysis of the glass layer,” *Solar Energy Materials and Solar Cells*, vol. 178, pp. 52–64, 2018, doi: 10.1016/j.solmat.2018.01.001.

[264] “THICK-FILM PASTES CONTAINING LEAD- AND TELLURIUM-OXIDES, AND THEIR USE IN THE MANUFACTURE OF SEMICONDUCTOR DEVICES - European Patent Office,” EP 3070062 A1.

[265] A. Ebong, N. Bezawada, and K. Batchu, “Understanding the influence of tellurium oxide in front Ag paste for contacting silicon solar cells with homogeneous high sheet resistance emitter,” *Jpn. J. Appl. Phys.*, vol. 56, 08MB07, 2017, doi: 10.7567/JJAP.56.08MB07.

[266] T. Aoyama, M. Aoki, I. Sumita, Y. Yoshino, Y. Ohshita, and A. Ogura, *EFFECTS OF TELLURIUM OXIDE IN SILVER PASTE ON THE ELECTRICAL LOSSES IN SILICON SOLAR CELLS*, 2017.

[267] K. Mikeska, M. Lu, and W. Liao, “Tellurium-based screen-printable conductor metallizations for crystalline silicon solar cells,” *Prog Photovolt Res Appl*, vol. 27, 2019, doi: 10.1002/pip.3185.

[268] T. Aoyama, M. Aoki, I. Sumita, Y. Yoshino, and A. Ogura, “An Evaluation of Constituents in Paste for Silicon Solar Cells with Floating Contact Method: A Case Study of Tellurium Oxide Effects,” *SSRN*, 2018, doi: 10.2139/ssrn.3152258.

[269] T. J. Trout, “PV module durability -connecting field results, accelerated testing, and materials,” in *44th IEEE*.

[270] M. Kempe, “Modeling of rates of moisture ingress into photovoltaic modules,” *Solar Energy Materials and Solar Cells*, vol. 90, no. 16, pp. 2720–2738, 2006, doi: 10.1016/j.solmat.2006.04.002.

[271] P. Hülsmann and K.-A. Weiss, “Simulation of water ingress into PV-modules: IEC-testing versus outdoor exposure,” *Solar Energy*, vol. 115, pp. 347–353, 2015, doi: 10.1016/j.solener.2015.03.007.

[272] A. Kraft *et al.,* “Investigation of Acetic Acid Corrosion Impact on Printed Solar Cell Contacts,” *Photovoltaics, IEEE Journal of*, vol. 5, pp. 736–743, 2015, doi: 10.1109/JPHOTOV.2015.2395146.

[273] T. Tanahashi, N. Sakamoto, H. Shibata, and A. Masuda, “Electrical detection of gap formation underneath finger electrodes on c-Si PV cells exposed to acetic acid vapor under hygrothermal conditions,” in *2016 IEEE 43rd Photovoltaic Specialists Conference (PVSC)*, 2016, pp. 1075–1079.

[274] C. Peike *et al.,* “Origin of damp-heat induced cell degradation,” (in af), *Solar Energy Materials and Solar Cells*, vol. 116, pp. 49–54, 2013, doi: 10.1016/j.solmat.2013.03.022.

[275] R. Asadpour, X. Sun, and M. A. Alam, “Electrical Signatures of Corrosion and Solder Bond Failure in c-Si Solar Cells and Modules,” *IEEE J. Photovoltaics*, vol. 9, no. 3, pp. 759–767, 2019, doi: 10.1109/JPHOTOV.2019.2896898.

[276] T. Tanahashi, N. Sakamoton, H. Shibata, and A. Masuda, “Corrosion-Induced AC Impedance Elevation in Front Electrodes of Crystalline Silicon Photovoltaic Cells Within Field-Aged Photovoltaic Modules,” *IEEE J. Photovoltaics*, vol. 9, no. 3, pp. 741–751, 2019, doi: 10.1109/JPHOTOV.2019.2893442.

[277] T. Tanahashi, N. Sakamoto, H. Shibata, and A. Masuda, “Localization and Characterization of a Degraded Site in Crystalline Silicon Photovoltaic Cells Exposed to Acetic Acid Vapor,” *IEEE J. Photovoltaics*, vol. 8, no. 4, pp. 997–1004, 2018, doi: 10.1109/JPHOTOV.2018.2839259.

[278] J.-H. Kim, J. Park, D. Kim, N. Park, and A. Umar, “Study on Mitigation Method of Solder Corrosion for Crystalline Silicon Photovoltaic Modules,” *International Journal of Photoenergy*, vol. 2014, p. 809075, 2014, doi: 10.1155/2014/809075.
[279] Y. Ino, S. Asao, K. Shirasawa, and H. Takato, “Investigation of Degradation Mode Spreading Interconnectors by Pressure-Cooker Testing of Photovoltaic Cells,” *IEEE J. Photovoltaics*, vol. 10, no. 1, pp. 188–196, 2020, doi: 10.1109/JPHOTOV.2019.2950079.
[280] T. Semba, T. Shimada, K. Y. K. Shirasawa, and H. Takato, “Corrosion of the Glass and Formation of Lead Compounds in the Metallization by High Temperature and High Humidity Test of Crystalline Silicon PV Module,” in *2018 IEEE 7th World Conference on Photovoltaic Energy Conversion (WCPEC) (A Joint Conference of 45th IEEE PVSC, 28th PVSEC & 34th EU PVSEC)*, 2018, pp. 1333–1335.
[281] Sulas-Kern, “Degradation mechanisms in fielded modules: Imaging for identification of resistance effects,” in *PV Reliability Workhop*.
[282] T. Tanahashi, N. Sakamoton, H. Shibata, and A. Masuda, “Corrosion-Induced AC Impedance Elevation in Front Electrodes of Crystalline Silicon Photovoltaic Cells Within Field-Aged Photovoltaic Modules,” *IEEE J. Photovoltaics*, vol. 9, no. 3, pp. 741–751, 2019, doi: 10.1109/JPHOTOV.2019.2893442.
[283] M. Köntges, I. Kunze, S. Kajari-Schröder, X. Breitenmoser, and B. Bjørneklett, “The risk of power loss in crystalline silicon based photovoltaic modules due to micro-cracks,” *Solar Energy Materials and Solar Cells*, vol. 95, no. 4, pp. 1131–1137, 2011, doi: 10.1016/j.solmat.2010.10.034.
[284] Gabor A., “Cracking the case: quantifying the impact of cell cracking,” in . [Online]. Available: https://www.pv-magazine.com/webinars/cracking-the-case-quantifying-the-impact-of-cell-cracking/
[285] J. Käsewieter, F. Haase, M. H. Larrodé, and M. Köntges, “Cracks in Solar Cell Metallization Leading to Module Power Loss under Mechanical Loads,” *Energy Procedia*, vol. 55, pp. 469–477, 2014, doi: 10.1016/j.egypro.2014.08.011.
[286] D. C. Jordan, T. J. Silverman, J. H. Wohlgemuth, S. R. Kurtz, and K. T. VanSant, “Photovoltaic failure and degradation modes,” *Prog. Photovolt: Res. Appl.*, vol. 25, no. 4, pp. 318–326, 2017, doi: 10.1002/pip.2866.
[287] E. Bellini, *UK researchers confirm correlation between micro-cracks and hot spots in polycrystalline cells*, 2020. [Online]. Available: https://www.pv-magazine.com/2020/01/07/uk-researchers-confirm-correlation-between-micro-cracks-and-hot-spots-in-polycrystalline-cells/
[288] O. K. Abudayyeh, N. D. Gapp, C. Nelson, D. M. Wilt, and S. M. Han, “Silver–Carbon-Nanotube Metal Matrix Composites for Metal Contacts on Space Photovoltaic Cells,” *IEEE J. Photovoltaics*, vol. 6, no. 1, pp. 337–342, 2016, doi: 10.1109/JPHOTOV.2015.2480224.
[289] O. Abudayyeh, C. Nelson, G. Bradshaw, S. Whipple, D. Wilt, and S. Han, “Crack-Tolerant Metal Composites as Photovoltaic Gridlines,” *IEEE J. Photovoltaics*, PP, pp. 1–5, 2019, doi: 10.1109/JPHOTOV.2019.2939096.
[290] O. Abudayyeh *et al., Development of Low-Cost, Crack-Tolerant Metallization Using Screen Printing*, 2019.
[291] T. J. Silverman, M. Bliss, A. Abbas, T. Betts, M. Walls, and I. Repins, “Movement of Cracked Silicon Solar Cells During Module Temperature Changes,” in *46th IEEE PVSC*.
[292] F. Haase, J. Kasewieter, S. R. Nabavi, E. Jansen, R. Rolfes, and M. Köntges, “Fracture Probability, Crack Patterns, and Crack Widths of Multicrystalline Silicon Solar Cells in PV Modules During Mechanical Loading,” *IEEE J. Photovoltaics*, PP, pp. 1–15, 2018, doi: 10.1109/JPHOTOV.2018.2871338.

[293] J. Gifford, *The weekend read: CIGS is back, back again.* [Online]. Available: https://www.pv-magazine.com/2018/07/21/the-weekend-read-cigs-is-back-back-again/
[294] E. Bellini, *Korean researchers announce flexible CIGS solar cell with 20.4% efficiency*, 2020. [Online]. Available: https://www.pv-magazine.com/2020/03/02/korean-researchers-announce-flexible-cigs-solar-cell-with-20-4-efficiency/
[295] R. Carron *et al.,* "Advanced Alkali Treatments for High-Efficiency Cu(In,Ga)Se2 Solar Cells on Flexible Substrates," *Adv. Energy Mater.*, vol. 9, no. 24, p. 1900408, 2019, doi: 10.1002/aenm.201900408.
[296] M. Hutchins, *MiaSolé breaks its own record for flexible CIGS*, 2019. [Online]. Available: https://www.pv-magazine.com/2019/11/11/miasole-breaks-its-own-record-for-flexible-cigs/
[297] Global Solar, *Flexible Solar Panels.* [Online]. Available: https://globalsolar.com/
[298] M. Osborne, *Midsummer offers complete BIPV CIGS thin-film metal roof systems.* [Online]. Available: https://www.pv-tech.org/products/midsummer-offers-complete-bipv-cigs-thin-film-metal-roof-systems
[299] MiaSolé, *MiaSolé - Home.* [Online]. Available: http://miasole.com/
[300] B. Weller, *Technologieentwicklung leichter,flexibler Photovoltaikelemente auf der Basis von ETFE und CIGS-Foliensolarzellen für die Architektur*.
[301] A. Gerthoffer *et al.,* "CIGS solar cells on flexible ultra-thin glass substrates: Characterization and bending test," *Thin Solid Films*, vol. 592, pp. 99–104, 2015, doi: 10.1016/j.tsf.2015.09.006.
[302] C. Yang, K. Song, X. Xu, G. Yao, and Z. Wu, "Strain dependent effect on power degradation of CIGS thin film solar cell," *Solar Energy*, vol. 195, pp. 121–128, 2020, doi: 10.1016/j.solener.2019.11.012.
[303] M. Theelen and F. Daume, "Stability of Cu(In,Ga)Se2 solar cells: A literature review," *Solar Energy*, vol. 133, pp. 586–627, 2016, doi: 10.1016/j.solener.2016.04.010.
[304] J. Rion, "Ultra-light photovoltaic composite sandwich structures," 2008, doi: 10.5075/epfl-thesis-4138.
[305] G. Oreski, A. Halm, V. Schenk, M. Edler, M. Klenk, and H. Nussbaumer, "Investigation of effects due to encapsulation thickness reduction in light weight modules," Halle an der Saale, Oct. 23 2018.
[306] H. Nussbaumer, M. Klenk, N. Keller, P. Ammann, and and J. Thurnheer, "Record-Light Weight c-Si Modules Based on the Small Unit Compound Approach – Mechanical Load Tests and General Results," in *33rd European Photovoltaic Solar Energy Conference and Exhibition*.
[307] M. Brown, "Hail Impact Testing on Crystalline Si Modules with Flexible Packaging," in *PV Module Reliability Workshop, Berlin, Germany, 2011*.

ISBN 978-3-907281-02-4